2017

Characterization of the SUF FE-S Pathway In Escherichia Coli

Naimah Bolaji
University of South Carolina

CHARACTERIZATION OF THE SUF FE-S PATHWAY IN *ESCHERICHIA COLI*

by

NAIMAH BOLAJI

Bachelor of Science
University of Ilorin, 2004

Submitted in Partial Fulfillment of the Requirements

For the Degree of Doctor of Philosophy in

Chemistry

College of Arts and Sciences

University of South Carolina

2017

Accepted by:

F. Wayne Outten, Major Professor

Ken Shimizu, Committee Member

Caryn Outten, Committee Member

Alan Decho, Committee Member

Cheryl L. Addy, Vice Provost and Dean of the Graduate School

DEDICATION

To my mom, sons and husband

ACKNOWLEDGEMENTS

I would like to thank my committee members. Thank you very much for your invaluable comments and feedback. Your guidance and tutoring were exceptional. Without you this would not be possible. Special thanks to my wonderful academic advisor Dr. F. Wayne Outten, for his support, guidance, and mentorship. Thank you for your thoughtfulness and patience - they meant the world to me! I am also grateful for the aid of my doctoral committee, Dr. Ken Shimizu and Dr. Tom Makris. They have assisted me through the years both academically and in other endeavors. I would also like to thank Dr. Alan Decho for agreeing to join my committee.

I would also like to express my thanks to my fellow colleagues in the two Outten labs. Crystal, Angela, Matt, Guangchao, Clorissa and to everybody else, you guys were amazing and I will miss you all. I would also like to thank Dr. Khaleh Thomas for putting me through the lab when I first arrived. I would like to express a special shout-out to my friends turned sisters- Bunmi and Nefe. Bunmi, thanks for feeding me and providing such well needed emotional assistance all these years. Love you guys.

Lastly, I would like to thank my dearest husband who believed in me even when I didn't believe in myself! Your support of my ambitions is a gift which I do not take for granted. Thank you for being there always! Love you forever.

ABSTRACT

Iron is an essential transition metal required by almost all organisms for use as a cofactor in many metabolic processes such as respiration and photosynthesis. Iron can be combined with elemental sulfur to form an iron-sulfur (Fe-S) cluster. In bacterial pathogens, Fe-S cluster cofactors carry out critical functions and the Fe-S cluster biogenesis pathway is essential for their survival. In *E. coli,* the Suf pathway assembles Fe-S clusters under conditions of iron starvation and oxidative stress. While some mechanistic details of the Fe-S cluster biogenesis have been well-characterized, the process of *in vivo* iron donation remains unclear. Iron storage proteins generally known as ferritins are capable of storing iron in a readily available and soluble form to serve as a reservoir of iron for metabolism. We are testing if these iron storage proteins can be *in vivo* iron donors for Suf Fe-S cluster assembly. Our results indicate that the bacterioferritin (Bfr) and DNA binding protein of starved cells (Dps) proteins may play roles in the *in vivo* donation to the Suf pathway. Our results also indicate the Ferritin A (FtnA) protein does not donate iron to this pathway. We also investigated what role the little characterized ferritin B protein may play in this iron donation. We found that the deletion of the FtnB and bacterioferritin proteins caused an inability for the strain to make Fe-S clusters. We therefore summarize that the three proteins: Bfr, Dps and FtnB donate iron to the Suf Fe-S cluster biogenesis pathway and have redundancy in their functions.

TABLE OF CONTENTS

DEDICATION iii

ACKNOWLEDGEMENTS iv

ABSTRACT v

LIST OF TABLES ix

LIST OF FIGURES x

LIST OFABBREVIATIONS xv

CHAPTER ONE - Introduction 1

1.1 Iron Acquisition and Regulation 1

1.2. Iron Sulfur Clusters 12

1.3 Iron-Sulfur (Fe-S) Cluster Biogenesis Pathway 13

1.4 Sulfur Utilization (Suf) pathway 18

1.5 Research Aims 22

1.6 Biomedical relevance 23

References 24

CHAPTER TWO – Bfr and Dps may serve as iron donors to the Suf pathway 32

Abstract 32

2.1 Introduction 33

2.2 Materials and Methods 36

2.3 Results 41

2.4 Discussion 78

References 83

CHAPTER THREE – FtnB may play a role in iron donation to the Suf pathway 86

Abstract 86

3.1 Introduction 87

3.2 Materials and Methods 89

3.3 Results 94

3.4 Discussion 108

References 112

CHAPTER FOUR – Wild-type *Escherichia coli* has multiple Non-Heme high spin iron species 113

Abstract 113

4.1 Introduction 114

4.2 Materials and Methods 116

4.3 Results 118

4.4 Discussion 125

References 132

APPENDIX A – SUPPLEMENTAL EXPERIMENTS AND RESULTS 134

APPENDIX B – SUPPLEMENTAL EXPERIMENTS AND RESULTS..... 151

LIST OF TABLES

Table 2.1 Bacterial Strains used in this study 43

Table 2.2 Mössbauer iron speciation and percentages.....57

Table 2.3 Mössbauer iron speciation and percentages.....69

Table 3.1 Bacterial Strains used in this study 91

Table 3.2 Mössbauer iron speciation and percentages.....103

Table 4.1 Offline ICP Metal Concentrations and Mössbauer Percentages.....122

Table 4.2 Offline ICP Metal Concentrations and Mössbauer Percentages.....126

Table A.1 Parameters for Wild-type Mossbauer analysis……..……143

LIST OF FIGURES

Figure 1.1 Schematic diagram of iron uptake in *E. coli* 5

Figure 1.2 Fur and RyhB regulation of iron and iron-containing enzymes 6

Figure 1.3 Crystal structure of apo-ferritin A and bacterioferritin 7

Figure 1.4 Crystal structure of DNA-binding proteins of starved cells 8

Figure 1.5 FtnA regulation by Fur 11

Figure 1.6 Structure of *E. coli* hydrognase-1 in complex with cytochrome b 14

Figure 1.7 General Fe-S cluster biogenesis pathway 15

Figure 1.8 The Isc pathway biogenesis operon 17

Figure 1.9 Transcriptional regulation of the *suf* operon in *E. coli* 20

Figure 1.10 Proposed mechanism of *suf* [Fe-S] cluster biogenesis 21

Figure 2.1 The parent Δ*iscU-fdx* strain 42

Figure 2.2 Deletion of individual ferritins in the parent Δ*iscU-fdx* strain does not make it sensitive to bipyridyl stress. 45

Figure 2.3 The Δ*iscU-fdx* Δ*bfr* Δ*dps* strain shows an extended increase in lag phase duration when pre-grown in minimal media with no stress 46

Figure 2.4 The Δ*iscU-fdx* Δ*bfr* Δ*dps* strain shows a less severe lag phase duration when pre-grown in minimal media with no stress 48

Figure 2.5 The deletion of both *bfr* and *dps* sensitizes the Δ*iscU-fdx* strain to bipyridyl stress. 49

Figure 2.6 The deletion of both *bfr* and *dps* sensitizes the Δ*iscU-fdx* strain to oxidative stress. 50

Figure 2.7 Deletion of Bfr and Dps in the presence of a functional Isc pathway doesn't make the strain sensitive to iron starvation stress 51

Figure 2.8 Pre-adaptation to low iron media rescues the sensitivity of the Δ*iscU-fdx*Δ*bfr*Δ*dps* strain to bipyridyl stress. 52

Figure 2.9 Addition of iron to the pre-stress growth media likely enhances the sensitivity of the Δ*iscU-fdx*Δ*bfr*Δ*dps* strain 54

Figure 2.10 The Δ*iscU-fdx*Δ*bfr*Δ*dps* strain has virtually no Fe-S cluster assembly function 55

Figure 2.11 The Δ*iscU-fdx*Δ*bfr*Δ*dps* mutant strain accumulates more iron than the WT when pre-grown in 100 μM ^{57}ferric citrate. 58

Figure 2.12 The Δ*iscU-fdx*Δ*bfr*Δ*dps* strain shows a defective growth phenotype in M9 acetate growth with no stress 59

Figure 2.13 Additional deletion of *ftnA* rescues the mild increase in lag phase duration in LB media with no stress of the Δ*iscU-fdx*Δ*bfr*Δ*dps* strain 61

Figure 2.14 Additional deletion of *ftnA* rescues the mild increase in lag phase duration in minimal media with no stress of the Δ*iscU-fdx*Δ*bfr*Δ*dps* strain 62

Figure 2.15 Additional deletion of *ftnA* rescues the sensitivity of the Δ*iscU-fdx*Δ*bfr*Δ*dps* strain to bipyridyl 63

Figure 2.16 Additional deletion of *ftnA* rescues the sensitivity of the Δ*iscU-fdx*Δ*bfr*Δ*dps* strain to oxidative stress 64

Figure 2.17 Additional deletion of *ftnA* increases the sensitivity of the Δ*iscU-fdx*Δ*bfr*Δ*dps* strain to bipyridyl when pre-grown in M9 minimal media. 65

Figure 2.18 Addition of iron to the pre-stress growth media does not alter the sensitivity of the Δ*iscU-fdx*Δ*ftnA*Δ*bfr*Δ*dps* to BIPY 66

Figure 2.19 The Δ*iscU-fdx*Δ*ftnA*Δ*dps*Δ*bfr* strain has restored Fe-S cluster assembly function. 68

Figure 2.20 The Δ*iscU-fdx*Δ*ftnA*Δ*dps*Δ*bfr* mutant strain accumulates less iron than the WT when pre-grown in 100 μM ^{57}ferric citrate though it has restored Fe-S cluster function 70

Figure 2.21 The Δ*iscU-fdx*Δ*ftnA*Δ*dps*Δ*bfr* strain shows no defective growth phenotype in M9 acetate growth without stress**.** 71

Figure 2.22 Suf regulation is upregulated in the mutants with the Δ*iscU-fdx* background 72

Figure 2.23 Transcriptional activity of FepA 74

Figure 2.24 The additional deletion of *ftnA* does not alter the low iron content of the Δ*iscU-fdx*Δ*bfr*Δ*dps* strain.....76

Figure 2.25 Labile iron pools are highest in the Δ*iscU-fdx*Δ*bfr*Δ*dps* strain. 77

Figure 3.1 Sequence comparison of Ferritin A and Ferritin B 88

Figure 3.2 The Δ*iscU-fdx*Δ*ftnB*Δ*bfr* strain shows an extended lag phase duration when pre-grown in minimal media with no stress which becomes more severe with addition of iron. 96

Figure 3.3 The deletion of both *ftnB* and *bfr* sensitizes the Δ*iscU-fdx* strain to bipyridyl stress……...98

Figure 3.4 The deletion of both *ftnB* and *bfr* sensitizes the Δ*iscU-fdx* strain to oxidative stress.....100

Figure 3.5 Pre-adaptation to low iron media rescues the sensitivity of the Δ*iscU-fdx*Δ*ftnB*Δ*bfr* strain to bipyridyl stress 101

Figure 3.6 The Δ*iscU-fdx*Δ*ftnB*Δ*bfr* strain has virtually no Fe-S cluster assembly function 102

Figure 3.7 The Δ*iscU-fdx*Δ*ftnB*Δ*bfr* strain shows a growth phenotype in M9 acetate growth. 105

Figure 3.8 Suf regulation is upregulated in Δ*iscU-fdx*Δ*ftnB*Δ*bfr* mutant strain 106

Figure 3.9 Transcriptional activity of FepA 107

Figure 3.10 Labile iron pools are higher in the Δ*iscU-fdx*Δ*ftnB*Δ*bfr* strain.....109

Figure 4.1 Whole-cell Mössbauer spectroscopy of wild-type *E. coli* grown in M9 glucose media with 100 μM ^{57}Fe (III)-citrate. 119

Figure 4.2 Whole-cell Mössbauer spectroscopy of wild-type *E. coli* grown in M9 glucose media with 1, 10 and 100 μM ^{57}Fe (III)-citrate. 121

Figure 4.3 Growth curves of the 3 wild-type strains in different iron concentrations were similar. 124

Figure 4.4 Whole-cell Mössbauer spectroscopy of Δ*fur::kan*^{R} *E. coli* grown in M9 glucose media with 1, 10 and 100 μM ^{57}Fe(III)-citrate. 127

Figure 4.5 Growth curves of the 3 Δ*fur::kan*^{R} strains in different iron concentrations were similar. 128

Figure 4.6 The Δ*fur::kan*^{R} strain shows a defective growth phenotype in M9 acetate growth without stress 129

Figure A.1 Transcriptional activity of FepA.....135

Figure A.2 Bfr and FtnA Plasmid re-insertion didn't rescue the sensitivity of the Δ*iscU-fdx*Δ*bfr*Δ*dps* strain.....136

Figure A.3 Additional deletion of *ftnA and ftnB* rescues the sensitivity of the Δ*iscU-fdx*Δ*bfr*Δ*dps* strain to bipyridyl. 138

Figure A.4 Additional deletion of *ftnA and ftnB* rescues the mild increase in lag phase duration in LB media with no stress of the Δ*iscU-fdx*Δ*bfr*Δ*dps* strain 139

Figure A.5 Transcriptional activity of FepA.....140

Figure A.6 Labile iron pools are lowest in the Δ*iscU-fdx*Δ*ftnA*Δ*dps*Δ*bfr*Δ*ftnB* strain... .141

Figure A.7 Mossbauer spectra (5K, 0.05T) of Wild-Type *E.* coli grown in glucose medium... 142

Figure A.8 Mossbauer spectra (5K, 0.05T) of E coli strain Δ*iscU-fdx* grown in glucose medium. 144

Figure A.9 Mossbauer spectra (5K, 0.05T) of E coli strain Δ*iscU-fdx*Δ*bfr*Δ*dps* grown in glucose medium.. 146

Figure A.10 Mossbauer spectra (5K, 0.05T) of E coli strain Δ*iscU-fdx*Δ*ftnA*Δ*dps*Δ*bfr* grown in glucose medium... 148

Figure A.11 Mossbauer spectra (5K, 0.05T) of E coli strain Δ*iscU-fdx*Δ*ftnB*Δ*bfr* grown in glucose medium... 149

Figure B.1 FtnA expression slightly upregulated in higher iron concentrations in the Wild-type strain. 152

Figure B.2 Iron LC-ICPMS on (A) wild type and (B) 10 μM Δ*fur* samples.....153

Figure B.3 Phosphorus LC-ICPMS on (A) wild type and (B) 10 μM Δ*fur* samples.....154

Figure B.4 Sulfur LC-ICPMS on (A) wild type and (B) 10 μM Δ*fur* samples. 155

Figure B.5 Copper LC-ICPMS on (A) wild type and (B) 10 μM Δ*fur* samples.....156

Figure B.6 Zinc LC-ICPMS on (A) wild type and (B) 10 µM Δ*fur* samples. 157

Figure B.7 Manganese LC-ICPMS on (A) wild type and (B) 10 µM Δ*fur* samples. 158

Figure B.8 Cobalt LC-ICPMS on wild type and 10 µM Δ*fur* samples.....159

LIST OFABBREVIATIONS

AAS.....Atomic absorption spectroscopy

Bfr .....Bacterioferritin

CD .....Central Doublet

BIPY ..... 2,2 Bipyridyl

Dps ..... DNA binding protein of starved cells

E. coli ..... *Escherichia coli*

EPR .....Electron Paramagnetic Resonance

[Fe-S] .....Iron Sulfur

FtnA .....Ferritin A

FtnB.....Ferritin B

Fur .....Ferric Uptake Regulator

ICP-MS ..... Inductively coupled plasma mass spectrometry

isc ..... Iron Sulfur Cluster

NHHS..... Non-Heme High Spin

PCR ..... Polymerase Chain Reaction

PMS..... Phenazine methosulfate

ROS.....Reactive Oxygen Species

Suf .....mobilization of Sulfur

CHAPTER ONE
Introduction

1.1 Iron Acquisition and Regulation

Iron. Iron is the fourth most abundant element in the Earth's crust, and one of the most versatile elements in terms of its biological uses.[1] It belongs to the group of elements known as "Transition Metals". In biological systems, iron predominantly exists in one of two oxidation states: Fe^{3+} (ferric), or Fe^{2+} (ferrous), but can also accommodate other oxidation states (+4).[2] The ability of iron to accept or donate an electron modulates the transition from Fe^{3+} to Fe^{2+} or vice versa. This redox chemistry allows iron to have fundamental roles in major biological processes including: photosynthesis, nitrogen fixation, oxygen transport, gene regulation, DNA synthesis, and citric acid cycle.[3] Iron's biological functionality is dependent on its incorporation into iron-sulfur [Fe-S] proteins, mono- or binuclear iron proteins, ferritins, hemosiderins, lactoferrins, and transferrins.[4-8] Iron availability in the cell is tightly controlled to prevent the accumulation of reactive oxygen species via the Fenton reaction (shown below)

$$Fe^{2+} + H_2O_2 \longrightarrow Fe^{3+} + {}^{-}OH + {}^{\cdot}OH$$

Iron Acquisition and Storage. Despite the indispensability of iron, it is also potentially toxic due to its tendency to catalyze the formation of toxic reactive oxygen species (ROS) (shown above). The Fenton reaction produces the hydroxyl radical (·OH), a ROS capable of oxidizing macromolecules and lipids. Therefore, cells must tightly regulate the

concentration of Fe to avoid ROS-mediated cell damage.[9]

In ancient environments, bacteria had no challenges acquiring ferrous iron (Fe^{2+}) for its utilization. Oxygenation of the world challenged bacteria to acquire the insoluble ferric iron (Fe^{3+}) which has very low solubility and this lead to bioavailability problems.[10] To overcome this challenge, bacteria evolved with pathways for the solubilization of extracellular iron either by reduction or chelation, followed by internalization via specific transporters. In order to acquire iron in iron-limiting environments, bacteria and fungi synthesize and secrete low molecular weight compounds, called siderophores which form a ferric-siderophore complex with the ferric ions.[11-15] These are then taken up via specific receptors and shuttled via periplasmic-binding proteins into the inner membrane transporters. These transporters ultimately deliver the complexes into the cytoplasm where they are dissociated by reduction.[16] Cytosolic iron may be deposited in inert forms such as ferric oxyhydroxide or ferrihydrite minerals within proteins known as Ferritins. This iron storage process requires a ferroxidation step which is catalyzed by specific sites within them known as ferroxidase centres.[17-18]

These ferritins can reduce the ferric iron stored and supply it to the cell when iron availability is limited. *E. coli* has 3 main iron storage proteins Ferritin A (FtnA), Bacterioferritin (Bfr) and DNA-Binding protein of starved cells (Dps).[19-21]

Iron acquisition and storage systems are regulated in response to iron availability. This regulation is mediated by Fur (Ferric uptake regulator), a transcriptional repressor which forms a Fe^{2+}-Fur complex.[22] The Fe^{2+}-Fur complex is a global transcriptional regulator involved in the regulation of many iron-dependent metabolic functions in the

cell. Fe^{2+}-Fur represses transcription by binding to a 19-bp sequence, designated the "iron box," normally located near the Pribnow box of cognate promoters.[1,21,23] Fur can also act as a transcriptional activator switching on genes encoding some iron-containing proteins including aconitase A, Bfr and FtnA. This activation appears to be to be indirect and seems to involve (at least in some cases) Fe^{2+}-Fur repression of a regulatory RNA, RyhB. (Figure 1.2) [24-25]

Ferritins. Ferritins constitute a broad superfamily of iron storage proteins that have been identified in all forms of life except lactobacilli. Bacterioferritins also belong to this ferritin superfamily but are unique to bacteria and contain heme.[26] The main function of the ferritin family is to sequester intracellular ferric iron in a non-toxic form. Under high iron concentrations, ferritins will oxidize Fe^{2+} to Fe^{3+} and sequester it as an inert ferrihydrite mineral inside the protein core. Under iron limiting conditions, these ferritins will release iron upon reduction.[27-29]

Ferritins usually consist of homopolymers of 24 subunits for the maxi-ferritins (FtnA and Bfr) and 12 subunits for the mini-ferritins (Dps). Usually, individual polypeptides are ~20 kD and contain a four-helical bundle motif. They possess internal catalytic sites (FtnA and Bfr) or sites at the interface of adjacent subunits (Dps).[1, 29, 30] The subunit structure forms a spherical protein shell and the ferroxidase centers are located in the inner surface of the protein. These ferroxidase centers oxidize soluble ferrous ions to ferrihydrite mineral in which form iron is stored in these proteins. FtnA and Bfr are larger proteins and have 24 subunits and can accommodate up to 4,500 iron atoms (Figure 1.3) while Dps which is smaller has 12 subunits and can accommodate about 500 iron atoms (Figure 1.4).[21]

E. coli contains at least 5 genes that may play a role in iron storage. These are *bfd* encoding bacterioferritin-associated ferredoxin (Bfd), *bfr* encoding bacterioferritin, *dps* encoding Dps, *ftnA* encoding ferritin A, and the *ftnB* encoding a ferritin-like protein FtnB. FtnB has not been well characterized and its role as an iron storage protein is still unclear because its primary sequence suggests that it lacks the presence of conserved dinuclear center ligands required for ferroxidase activity conserved in other ferritins.[31] Bfr and FtnA have been well characterized to be iron storage proteins while Bfd is required for in vivo iron reduction and release from Bfr.[32]

The reason why *E. coli* has multiple iron storage proteins is unknown. FtnA has been shown to be involved in the storage of iron during stationary phase and release during iron starved conditions. Bfr is an oligomeric protein containing both a binuclear iron centre and haem b. The tertiary and quaternary structure of Bfr is very similar to that of Ferritin A. The physiological role of Bfr remains slightly uncertain. While it has been implicated as the main storage protein in other microorganisms, its role in cells may involve more than iron uptake.

Dps has been shown to have the ability to bind and physically sequester DNA, and during stationary phase forms a highly ordered and stable dps-DNA co-crystal within which chromosomal DNA is condensed and protected from diverse damages.[33-35] It protects DNA from oxidative damage by sequestering intracellular Fe^{2+} ion and storing it in the form of Fe^{3+} oxyhydroxide mineral, which can be released after reduction. In Dps one hydrogen peroxide oxidizes two Fe^{2+} ions, which prevents hydroxyl radical production by the Fenton reaction. Dps also protects the cell from UV and gamma irradiation, iron and copper toxicity, thermal stress and acid and base shocks. [36]

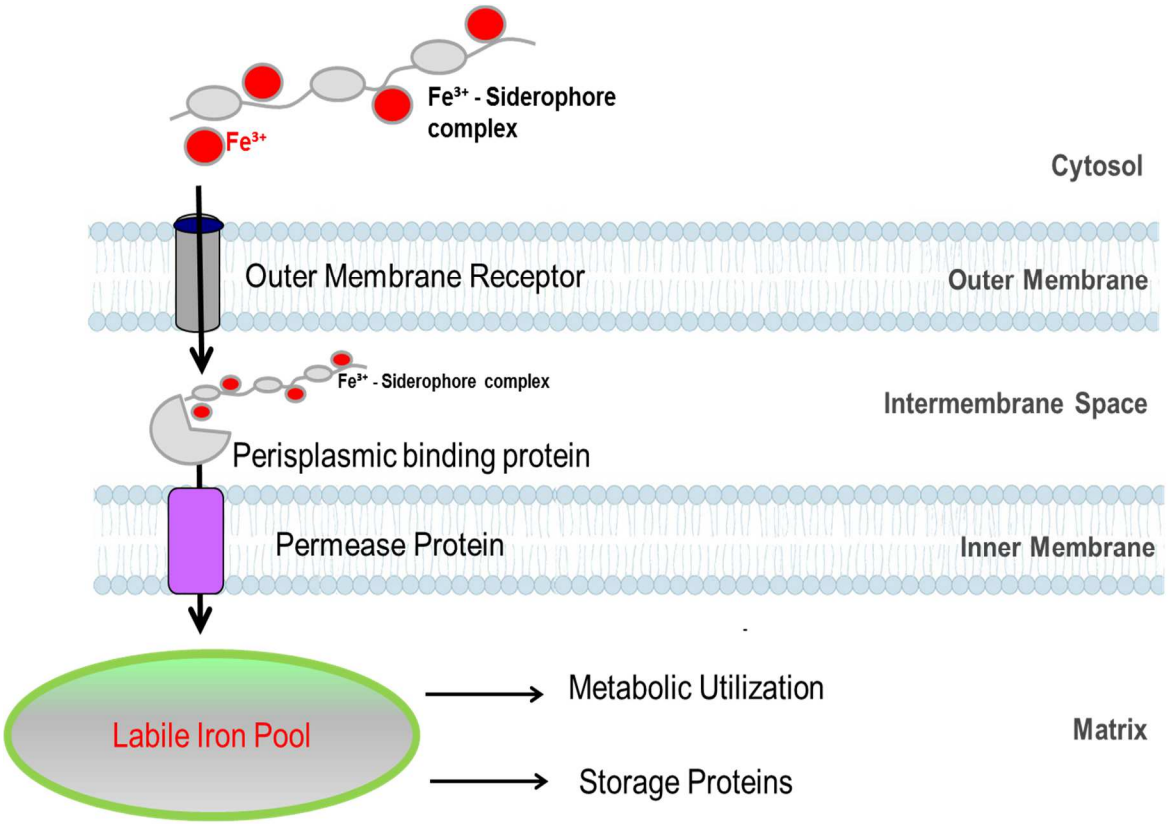

Figure 1.1. Schematic diagram of iron uptake in *E. coli*

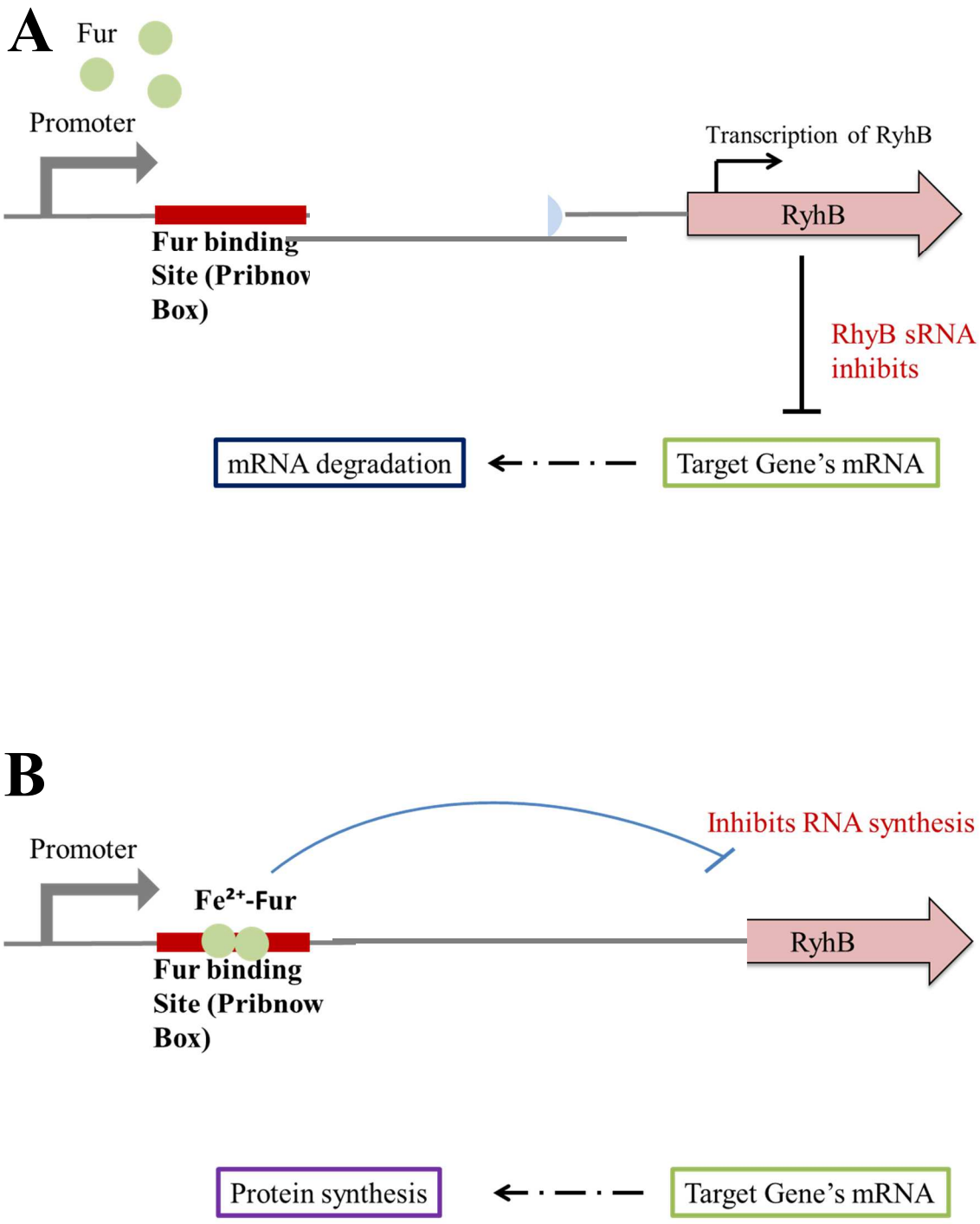

Figure 1.2. Fur and RyhB regulation of iron and iron containing proteins. (A) In the absence of Fe^{2+}, Fur doesn't bind to its promoter region; RyhB inhibits synthesis of target genes mRNA and causes degradation. (B) In presence of iron, the Fe^{2+}-Fur complex binds the Pribnow box, and inhibits RyhB synthesis. The repression of target genes is stopped and protein is synthesized.

A

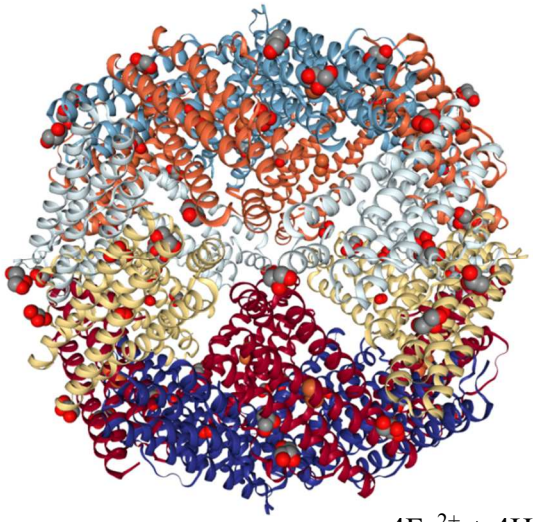

$4Fe^{2+} + 4H^{+} + O_2 \longrightarrow 4Fe^{3+} + 2H_2O$

(Ferroxidase reaction in FtnA and Bfr)

B

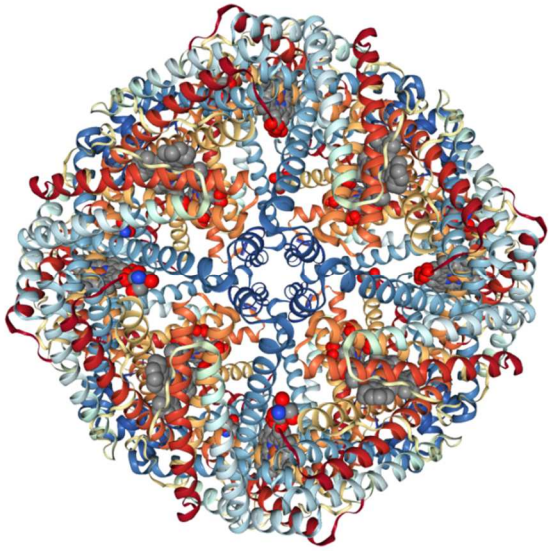

Figure 1.3. (A) Crystal structure of apo-Ferritin A from *E. coli* (PDB entry 4ZTT). (B) Crystal structure of apo-bacterioferritin from *E. coli* (PDB entry 2Y3Q). The heme is the grey balls buried in interior of molecule. Oxygen (O_2) is the physiological oxidant in FtnA and Bfr.

$H_2O_2 + 2Fe^{2+} \longrightarrow 2Fe^{3+} + 2H_2O$
(Ferroxidase reaction in Dps)

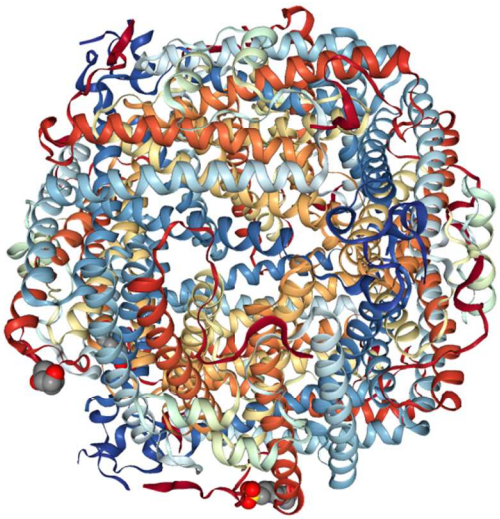

Figure 1.4. Crystal structure of DNA-binding protein of starved cells (DPS) from *E. coli* (PDB entry 5HJH). Hydrogen peroxide (H_2O_2) is the physiological oxidant in Dps.

The reason why *E. coli* has multiple iron storage proteins is unknown. FtnA has been shown to be involved in the storage of iron during stationary phase and release during iron starved conditions. Bfr has also been implicated as the main iron storage protein in other microorganisms. The role of Bfr remains uncertain. Dps has been shown to have the ability to bind and physically sequester DNA, and during stationary phase forms a highly ordered and stable dps-DNA co-crystal within which chromosomal DNA is condensed and protected from diverse damages.[33-35] It protects DNA from oxidative damage by sequestering intracellular Fe^{2+} ion and storing it in the form of Fe^{3+} oxyhydroxide mineral, which can be released after reduction. In Dps one hydrogen peroxide oxidizes two Fe^{2+} ions, which prevents hydroxyl radical production by the Fenton reaction. Dps also protects the cell from UV and gamma irradiation, iron and copper toxicity, thermal stress and acid and base shocks. [36]

The mechanism by which iron is sequestered inside the maxi-ferritins can be divided into three distinct steps. The first step involves ferrous iron binding at the ferroxidase center. The ferroxidase center is a di-iron binding site composed of conserved glutamate and histidine residues although the different types of ferritins contain somewhat different arrangements.[37-39] The second step involves catalytic oxidation of ferrous iron to ferric iron using molecular O_2 as the oxidant and the final step involves the storage of the ferric iron in its ferric oxyhydroxide mineral inert form. In Dps, the oxidant for oxidation of ferrous iron has been shown to be hydrogen peroxide (H_2O_2). It therefore has an extra role in protecting DNA from oxidative damage by consuming H_2O_2 as it sequesters intracellular $Fe2^{+}$ ion in the form of Fe^{3+} oxyhydroxide mineral.[34] One hydrogen peroxide oxidizes two Fe^{2+} ions, which prevents uncontrolled hydroxyl radical

production by the Fenton reaction.[9]

Regulation of the ferritin genes is necessary to provide the cell with a balance between iron- mediated toxicity and the iron necessary for metabolism. In *E. coli*, the *ftnA* and *bfr* genes are regulated using an elegant mechanism under iron replete or iron depleted conditions. Both genes are upregulated by the Fur-Fe^{2+} repressor relaying the signal that iron is abundant in the cell. While Bfr is regulated by Fe^{2+}– Fur through the regulation of RyhB (Figure 1.2), FtnA is induced by Fur in a mechanism independent of it (Figure 1.5). This involves direct interaction of Fe^{2+}–Fur with an 'extended' Fur binding site located upstream (−83) of the *ftnA* promoter. In iron poor environments, histone-like nucleoid associated protein (H-NS), a direct repressor of *ftnA,* binds at multiple sites upstream of the *ftnA* promoter and subsequently prevents *ftnA* transcription. When the cell is replete with iron, Fe^{2+}–Fur directly competes with H-NS binding at upstream sites and consequently displaces H-NS from the *ftnA* promoter which in turn leads to derepression of *ftnA* transcription. Fur displacement of H-NS from the upstream sites prevents cooperative H-NS binding at the downstream sites within the promoter, thus allowing access to RNA polymerase to the *ftnA* promoter.[40]

On the other hand, most iron acquisition genes are negatively regulated by Fur-Fe^{2+}.[22] One such negatively regulated gene is a small RNA called RyhB.[26] When Fe^{2+} dissociates from Fur, transcription of *ryhB* is activated. RyhB targets the mRNA of *ftnA*, *bfr*, and many [Fe-S] proteins for degradation. This reduces cellular demand for iron while also blocking further iron storage in FtnA and Bfr.

Dps is one of the most abundant proteins in stationary phase and forms biocrystals with the chromosomal DNA through nonspecific binding. The ability of Dps to

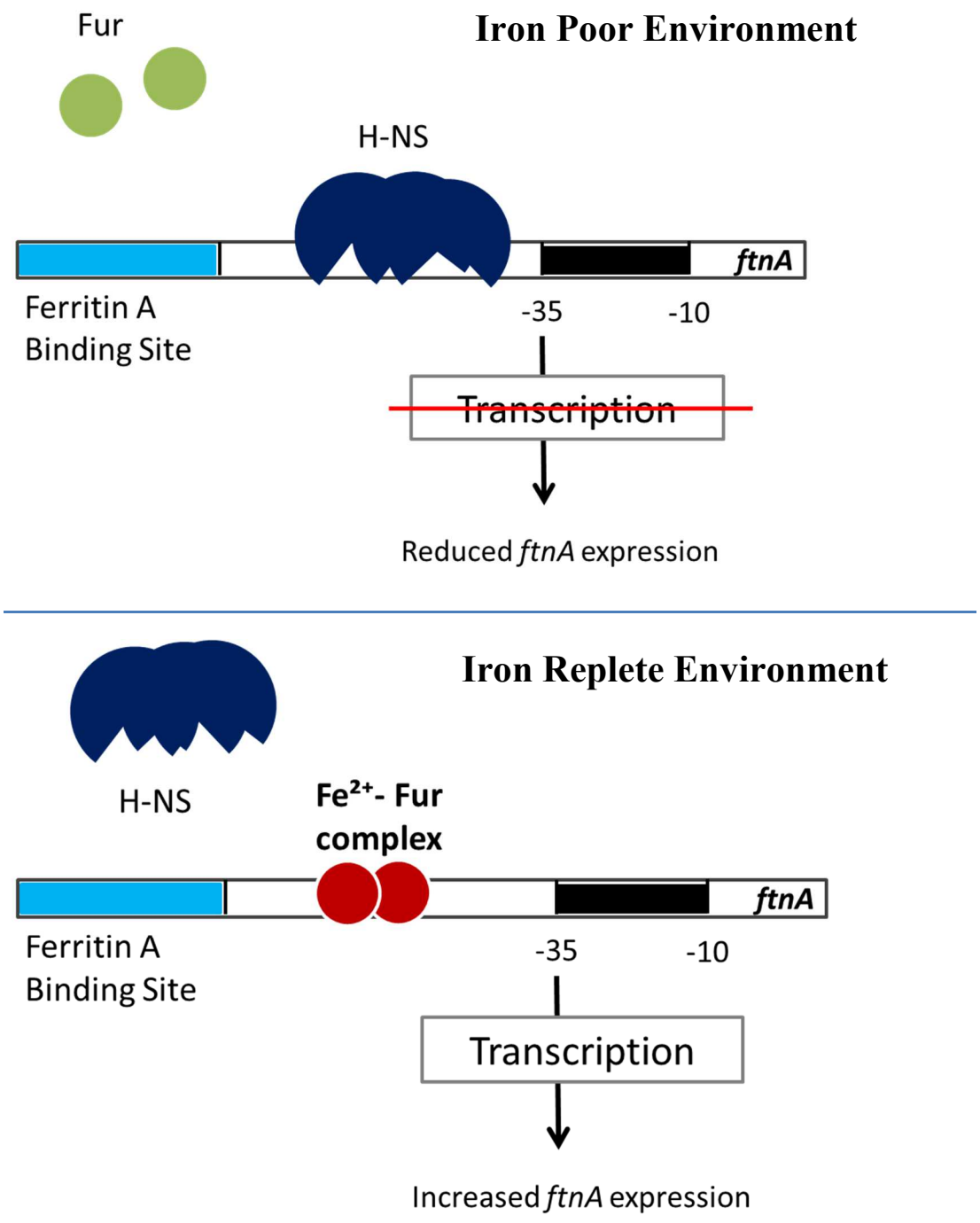

Figure 1.5. FtnA regulation by Fur. Direct interaction of Fe^{2+}–Fur at the Fur binding site directly displaces histone-like nucleoid associated protein (H-NS) a *ftnA* repressor and increases its transcription in iron replete environments.

nonspecifically bind DNA and the fact that it uses H_2O_2 as the oxidant for iron mineralization suggests a different oxidative stress defense system whereby the DNA is crystallized like eukaryotic chromosomes. Dps forms bio-crystals with the DNA and thus protects it from oxidative stress. It has also been shown to act as a component of several other stress pathways by enhancing bacterial survival of other different stresses including heat shock, starvation and over exposure to iron. Unlike the indirect activation of *ftnA* or *bfr* due to oxidative stress, direct activation of *dps* can occur in exponential phase via oxidized OxyR, a transcriptional activator that responds to H_2O_2.[41]

1.2. Iron Sulfur Clusters

Iron-sulfur (Fe-S) clusters are among the most ancient and versatile protein cofactors. These clusters consist of iron in the Fe^{2+} or Fe^{3+} oxidation states bound to sulfide (S^{2-}).[42] These clusters are typically ligated to proteins via cysteine residues; however, histidine, serine, aspartate, or backbone amides have been also seen to coordinate clusters in specific examples.[43] Fe-S clusters are essential metal co-factors and serve both catalytic and structural roles in a large and diverse group of proteins. They have the ability to delocalize electron density over both Fe and S atoms and this makes them ideally suited for their primary role in mediating biological electron transport.[44] They are also vital in several other essential central metabolic processes such as redox chemistry, enzyme catalysis, and regulating gene expression. The process by which Fe-S clusters have to be assembled has to be highly regulated since the reactive oxygen species generated as byproducts of aerobic respiration are highly damaging to Fe-S clusters, and free iron and free sulfide are toxic to the cell.[45-47]

Different cluster types are named based on the ratios of iron and sulfide that

are present in those clusters with the most common being [2Fe-2S], [3Fe-4S] and [4Fe-4S] clusters (Figure 1.6). Examples of Fe-S containing enzymes in *E. coli* include ferredoxins, hydrogenases, oxygenases and enzymes of the tricarboxylic acid (TCA) cycle such as Aconitase A and Aconitase B. [48]

[Fe-S] clusters can be assembled in vitro by adding ferrous iron, sulfide, and a reductant to an apo-protein. However, the concentrations of free iron and sulfide required for in vitro [Fe- S] cluster assembly are toxic to the cell. A complex Fe-S cluster assembly machinery therefore characterizes the formation of Fe-S clusters *in vivo*.[49]

1.3 Iron-Sulfur (Fe-S) Cluster Biogenesis Pathway

Fe-S cluster biogenesis pathways all follow the same basic principles. The first step is the liberation of sulfur by a cysteine desulfurase, which forms a persulfide intermediate on a conserved cysteine residue. Iron is donated from a source yet to identified and the newly formed nascent cluster is then assembled on scaffold proteins with the help of electron donors, which are needed for the reduction of sulfur to sulfide.[50] The fully formed cluster is transferred to apoproteins via chaperones that facilitate the correct substrate specificity and proper assembly of the cluster to form the mature holoprotein (Figure 1.7).

Two Fe-S biogenesis pathways have been identified in *E. coli;* The Isc (Iron Sulfur Cluster) pathway and the Suf (mobilization of Sulfur) pathway which was the last Fe-S biogenesis pathway to be discovered. All pathways require a cysteine desulfurase (designated IscS, SufS) to liberate a persulfide from free L-cysteine.[51] Secondly; clusters are primarily assembled and transported within a scaffold protein (IscU, SufB, SufU),

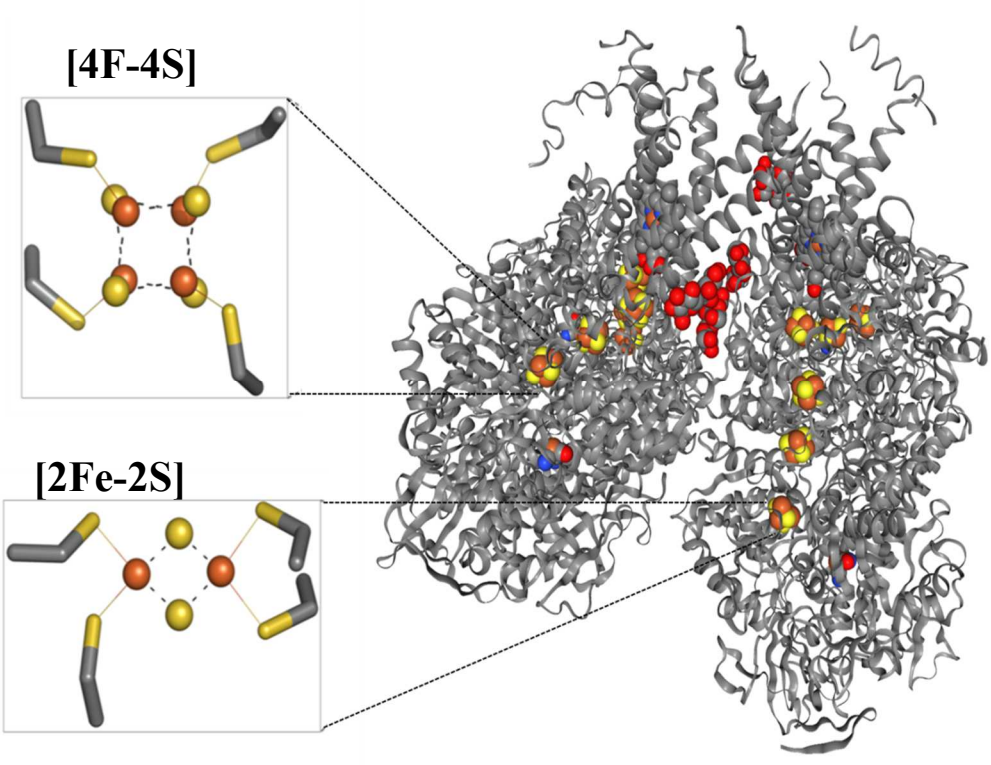

Figure 1.6. Structure of *E. coli* hydrogenase-1 in complex with cytochrome b (PDB entry 4GD3)

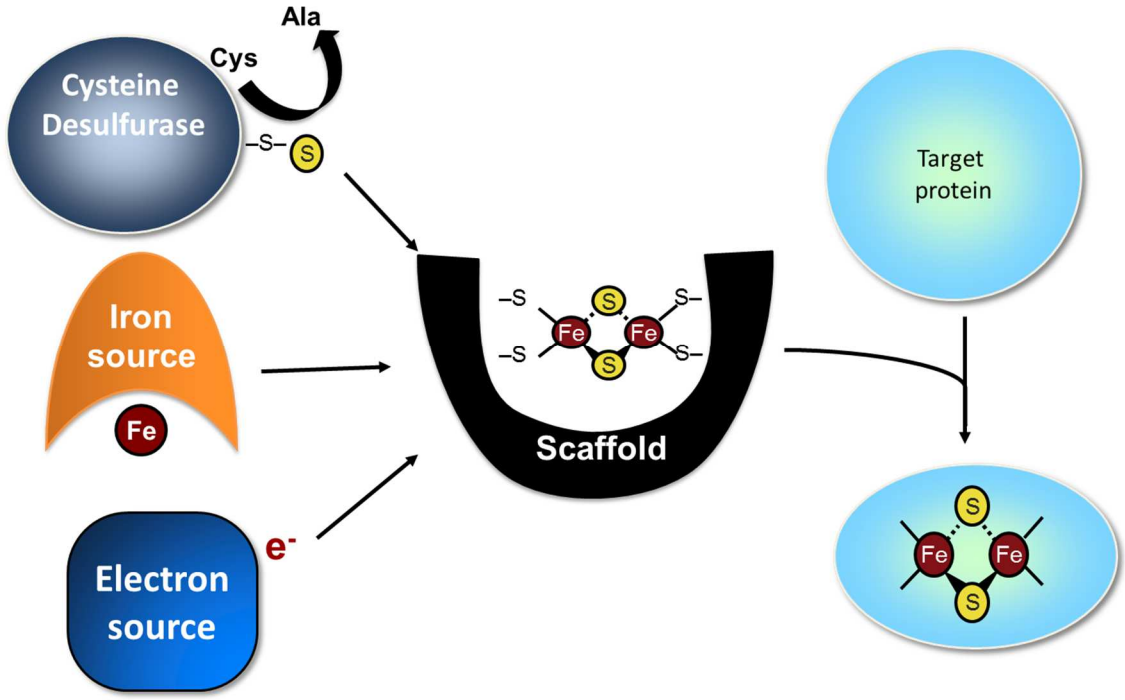

Figure 1.7. General Fe-S cluster biogenesis pathway

from which they are then transferred to recipient protein either directly or via transport proteins (IscA, SufA).[52] These different Fe-S cluster biogenesis pathways are sometimes found in combination in different microorganisms. In *E. coli*, the Isc pathway is the housekeeping pathway and functions under normal cellular conditions.

The *suf* operon functions under conditions of iron starvation and oxidative stress to repair or replace damaged Fe-S clusters.[53-57] Regulation of s*uf* is mediated by OxyR, Fur and IscR.[54,58,59] The presence of these global regulators of oxidative stress and iron limitation suggest that the function of the *suf* operon is to activate, protect, or repair [Fe-S] proteins under those stress conditions. Our lab studies the mechanism of Suf Fe-S cluster biogenesis in *E. coli* and my research focuses on the iron donation to the pathway.

Iron Sulfur Cluster pathway (Isc pathway). The Isc cluster biogenesis pathway in *E. coli* requires at least 6 proteins in both bacteria and eukaryotes (Figure 1.8). The IscU is the scaffold protein where nascent Fe-S clusters are formed. IscU receives sulfur from the action of IscS. IscA has been implicated in both being an alternative scaffold protein for Fe-S cluster assembly and also in functioning as the iron donor for [Fe-S] cluster assembly on IscU.[60] This hypothesis is supported by the fact that IscA binds iron very tightly with an apparent iron association constant of 3.0×10^{19}M in reducing conditions.[61] Iron-loaded IscA has also been shown experimentally to transfer iron to IscU for [Fe-S] cluster assembly under physiologically relevant reducing conditions.[62] In addition to IscA, eukaryotic frataxin has been implicated as a potential iron donor and also an activator. Frataxin/CyaY is a highly conserved protein implicated in Freidreich's ataxia (an incurable ataxia) in humans. *S. cerevisiae* knockouts of frataxin homolog YFH1 have deficiencies in [Fe-S] cluster maturation and increased oxidative stress.

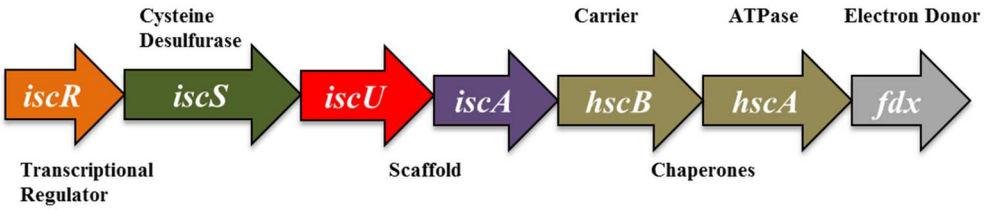

Figure 1.8. The Isc pathway (housekeeping) biogenesis operon in *E. coli*

Recently it has been suggested that CyaY and IscA may exist as dual iron donors depending on oxidative stress levels in.[63] IscA is believed to be the iron donor for Fe-S cluster assembly under physiologically relevant reducing conditions, whereas CyaY is thought to mediate Fe-S cluster assembly during periods of enhanced oxidative stress. Hydrogen peroxide which induces oxidative stress has been shown to oxidize the thiol groups of IscA and thus blocks its iron binding. The carbonyl group of CyaY however, remains unaffected by hydrogen peroxide and its iron binding ability is thus retained. The fact that both of these protein architectures exist in organisms ranging from bacteria to humans implies the importance of having two iron donors for Fe-S cluster biogenesis.[64-65]

Heat shock protein A (HscA) and Heat shock protein B (HscB) are two co-chaperones that are in the Isc pathway. HscA has ATPase activity and selectively interacts with scaffold IscU and HscB to simulate transfer of Fe-S cluster from IscU to acceptor proteins. HscB facilitates the interaction between HscA and IscU and helps serve as a bridge between the two proteins.[65-68]

1.4 Sulfur Utilization (Suf) pathway

Transcriptional Regulation of Suf pathway. The Suf pathway was first identified as part of the Fur and OxyR regulons in *E. coli*. The *suf* operon encodes *sufABCDSE* . During iron starvation Fur converts to its iron-free (apo) form, which de-represses target promoters and facilitates *suf* repression allowing increased transcription of the suf operon. Oxidative stress activates OxyR, which increases *suf* transcription in conjunction with the DNA-bending protein IHF. IscR, an Fe-S cluster binding transcription factor also regulates the *isc* and *suf* operons. Apo-IscR binds the *suf* promoter to activate

transcription of the *suf* operon in response to oxidative stress, iron limitation, and other conditions that perturb Fe-S cluster biogenesis by the Isc pathway. RyhB a small RNA molecule also regulates the *isc* operon.[69-71] The expression of RyhB is repressed by Fur-Fe^{2+} when iron is replete in the cell. Under limited iron, apo-Fur loses the ability to bind DNA, which releases *ryhB* repression. The *isc* mRNA transcript base pairs with RyhB causing it to be degraded when iron is limited (Figure 1.9).

Deletion of the *suf* pathway in *E. coli* has been shown to be lethal in conditions of iron starvation and oxidative stress.[72]

Suf Pathway biogenesis. In *E. coli* SufA, SufB, SufC, SufD, SufS and SufE form at least two stable complexes $SufBC_2D$ and SufSE. SufS is a PLP-dependent cysteine desulfurase that liberates sulfur from free cysteine molecules resulting in formation of a persulfide. SufE, a structural homolog of IscU, accepts the persulfide and releases it in the form of a reduced sulfide (S^{2-}) to $SufBC_2D$ for cluster assembly (Figure 1.10). The SufS activity has been shown to be enhanced by the action of SufE. This activity has been further shown to be enhanced by $SufBC_2D$. This scaffold has also been shown to be resistant to oxidative stress. This transfer has also be shown to be protected in the presence of reducing agents.[73-74]

SufA appears to function as a cluster transfer protein to move intact Fe-S clusters from $SufBC_2D$ to target metalloproteins. Experimental *in vitro* studies indicate that SufA preferentially binds Free S bound $SufBC_2D$ and that the Fe-S transfer is unidirectional from $SufBC_2D$ to SufA.[75-76] SufA has also been shown to bind Fe. SufB is the scaffold protein of the Suf pathway. It assembles stable [4Fe-4S] and [2Fe-2S] clusters. SufD

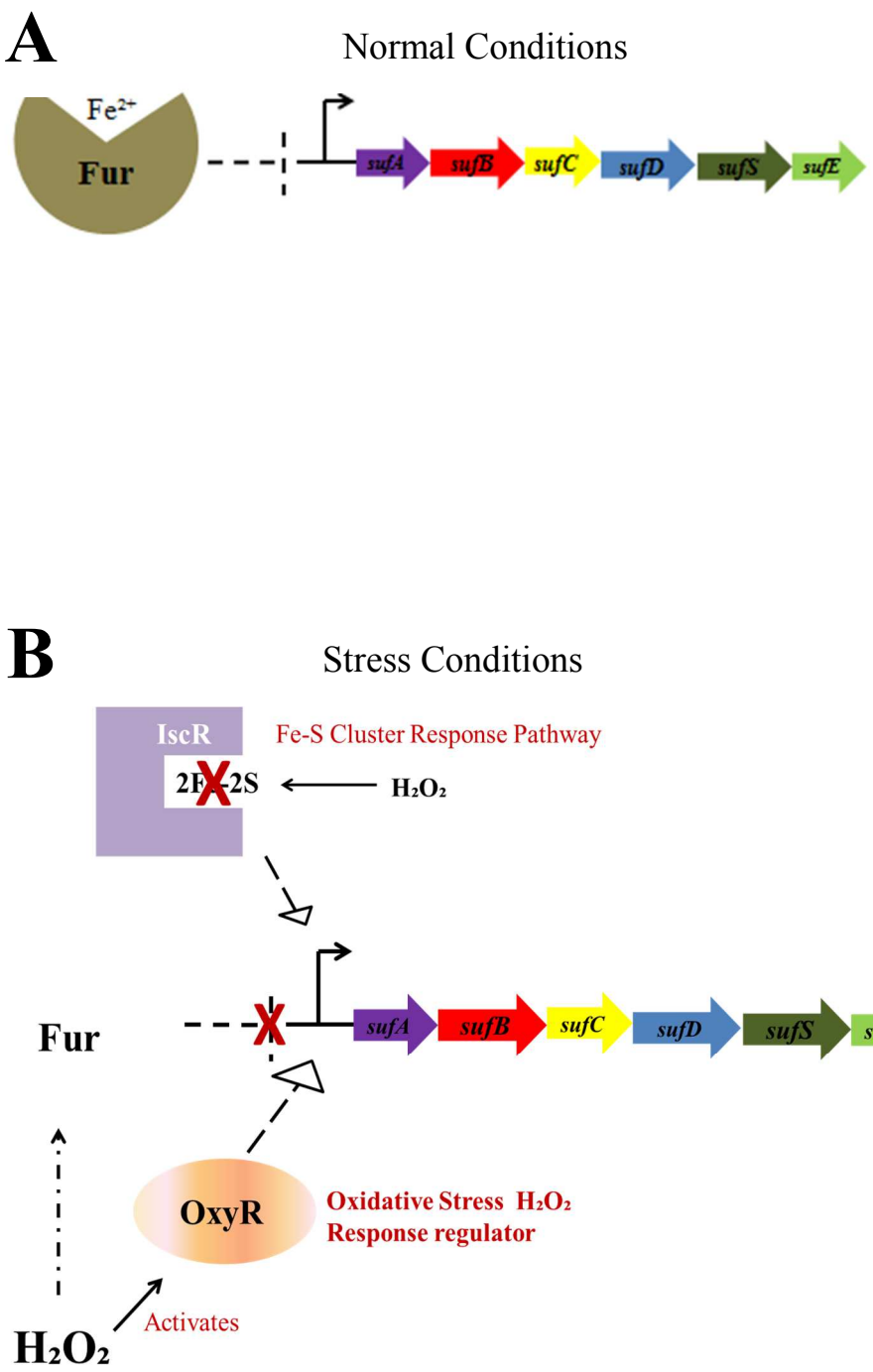

Figure 1.9. Transcriptional regulation of the *suf* operon in *E. coli* under (A) normal and (B) H□O□ stress conditions. (A) Fe^{2+} bound Fur represses *suf* expression under normal growth conditions. (B) H□O□ stress depresses Fur regulation of *suf* and apo-IscR and OxyR activate *suf* expression.

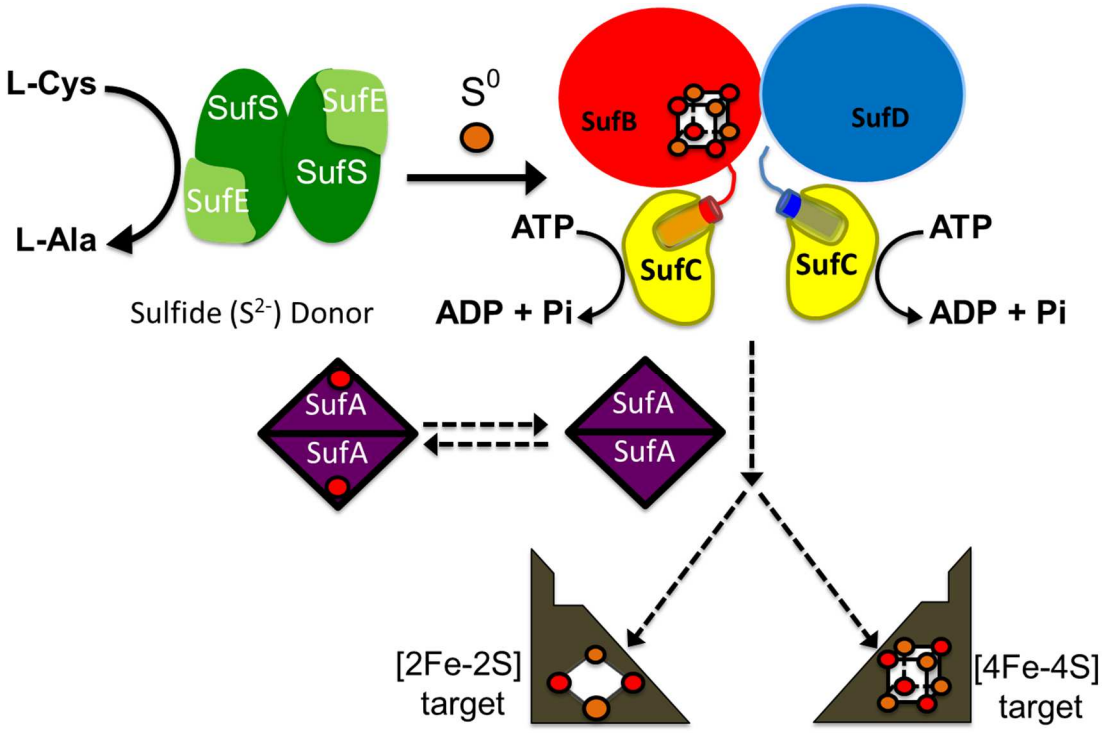

Figure 1.10. Proposed mechanism of *suf* [Fe-S] cluster biogenesis

paralog of SufB and interacts with SufB and SufC (an ATPase) to form a stable $SuBC_2D$ complex. Similar to SufB alone, the $SuBC_2D$ complex reconstitutes a [4e-4S] cluster *in vitro.* Interactions of SufA and SufE have also been shown to be enhanced when SufB is in SufB is in the $SuBC_2D$ complex.[77]

Studies have also shown that the Fe-S clusters assembled on the complex are more resistant to oxidants than the ones assembled on SufB alone. This protected environment provides more evidence for a protected Fe-S cluster assembly process by the Suf Pathway under oxidative stress conditions. In the absence of SufB, SufD has been shown to form a complex with Suf C; $SufC_2D_2$. This is however not been shown to act as a scaffold for Fe-S cluster biogenesis.[77-78]

The source of iron to the suf pathway is still unclear. The labile iron pool may be a source of iron to the pathway but the iron will be susceptible to oxidative stress possibly depleting the labile iron pool. The iron source must therefore be one that is protected under these conditions. A possible source could therefore be a group of iron storage proteins known as ferritins that are conserved across all domains of life.

1.5 Research Aims

A critical gap in the knowledge of Suf function is in the iron donor source. Our hypothesis is the iron would be obtained from a protected source that is resistant to oxidative stress (like the persulfide donation). We decided to test if iron storage proteins could serve as a potential donor. The overall strategy of this project is to identify and characterize mutant strains of *E. coli* where the cellular iron pools are perturbed, and to use genetic and bio-analytical techniques to characterize iron speciation, trafficking, and

regulation in intact cells from these strains. These studies also will determine how loss of iron storage proteins alters iron utilization for iron cofactor biogenesis

It's been proposed that organisms have more than one iron pool in the cell. We have chosen to better define the pools of iron that exist in prokaryotic species beginning with the well-characterized model organism, *E. coli*. We analyzed the iron environment in the MG1655 strains and that lacking the global iron regulator *fur* to determine the differences in the iron speciation and pools.

1.6 Biomedical relevance

Many pathogenic bacteria e.g. *Mycobacterium tuberculosis* only encode the Suf pathway as their iron sulfur cluster assembly machinery. Disruption of this pathway has been proven to be lethal to the pathogens.[79] Fe-S clusters are incorporated into metalloproteins essential to survival of the bacterial cells in the host during infection. Human beings lack the Suf pathway and this makes the Suf pathway an attractive drug target. The aim of our research is therefore to provide a foundation for this drug development.

A number of human diseases, including Friedreich's ataxia and some neurodegenerative disorders, occur as a result of disruption of cellular iron metabolism. Further understanding of the iron pools in cells could therefore lead to a better management of understanding of these diseases.

References

[1] Andrews, S.C., Robinson, A.K. and Rodriguez-Quinones, F. (2003). Bacterial iron homeostasis. *FEMS Microbiol Rev* 27, 215-37.

[2] Touati, D. (2000). Iron and oxidative stress in bacteria. *Arch Biochem Biophys* 373, 1-6.

[3] Winterbourn, C. C. (1995). Toxicity of iron and hydrogen peroxide: the fenton reaction. *Toxicol Lett* 82-83, 969-974.

[4] Gupta, N., Bonomi, F., Kurtz, D.M., Jr., Ravi, N., Wang, D.L. and Huynh, B.H. (1995). Recombinant Desulfovibrio vulgaris rubrerythrin. Isolation and characterization of the diiron domain. *Biochem* 34, 3310-8.

[5] Aisen, P., Leibman, A. and Zweier, J. (1978). Stoichiometric and site characteristics of the binding of iron to human transferrin. *J Biol Chem* 253, 1930-7.

[6] Hall, D.O. and Evans, M.C. (1969). Iron-sulfur proteins. *Nature* 223, 1342-8.

[7] Chen, V.J., Orville, A.M., Harpel, M.R., Frolik, C.A., Surerus, K.K., Munck, E. and Lipscomb, J.D. (1989). Spectroscopic studies of isopenicillin N synthase. A mononuclear nonheme Fe^{2+} oxidase with metal coordination sites for small molecules and substrate. *J Biol Chem* 264, 21677-81.

[8] ImLay, J.A. and Linn, S. (1988). DNA damage and oxygen radical toxicity. *Science* 240, 1302-9.

[9] ImLay, J.A. (2006). Iron-sulfur clusters and the problem with oxygen. *Mol Microbiol* 59, 1073-82.

[10] Boyd, E. S., Thomas, K. M., Dai, Y., Boyd, J. M and Outten, F. W. (2014). Interplay between oxygen and Fe-S cluster biogenesis: insights from the Suf pathway. *Biochem* 53, 5834-5847

[11] Grass, G. (2006). Iron transport in *Escherichia coli*: all has not been said and done. *Biometals* 19, 159-72.

[12] Andrews, S.C. (1998). Iron storage in bacteria. *Adv Microb Physiol* 40, 281-351.

[13] Matzanke, B.F., Anemuller, S., Schunemann, V., Trautwein, A.X. and Hantke, K. (2004). FhuF, part of a siderophore-reductase system. *Biochem* 43, 1386-92.

[14] Hantke, K. (2001). Iron and metal regulation in bacteria. *Curr Opin Microbiol* 4,

172-7.

[15] Carrondo, M.A. (2003). Ferritins, iron uptake and storage from the bacterioferritin viewpoint. *Embo J* 22, 1959-68.

[16] Funk, F., Lenders, J.P., Crichton, R.R. and Schneider, W. (1985). Reductive mobilization of ferritin iron. *Eur J Biochem* 152, 167-72.

[17] Le Brun, N.E., Andrews, S.C., Guest, J.R., Harrison, P.M., Moore, G.R. and Thomson,
A.J.(1995). Identification of the ferroxidase centre of *Escherichia coli* bacterioferritin. *Biochem* J3122 (Pt 2), 385-92.

[18] Yang, X., Le Brun, N.E., Thomson, A.J., Moore, G.R. and Chasteen, N.D. (2000). The iron oxidation and hydrolysis chemistry of *Escherichia coli* bacterioferritin. *Biochem* 39, 4915-23.

[19] Hudson, A.J. et al. (1993). Overproduction, purification and characterization of the *Escherichia coli* ferritin. *Eur J Biochem* 218, 985-95.

[20] Smith, J.L. (2004). The physiological role of ferritin-like compounds in bacteria. *Crit Rev Microbiol* 30, 173-85.

[21] Abdul-Tehrani, H., Hudson, A. J., Chang, Y.S., Timms, A.R., Hawkins, C., Williams, J.M., Harrison, P.M., Guest, J.R. and Andrews, S.C. (1999). Ferritin mutants of *Escherichia coli* are iron deficient and growth impaired, and fur mutants are iron deficient. *J Bacteriol* 181, 1415-28.

[22] McHugh, J.P., Rodriguez-Quinones, F., Abdul-Tehrani, H., Svistunenko, D.A., Poole, R.K., Cooper, C.E. and Andrews, S.C. (2003). Global iron-dependent gene regulation in *Escherichia coli*. A new mechanism for iron homeostasis. *J Biol Chem* 278, 29478-86.

[23] Bereswill, S., Greiner, S., Van Vliet, A.H., Waidner, B., Fassbinder, F., Schiltz, E. (2000). Regulation of ferritin-mediated cytoplasmic iron storage by the ferric uptake regulator homolog (Fur) of Helicobacter pylori. *J Bacteriol* 182, 5948–5953

[24] Masse, E. and Arguin, M. (2005). Ironing out the problem: new mechanisms of iron homeostasis. *Trends Biochem Sci* 30, 462-8.

[25] Masse, E., Escorcia, F.E. and Gottesman, S. (2003). Coupled degradation of a small regulatory RNA and its mRNA targets in *Escherichia coli*. *Genes Dev* 17, 2374-83.

[26] Masse, E., Vanderpool, C.K. and Gottesman, S. (2005). Effect of RyhB small

RNA on global iron use in *Escherichia coli*. *J Bacteriol* 187, 6962-71.

[27] Frolow, F., Kalb, A.J. and Yariv, J. (1993). Location of haem in bacterioferritin of *E. coli*. *Acta Crystallogr D Biol Crystallogr* 49, 597-600

[28] Bradley, J. M., Le Brun, N. E. and Moore, G. (2016). Ferritins, furnishing the cells with iron. *J Biol Inorg Chem* 21, 13-28.

[29] Le Brun, N. E., Crow, A., Murphy, M. E. P., Mauk, A. G. and Moore, G. R. (2010). *Biochim Biophys Acta 1800*, 732-744

[30] Andrews, S. C. (2010). The Ferritin-like superfamily: Evolution of the biological iron storeman from a rubrerythrin-like ancestor, *Biochim Biophys Acta* 1800, 691-705

[31] Trefrey, A., Zhao, Z., Quail, M. A., Guest, J. and Harrison, P. (2009). How the presence of three iron binding sites affects the iron storage function of the ferritin (EcFtnA) of *Escherichia coli*. *FEBS Lett* 432, 231-218

[32] Yao, H., Wang, Y., Lovell, S., Kumar, R., Ruvinsky, A. M., Battaile, K. P., Vakser, I. and Rivera, M. (2012). The structure of the BfrB-Bfd complex reveals protein-protein interactions enabling iron release from bacterioferritin. *J Am Chem Soc* 134, 13470-13481.

[33] Altuvia, S., Almiron, M., Huisman, G., Kolter, R. and Storz, G. (1994). The dps promoter is activated by OxyR during growth and by IHF and sigma S in stationary phase. *Mol Microbiol* 13, 265-72.

[34] Grant, R.A., Filman, D.J., Finkel, S.E., Kolter, R. and Hogle, J.M. (1998). The crystal structure of Dps, a ferritin homolog that binds and protects DNA. *Nat Struct Biol* 5, 294- 303.

[35] Zhao, G., Ceci, P., Ilari, A., Giangiacomo, L., Laue, T.M., Chiancone, E. and Chasteen,
N.D.(2002). Iron and hydrogen peroxide detoxification properties of DNA-binding protein from starved cells. A ferritin-like DNA-binding protein of *Escherichia coli*. *J Biol Chem* 277, 27689-96

[36] Kauko, A., Haataja, S., Pulliainen, A.T., Finne, J. and Papageorgiou, A.C. (2004). Crystal structure of Streptococcus suis Dps-like peroxide resistance protein Dpr: implications for iron incorporation. *J Mol Biol* 338, 547-58.

[37] Jameson, G.N., Jin, W., Krebs, C., Perreira, A.S., Tavares, P., Liu, X., Theil, E.C. and Huynh, B.H. (2002). Stoichiometric production of hydrogen peroxide and parallel formation of ferric multimers through decay of the diferric-peroxo complex, the first detectable intermediate in ferritin mineralization. *Biochem* 41, 13435-43.

[38] Hwang, J., Krebs, C., Huynh, B.H., Edmondson, D.E., Theil, E.C. and Penner-Hahn, J.E. (2000). A short Fe-Fe distance in peroxodiferric ferritin: control of Fe substrate versus cofactor decay? *Science* 287, 122-5.

[39] Moenne-Loccoz, P., Krebs, C., Herlihy, K., Edmondson, D.E., Theil, E.C., Huynh, B.H. and Loehr, T.M. (1999). The ferroxidase reaction of ferritin reveals a diferric mu-1,2 bridging peroxide intermediate in common with other O_2-activating non-heme diiron proteins. *Biochem* 38, 5290-5.

[40] Nandal, A., Huggins, C. O., Woodhall, M. R., McHugh, j., Rodriguez-Quinones, F., Quail, M. A., Guest, j. R., Andrews, S. C. (2010). Induction of the ferritin gene (*ftnA*) of *Escherichia coli* by Fe^{2+} - Fur is mediated by reversal of H-NS silencing and is RyhB independent. *Mol Micro* 75, 637-657

[41] Martinez, A. and Kolter, R. (1997). Protection of DNA during oxidative stress by the nonspecific DNA-binding protein Dps. *J Bacteriol* 179, 5188-94.

[42] Beinert, H., Holm, R.H. and Munck, E. (1997). Iron-sulfur clusters: nature's modular, multipurpose structures. *Science* 277, 653-659.

[43] Johnson, D.C., Dean, D.R., Smith, A.D. and Johnson, M.K. (2005). Structure, function, and formation of biological iron-sulfur clusters. *Annu Rev Biochem* 74, 247-81.

[44] Yoch, D.C. and Carithers, R.P. (1979). Bacterial iron-sulfur proteins. *Microbiol* Rev 43, 384-421.

[45] Moulis, J.M., Davasse, V., Golinelli, M.P., Meyer, J. and Quinkal, I. (1996). The coordination sphere of iron-sulfur clusters: Lessons from site-directed mutagenesis experiments. *J Biol Inorg Chem* 1, 2-14.

[46] Agar, J.N., Krebs, C., Frazzon, J., Huynh, B.H., Dean, D.R. and Johnson, M.K. (2000). IscU as a scaffold for iron-sulfur cluster biosynthesis: sequential assembly of [2Fe-2S] and [4Fe-4S] clusters in IscU. *Biochem* 39, 7856-62.

[47] Zheng, L., Cash, V.L., Flint, D.H. and Dean, D.R. (1998). Assembly of iron-sulfur clusters. Identification of an *iscSUA-hscBA-fdx* gene cluster from *Azotobacter vinelandii*. *J Biol Chem* 273, 13264-72.

[48] Kennedy, M.C., Kent, T.A., Emptage, M., Merkle, H., Beinert, H. and Munck, E. (1984). Evidence for the formation of a linear [3Fe-4S] cluster in partially unfolded aconitase. *J Biol Chem* 259, 14463-71.

[49] Johnson, M.K. (1998). Iron-sulfur proteins: new roles for old clusters. *Curr Opin Chem Biol* 2, 173-181.

[50] ImLay, J.A. (2006). Iron-sulfur clusters and the problem with oxygen. *Mol Microbiol* 59, 1073-82.

[51] Djaman, O., Outten, F.W. and ImLay, J.A. (2004). Repair of oxidized iron-sulfur clusters in *Escherichia coli*. *J Biol Chem* 279, 44590-9.

[52] Blanc, B., Clemancey, M., Latour, J.-M., Fontecave, M., and de Choudens, S. O. (2014) Molecular investigation of iron sulfur cluster assembly scaffolds under stress, *Biochem* 53, 7867-7869.

[53] Outten, F.W., Djaman, O. and Storz, G. (2004). A suf operon requirement for Fe-S cluster assembly during iron starvation in Escherichia coli. *Mol Microbiol* 52, 861-72.

[54] Lee, J.H., Yeo, W.S. and Roe, J.H. (2004). Induction of the *sufA* operon encoding Fe-S assembly proteins by superoxide generators and hydrogen peroxide: involvement of OxyR, IHF and an unidentified oxidant-responsive factor. *Mol Microbiol* 51, 1745-55.

[55] Takahashi, Y. and Tokumoto, U. (2002). A third bacterial system for the assembly of iron-sulfur clusters with homologs in Achaea and Plastids. *J Biol Chem* 277, 28380-3.

[56] Blanc, B., Clemancey, M., Latour, J.-M., Fontecave, M., and de Choudens, S. O. (2014). Molecular investigation of iron sulfur cluster assembly scaffolds under stress. *Biochem* 53, 7867-7869.

[57] Dai, Y., and Outten, F. W. (2012). The *E. coli* SufS-SufE sulfur transfer system is more resistant to oxidative stress than IscS-IscU. *FEBS Lett 586*, 4016-4022.

[58] Jang, S., and ImLay, J. A. (2010). Hydrogen peroxide inactivates the *Escherichia coli* Isc iron-sulfur assembly system, and OxyR induces the Suf system to compensate. *Mol Microbiol 78*, 1448-1467.

[59] Mettert, E. L., and Kiley, P. J. (2014). Coordinate regulation of the Suf and Isc Fe-S cluster biogenesis pathways by IscR is essential for viability of *Escherichia coli*. *J Bacteriol 196*, 4315-4323.

[60] Zheng, L., Cash, V.L., Flint, D.H. and Dean, D.R. (1998). Assembly of iron-sulfur clusters. Identification of an *iscSUA-hscBA-fdx* gene cluster from *Azotobacter vinelandii*. *J Biol Chem* 273, 13264-72.

[61] Ding, H., Clark, R.J. and Ding, B. (2004). IscA mediates iron delivery for assembly of iron-sulfur clusters in IscU under the limited accessible free iron conditions. *J Biol Chem* 279, 37499-37504.

[62] Ding, H. and Clark, R.J. (2004). Characterization of iron binding in IscA, an ancient iron- sulfur cluster assembly protein. *J Biochem* 379, 433-40.

[63] Ding, H., Yang, J., Coleman, L.C. and Yeung, S. (2007). Distinct Iron Binding Property of Two Putative Iron Donors for the Iron-Sulfur Cluster Assembly: IscA and the bacterial frataxin orthologue CyaY under physiological and oxidative stress conditions. *J Biol Chem 282, 7997-8004.*

[64] Li, D.S., Ohshima, K., Jiralerspong, S., Bojanowski, M.W. and Pandolfo, M. (1999). Knock-out of the *cyaY* gene in *Escherichia coli* does not affect cellular iron content and sensitivity to oxidants. *FEBS Lett* 456, 13-6.

[65] Bou-Abdallah, F., Adinolfi, S., Pastore, A., Laue, T.M. and Dennis Chasteen, N. (2004). Iron Binding and Oxidation Kinetics in Frataxin CyaY of *Escherichia coli. J Mol Biol* 341, 605-15.

[66] Hoff, K.G., Silberg, J.J. and Vickery, L.E. (2000). Interaction of the iron-sulfur cluster assembly protein IscU with the Hsc66/Hsc20 molecular chaperone system of Escherichia coli. *Proc Natl Acad Sci USA* 97, 7790-5.

[67] Silberg, J.J., Tapley, T.L., Hoff, K.G. and Vickery, L.E. (2004). Regulation of the HscA ATPase reaction cycle by the co-chaperone HscB and the iron-sulfur cluster assembly protein IscU. *J Biol Chem* 279, 53924-31.

[68] Chandramouli, K. and Johnson, M.K. (2006). HscA and HscB stimulate [2Fe-2S] cluster transfer from IscU to apoferredoxin in an ATP-dependent reaction. *Biochem* 45, 11087-95.

[69] Lee, J.H., Yeo, W.S. and Roe, J.H. (2004). Induction of the sufA operon encoding Fe-S assembly proteins by superoxide generators and hydrogen peroxide: involvement of OxyR, IHF and an unidentified oxidant-responsive factor. *Mol Microbiol* 51, 1745-55.

[70] Jang, S., and ImLay, J. A. (2010). Hydrogen peroxide inactivates the *Escherichia coli* Isc iron-sulfur assembly system, and OxyR induces the Suf system to compensate, *Mol Microbiol 78*, 1448-1467.

[71] Mettert, E. L., and Kiley, P. J. (2014). Coordinate regulation of the Suf and Isc Fe-S cluster biogenesis pathways by IscR is essential for viability of *Escherichia coli*. *J Bacteriol* 196, 4315-4323.

[72] Outten, F. W., Djaman, O., and Storz, G. (2004). A suf operon requirement for Fe-S cluster assembly during iron starvation in *Escherichia coli*. *Mol Microbiol 52*, 861-872.

[73] Boyd, E. S., Thomas, K. M., Dai, Y., Boyd, J. M and Outten, F. W. (2014).

Interplay between oxygen and Fe-S cluster biogenesis: insights from the Suf pathway. *Biochem* 53, 5834-5847.

[74] Dai, Y., and Outten, F. W. (2012). The *E. coli* SufS-SufE sulfur transfer system is more resistant to oxidative stress than IscS-IscU. *FEBS Lett 586*, 4016-4022.

[75] Ollagnier-de-Choudens, S., Mattioli, T., Takahashi, Y. and Fontecave, M. (2001). Iron- sulfur cluster assembly: characterization of IscA and evidence for a specific and functional complex with ferredoxin. *J Biol Chem* 276, 22604-7.

[76] Gupta, V., Sendra, M., Naik, S.G., Chahal, H.K., Huynh, B.H., Outten, F.W., Fontecave, M. and Ollagnier de Choudens, S. (2009). Native *Escherichia coli* SufA, coexpressed with SufBCDSE, purifies as a [2Fe-2S] protein and acts as an Fe-S transporter to Fe-S target enzymes. *J Am Chem Soc* 131, 6149-53.

[77] Saini, A., Mapolelo, D. T., Chahal, H. K., Johnson, M. K., and Outten, F. W. (2010). SufD and SufC ATPase activity are required for iron acquisition during in vivo Fe-S cluster formation on SufB. *Biochem 49*, 9402-9412.

[78] Petrovic, A., Davis, C. T., Rangvhari, K., Clough, B., Wilson, R. J. and Eccleston, J. F. (2008). Hydrodynamic characterization of the SufBC and SufCD complexes and their interaction with fluorescent adenosine nucleotides. *Protein Sci* 17, 1264-1274.

[79] Huet, G., Castain, J. P., Fournier, D., Daffe, M. and Saves, I. (2006). Protein splicing of SufB is crucial for the functionality of the *Mycobacterium tuberculosis* SUF machinery. *J Bacteriol* 188, 3412-3414.

CHAPTER TWO
Bfr and Dps may serve as iron donors to the Suf pathway

Abstract

Iron is an essential transition metal required by almost all organisms for use as a cofactor in many metabolic processes such as respiration and photosynthesis. Iron can be combined with elemental sulfur to form an iron-sulfur (Fe-S) cluster. In bacterial pathogens, Fe-S cluster cofactors carry out critical functions and the Fe-S cluster biogenesis pathway is essential for their survival. In *E. coli,* the Suf pathway assembles Fe-S clusters under conditions of iron starvation and oxidative stress. There has been considerable characterization of the sulfide donation to the *suf* Fe-S pathway; however, the process of *in vivo* iron donation remains unclear. Iron storage proteins generally known as ferritins are capable of storing iron in a readily available and soluble form to serve as a reservoir of iron for metabolism. We investigate if these iron storage proteins can be *in vivo* iron donors for Suf Fe-S cluster assembly in *E. coli*. We establish that the bacterioferritin (Bfr) and DNA binding protein of starved cells (Dps) may play a role in the *in vivo* donation. Our results also indicate the ferritin A (FtnA) protein does not play a role in this iron donation.

2.1 Introduction

Iron is a key cofactor for metalloproteins that perform essential roles in important metabolic processes such as electron transport, oxygen transport and oxygen storage. In vivo iron levels have to be regulated carefully because excessive or loosely chelated ferrous ion may lead to production of hydroxyl radicals from hydrogen peroxide through the Fenton reaction**.** The cell therefore has specialized proteins for the storage and trafficking of iron to limit the release of ferrous iron into the cytoplasm.[1-3]

Three main types of iron storage proteins have been found in bacteria. They are the ferritins (Ftns), the heme-containing bacterioferritins (Bfr), and the DNA binding protein of starved cells (Dps). These have all been determined to play a role in iron homeostasis in bacteria.[4] These all belong to a broad family of ferritins and generally share similar physical characteristics. Their multimeric quaternary structure occurs in 2 sizes: 24 subunits and 12 subunits and they possess catalytic sites known as ferroxidase centers located either within the individual subunits (FtnA and Bfr) or at the interface of adjacent subunits (Dps). The subunits assemble into a spherical protein shell and the ferroxidase centers are located in the inner surface of the protein shell. These ferroxidase centers oxidize soluble ferrous ions to ferrihydrite mineral and that it is the form in which the ferric iron that is stored in these proteins.[5,6] FtnA, coded by *ftnA* and Bfr coded by *bfr* are larger proteins and have 24 subunits that can accommodate up to 4,500 iron atoms. Also associated with Bfr is Bacterioferritin-associated ferrodoxin Bfd, coded by *bfd.* Bfd facilitates release of iron from Bfr. Dps coded by *dps* is a mini-ferritin comprising 12 subunits and can accommodate about 500 iron atoms.[7,8]

In *E. coli,* FtnA has been shown to be involved in the storage of iron during

stationary phase and release of iron during iron starved conditions. Bfr has also been implicated as the main iron storage protein in other microorganisms but its role remains uncertain in *E. coli*. In *E. coli*, under iron-replete conditions such as in rich media, about 25% of the total iron isolated in the soluble protein fraction is found in FtnA, Bfr, and to a lesser extent Dps.[8] Under high iron conditions the amount of iron specifically associated with FtnA increases 10-fold while that sequestered in Bfr and Dps remains constant. Based on these results FtnA is thought to be the primary storage protein for excess iron in *E. coli*. Dps has the additional ability to bind and physically sequester DNA, possibly to limit oxidative DNA cleavage caused by the toxic products of the Fenton reaction. Dps binds chromosomal DNA non-specifically, forming a highly ordered and stable dps-DNA co-crystal within which chromosomal DNA is condensed and protected from diverse damages in stationary phase.[9-12]

Iron-sulfur (Fe-S) clusters are critical iron co-factors that are used to carry out important metabolic processes in a cell. These Fe-S cluster proteins are widely distributed in nature and can be found in all kingdoms of life.[13] Examples of these Fe-S proteins include enzymes of the electron transport chain such as NADH dehydrogenase and coenzyme Q – cytochrome c reductase. The most common forms of Fe-S clusters are the rhombic [2Fe-2S] and the cubic [4Fe-4S] clusters.[13]

Fe-S clusters must be carefully assembled in vivo because they are sensitive to reactive oxygen species.[14] Oxidation and degradation of the cluster also releases free ferrous iron and sulfide that are toxic to the cell. Fe-S cluster biogenesis pathways have a common set of core components. Each pathway consists of a cysteine desulfurase, that donates sulfide to the pathway, and a scaffold protein on which transient clusters are assembled and

transferred to apo proteins. The Isc pathway is the main Fe-S assembly pathway in *E. coli* under normal conditions.[14] The *isc* operon is composed of eight genes, *iscR-iscS-iscU-iscA-hscB-hscA-fdx-iscX*. IscR is a transcriptional regulator of the Isc pathway, IscS is the cysteine desulfurase, IscU is a Fe-S cluster scaffold protein, IscA is a Fe-S cluster carrier protein, HscA and HscB are molecular chaperones, and Fdx is a ferredoxin that likely provides electrons for some step in cluster assembly or trafficking. IscX is a protein whose function has not been clearly elucidated but may play a role as a regulator of cysteine desulfurase activity.[15-16]

The Suf pathway in *E. coli* is the Fe-S cluster biogenesis pathway during environmental stress which includes oxidative stress and iron limited environments.[17] The sulfur donation to the scaffold assembly complex and the Fe-S cluster on the scaffold has been proven to be resistant to oxidative stress.[18] The iron donation step which hasn't been discovered may also be from a source resistant to oxidative stress, metal poisoning and iron starvation.

Our hypothesis is that iron could be donated from one of the aforementioned iron storage proteins to the Suf pathway. In this study, we characterize the relative roles of the three main ferritin proteins as possible iron donor sources to the Suf Fe-S cluster biogenesis pathway. To test whether the Suf system directly or indirectly accesses iron from one or more iron storage proteins *in vivo*, we constructed a mutant strain with the Isc housekeeping pathway inactivated. This mutation ensured that the strain was completely dependent on the Suf pathway for its Fe-S cluster biogenesis. Various mutants were then constructed by further deleting iron storage proteins either individually or in combination in this Isc inactivated background. Our results show that

bacterioferritin (Bfr) and DNA binding protein of starved cells (Dps) may play a role in the *in vivo* donation to the Suf pathway.

2.2 Materials and Methods

Growth medium and conditions. For bacterial growth, an individual colony was transferred from fresh Lennox Broth (LB) agar plates into either LB media or M9 glucose minimal media containing 1X M9 minimal salts (Sigma-Aldrich), 0.2% (w/v) glucose (Acros Organics), 0.2% (w/v) magnesium chloride (Sigma-Aldrich) and 0.1mM calcium chloride (Sigma-Aldrich). Cultures were grown in LB or M9 minimal media for 18hours and 24 hours respectively at 37°C and 200rpm. When necessary, kanamycin (30µg/mL) or chloramphenicol (25 µg / mL) was added to the media. For cells grown under various iron conditions, different concentrations of ferric citrate were added to the 0.2% glucose M9 minimal media. For cell growth curves, the cell growth was monitored by UV-Vis absorption at 600nm and plotted versus time in hours. For sensitivity assays, the cells were collected, washed in sterile 1 X M9 minimal salts and normalized to a final OD_{600} of 0.04 in M9 minimal media with 0.2% (w/v) gluconate (Alfa Aesar) containing varying amounts of 2,2-bipyridyl (BIPY) or Phenazine Methosulfate (PMS). Cell density (final optical density at 600nm) was measured after 24-hr growth at 37 °C and assays were performed in triplicate.

ICP-MS Analysis*:* Preparatory cell growth in LB and glucose minimal media was conducted as described above. Cells were collected, washed and normalized to a final OD_{600} of 0.04 and grown in gluconate minimal media until they reached the desired growth phase. Cells were harvested, centrifuged at 4000 x g for 20 mins and then pelleted three times at 16,000 x g with intermediate washing in ICP-MS wash solution

consisting of 50mM EDTA tetrasodium salt, 100mm Sodium Oxalate, 300 mM NaCl and 10 mM KCl to remove any cell surface associated metal ions. Washed cell pellets were re-suspended in 1 mL 3% NaCl. The OD_{600} and volume of the cell suspension after the last wash was recorded. The re-suspended cells were transferred to an acid-washed, Perfluoroalkoxy (PFA) centrifuge tube (Savillex Corporaion) and centrifuged at 16,000 x g. After centrifugation, the supernatant was discarded and the cell pellets were frozen in liquid nitrogen. Cell pellets were stored at -80□C until ready for digestion and ICP-MS analysis.

For analysis, cells were thawed for 15 min on ice, and then dried at 80 C for 30 min. The pellet was then resuspended in 0.3 mL of trace metal grade ultra-pure nitric acid and incubated at 70 C for 10hours. 250 µL of the digested solution was transferred to an acid washed, 15-mL Trace Metal Grade VWR Falcon Tube and diluted to 5 mL with milli-Q H_2O to give a final sample solution with an HNO_3 matrix of 3.5% before analysis using the High Resolution Inductively Coupled Plasma Mass Spectrometer. Blanks consisting of 3.5% trace-metal grade HNO_3 only in MQ H_2O were simultaneously prepared in the same way as the samples. Samples were analyzed on a Thermo Element 2 High Resolution ICP-MS instrument operated by CEMS at the University of South Carolina. A cyclonic spray chamber (Elemental Scientific) was used for delivery of sample into the instrument.

Whole cell EPR spectroscopy: A protocol was adapted from the ImLay and Kiley Labs[19]. Cells were grown overnight aerobically in 250 mL of LB before harvesting by centrifugation. Cells were collected by centrifugation at 8,000 x g for 20 min at 4°C. The pellet was re-suspended using 10 mL of pre-warmed M9 gluconate media supplemented

with 10 mM diethylenetriaminepentaacetic acid (DTPA) (Sigma-Aldrich), 20 mM desferrioxamine mesylate salt (DFO) (CalBiochem) and incubated for 10 min at 37 °C at 200 rpm in a 250-mL flask for proper oxygenation. The cells were then centrifuged, washed with cold 20 mM Tris-HCl, pH 7.4 and re-suspended in a final volume of 0.5 volumes (relative to the pellet volume) of 20 mM Tris-HCl, pH 7.4, 30% glycerol to give a final glycerol concentration of approximately 10-15%. A 300-µL volume of the re-suspended cells was loaded into a 3-mm quartz EPR tube (Norell Incorporated, NC) and immediately frozen in liquid N_2. A sample of each cell suspension was diluted 200x to obtain a final OD_{600}. Samples were stored in liquid N_2 until EPR measurements were performed. Ferric-DFO standards were prepared over a range from 0 µm to 100 µm $FeCl_3$ in 20 mM Tris-HCl, 1 mM DFO, 10% glycerol, pH 7.4. The EPR signals were measured with a Bruker EMX X-band spectrometer (Rheinstetten, Germany). EPR parameters used were as follows: centerfield: 1564 G; sweep width: 500 G; Temp: 110K, Modulation frequency: 100 KHz, Modulation amplitude: 12.5 Gauss, Modulation phase: 0, Harmonic: 1, Receiver gain: 60, Time constant: 20.4 ms, Field: 301.25-2801.25 Gauss, g factor: 4.3, Attenuation: 16, Power: 5mW, number of scans, 10. Fe levels were quantified by normalizing the amplitude of the Fe signal of the samples to the Fe-DFO standards, and internal concentrations were calculated using the cell density and intracellular volume.

Western Blot Analysis: Cells were prepared as described above and pelleted at 6,000 x g for 20 mins. The pellets were lysed by sonicator or Bacterial Protein Extraction Reagent (B-PER) (ThermoScientific) and the protein concentration checked using the Bradford assay. Equal total protein amounts were electrophoresed on a 15% SDS PAGE

gel. Proteins were transferred to nitrocellulose membrane and blocked overnight with 80% Odyssey blocking buffer (Li-Cor) in 1 X TBS (50 mM Tris-HCl pH 8.0, 150 mM NaCl) at 4□C. Primary antibody incubations with α-SufD (1:5000), α-Bfr (1:1000), or α-FtnA (1:2000) were performed in 40% blocking buffer in 1 X TBST (TBS + 0.001% Tween-20). After 2 hours incubation at room temperature with shaking, membranes were washed 5 times (10 min each) with copious amounts of 1 X TBST. Then they were incubated with goat α-rabbit secondary antibody (1:20,000) at room temperature with shaking for 45 min. Membranes were washed with 1 X TBS and scanned using an Odyssey Infrared Imager (Li-Cor).

Primer extension assay: RNA was extracted from MG1655 and the mutant strains by using the acid phenol method. The *fepA* primer was labeled by [γ-^{32}P] ATP using T4 polynucleotide kinase (NEB). Primer extension with Superscript II reverse transcriptase (Invitrogen) was carried out according to manufacturer instructions. 8 µg of total RNA was used as a template for cDNA synthesis. The cDNA products were separated on an 8% polyacrimide gel. The gel was dried and exposed to CL-XPosure film (ThermoScientific).

Mössbauer Analysis: Cells were initially grown in 35 mL M9 glucose minimal media for 24 hours at 37 C at 200 rpm. The overnight culture was then used to inoculate a 1 L M9 glucose minimal media supplemented with 10µM and 100 µM ^{57}Fe (III) citrate. 10 mM ^{57}Fe(III) citrate stock solution was prepared by dissolving 100 mg ^{57}Fe metal powder (IsoFlex USA) in 2 mL minimal amount aqua regia which is a 3:1 mixture of trace metal grade nitric acid (TMG) to trace metal grade hydrochloric acid (Fischer Scientific) while stirring. Once dissolved, the solution was further diluted to a final volume of 100 mL.

This stock was then treated with a 3-fold molar excess of sodium citrate (Fisher Scientific) while stirring. The solution was adjusted to pH 5 with 1 M NaOH (EMD Chemicals) resulting in a final ^{57}Fe concentration of 10 mM. Cells were grown to desired growth phase, harvested and centrifuged at 6,000 x g for 20 min. The pellet was washed in 40 mL wash solution comprising 50 mM EDTA tetrasodium salt, 100 mM Sodium Oxalate, 300 mM NaCl, 10 mM KCl and centrifuged for at 4,000 x g for 20min. The wash solution was fully removed from the pellet, washed with MilliQ water, packed into Mössbauer cups and immediately frozen in liquid nitrogen prior to analysis.

Mössbauer spectra were collected at the Texas A&M and analyzed in the Dr. Paul Lindahl lab by Joshua Wofford. Mössbauer spectra were recorded on MS4 WRC 4.5 to 300 K closed-cycle Helium-refrigerated system and a W106 temperature controller) and LHe6T spectrometers (SEE Co., Edina, MN), the latter of which is capable of generating 0–6 T fields. Both were calibrated using α-Fe foil. Spectra was analyzed at 5K and 0.05T and the resulting spectra were fitted over different iron species including Non-Heme Fe (II), Non Heme Fe (III) and Low Heme Fe fits.

Atomic Absorption Spectroscopy. Intracellular iron content was calculated using atomic absorption spectroscopy (AAS). Cells were grown to desired growth phase in M9 minimal media and harvested, centrifuged at 4000 x g for 20 min and then pelleted three times at 16,000 x g with intermediate washing in ICP-MS wash solution consisting of 50 mM EDTA tetrasodium salt, 100mm Sodium Oxalate, 300 mM NaCl and 10 mM KCl to remove any cell surface associated metal ions. Washed cell pellets were re-suspended in 1 mL 3% NaCl. The OD_{600} and volume of the cell suspension after the last wash was recorded. Cells digested in 300 µL concentrated nitric acid for 10 hours at 70°C and

diluted to get an avid matrix of 3.5% in MilliQ water. Iron standards were prepared in MilliQ water. Iron analysis of fractions was performed on a PerkinElmer PinAACle 900T graphite furnace atomic absorption spectrometer using the manufacturer's recommended conditions.

2.3 Results

Bfr and Dps may act as iron sources to the Suf Pathway during stress conditions. To test if any of the ferritins could donate iron to the Suf pathway we first had to construct a strain that was wholly dependent on the Suf pathway both during normal housekeeping and stress conditions. To do this, we selectively deleted part of the Isc pathway to create the Δ*iscU-fdx* strain (Figure 2.1). The parent Δ*iscU-fdx* strain thus retains *iscR* which is a global regulator of Fe-S cluster assembly and *iscS* which donates sulfur to other metabolic pathways (Figure 2.1). In this strain, Fe-S cluster assembly by Isc is therefore disrupted. In this parent strain, we then deleted individual ferritins alone or in combination (Table 2.1).

We first checked the growths of the mutants in the absence of stress in two types of media broth, the complex media Lennox Broth (LB) and the chemically defined M9 glucose minimal media. LB is a rich, iron replete complex media containing several carbon sources and optimal levels of small molecule metabolites (i.e. amino acids) required for proper cellular growth and metabolism.[20] In contrast, M9 minimal media is a media that is limited for most nutrients and metals. Compared to LB, it lacks its various rich nutrients and amino acids and only provides a single, controlled carbon source to support growth. Minimal media therefore allows a greater control over which nutrients and metals the cells are exposed to.

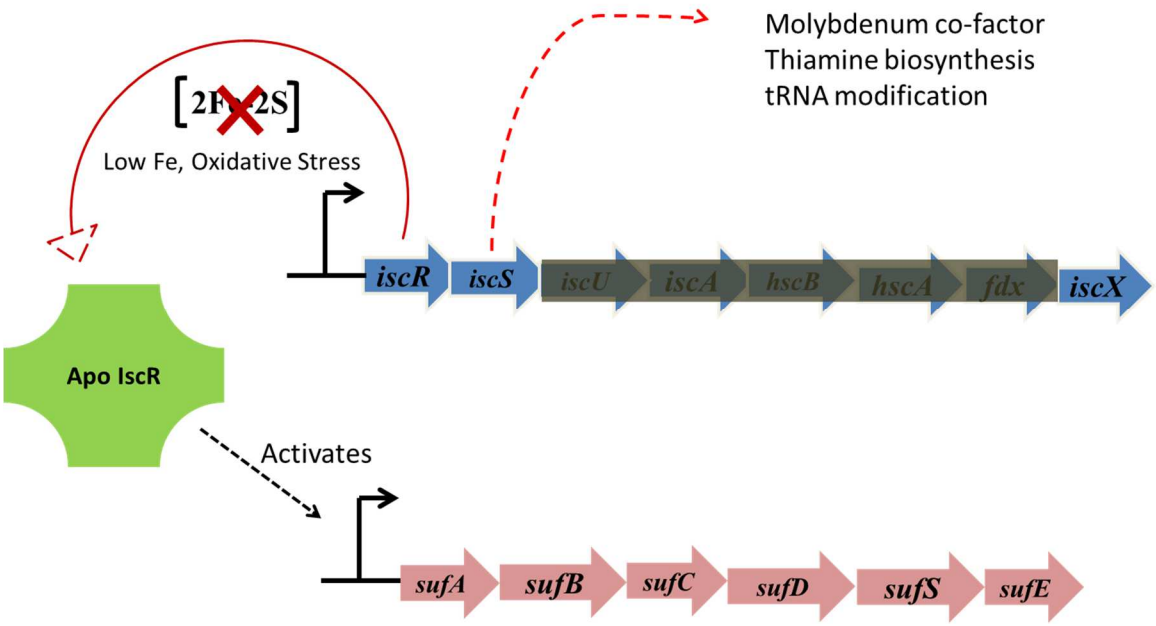

Figure 2.1. The parent Δ*iscU-fdx* strain. In this strain, all the genes in the genome from *iscU* to *fdx* have been deleted, effectively rendering the Isc pathway null. *iscR* is a transcriptional regulator for Suf pathway as its apo form (without [2Fe-2S] cluster) activates Suf transcription. *iscS* has also not been deleted because it serves as a substrate for other important cellular functions e.g. Molybdenum cofactor synthesis.

Table 2.1 Bacterial Strains utilized in this study

Strain	Relevant Genotype Or Phenotype	Reference or Source
E. coli Strains		
MG1655	Wild Type. *E. coli,* K12	Laboratory Strain
Δ*iscU-fdx*	Δ*iscU-fdx*	Laboratory Strain
Δ*sufA-E*	Δ*sufA-E*	Laboratory Strain
Δ*iscU-fdx*_Δ*bfr::kan*^{R}	Δ*iscU-fdx*_Δ*bfr::kan*^{R}	This Study (R. Drevelland unpublished)
Δ*iscU-fdx*_Δ*dps::cm*^{R}	Δ*iscU-fdx*_Δ*dps::cm*^{R}	This Study (R. Drevelland unpublished)
Δ*iscU-fdx*_Δ*ftnA::kan*^{R}	Δ*iscU-fdx*_Δ*ftnA::kan*^{R}	This Study (R. Drevelland unpublished)
BN001	Δ*iscU-fdx*_Δ*bfr::kan*^{R}_Δ*dps::cm*^{R}	This Study
BN002	Δ*iscU-fdx*_Δ*bfr::kan*^{R}_Δ*ftnA::cm*^{R}	This Study
BN003	Δ*iscU-fdx*_Δ*ftnA::kan*^{R}_Δ*dps::cm*^{R}	This Study
BN004	Δ*iscU-fdx*_Δ*ftnA*_Δ*dps*_Δ*bfr::kan*^{R}	This Study
BN005	Δ*bfr::kan*^{R}_Δ*dps::cm*^{R}	This Study
Δ*fur::kan*^{R}	Δ*fur::kan*^{R}	Laboratory Strain

To test whether disruption of iron storage proteins affects sensitivity to iron deprivation, varying concentrations of the cell permeable iron chelator 2,2-bipyridyl (BIPY) were added to the growth media and the final optical density measured after 24 hours of growth in M9 gluconate minimal media. Growth on M9 gluconate minimal media occurs via the Entner-Duodoroff pathway that requires phosphogluconate dehydratase (Edd) which has a [4Fe-4S] cluster.[21] Disruption of Suf Fe-S cluster biogenesis in the Δ*iscU-fdx* strains will therefore result in that mutant being sensitive to environmental stress in M9 gluconate media. None of the mutations were lethal.

Individual Δ*iscU-fdx* strains with only single mutations of *bfr*, *dps* or *ftnA*, did not show a marked difference in their sensitivity compared to the MG1655 (wild type) and parent Δ*iscU-fdx* strains (Figure 2.2). As a control, the Δ*sufA-E* strain where the entire *suf* operon is deleted was included. This strain has been previously shown to be sensitive to iron starvation and oxidative stress conditions.[17]

Next, we tested if combinations of iron storage mutations would lead to disruption of Suf function in the Δ*iscU-fdx* mutant background. We observed that the Δ*iscU-fdx*Δ*bfr*Δ*dps* strain had an extended lag phase compared to the wild-type when pre-grown in LB media and transferred to the M9 minimal media even in the absence of stress (Figure 2.3) although it grew to a comparable final cell density (Figure 2.3). This extended lag phase was reduced by 50% from 8 hours to 4 hours when the Δ*iscU-fdx* Δ*bfr* Δ*dps* strain was pre-grown in M9 glucose minimal media and transferred to M9 gluconate minimal media (Figure 2.4). Although this lag phase got reduced in the M9 minimal media, it was still longer than both the wild-type strain and parent Δ*iscU-fdx* strain.

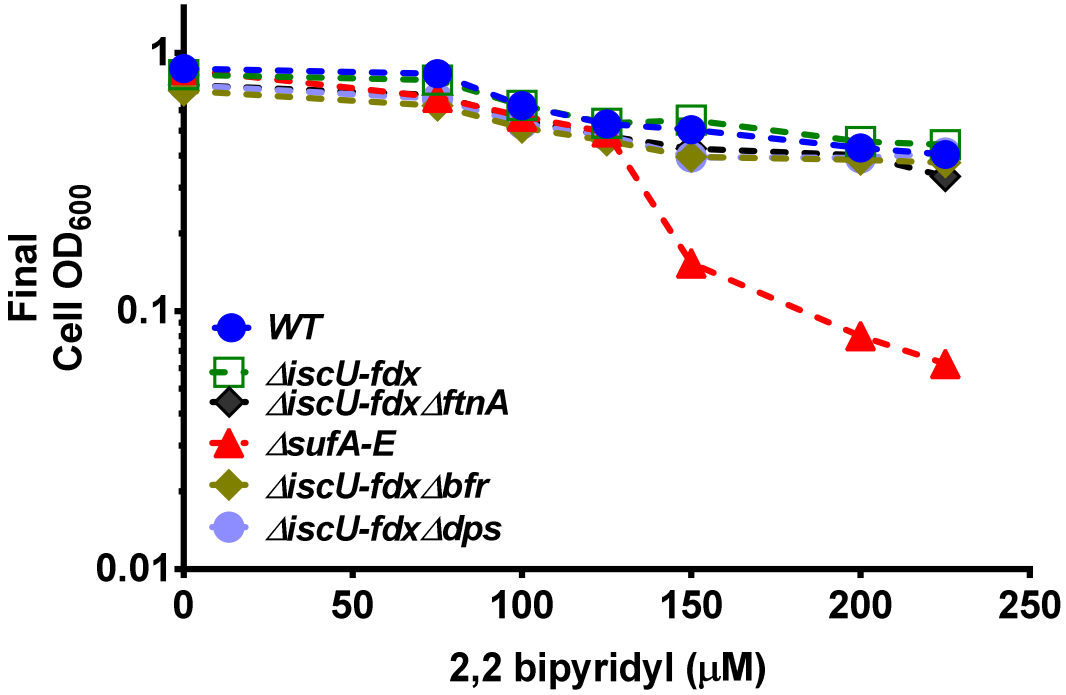

Figure 2.2. Deletion of individual ferritins in the parent Δ*iscU-fdx* strain does not make it sensitive to bipyridyl stress. All strains were grown in LB for 18 hours. After this, they were washed and inoculated into fresh M9 gluconate minimal media with varying concentrations of BIPY. The final cell density was measured after 24 hours. All growths were repeated in triplicate (n=3) and error bars indicate one standard deviation from the mean value.

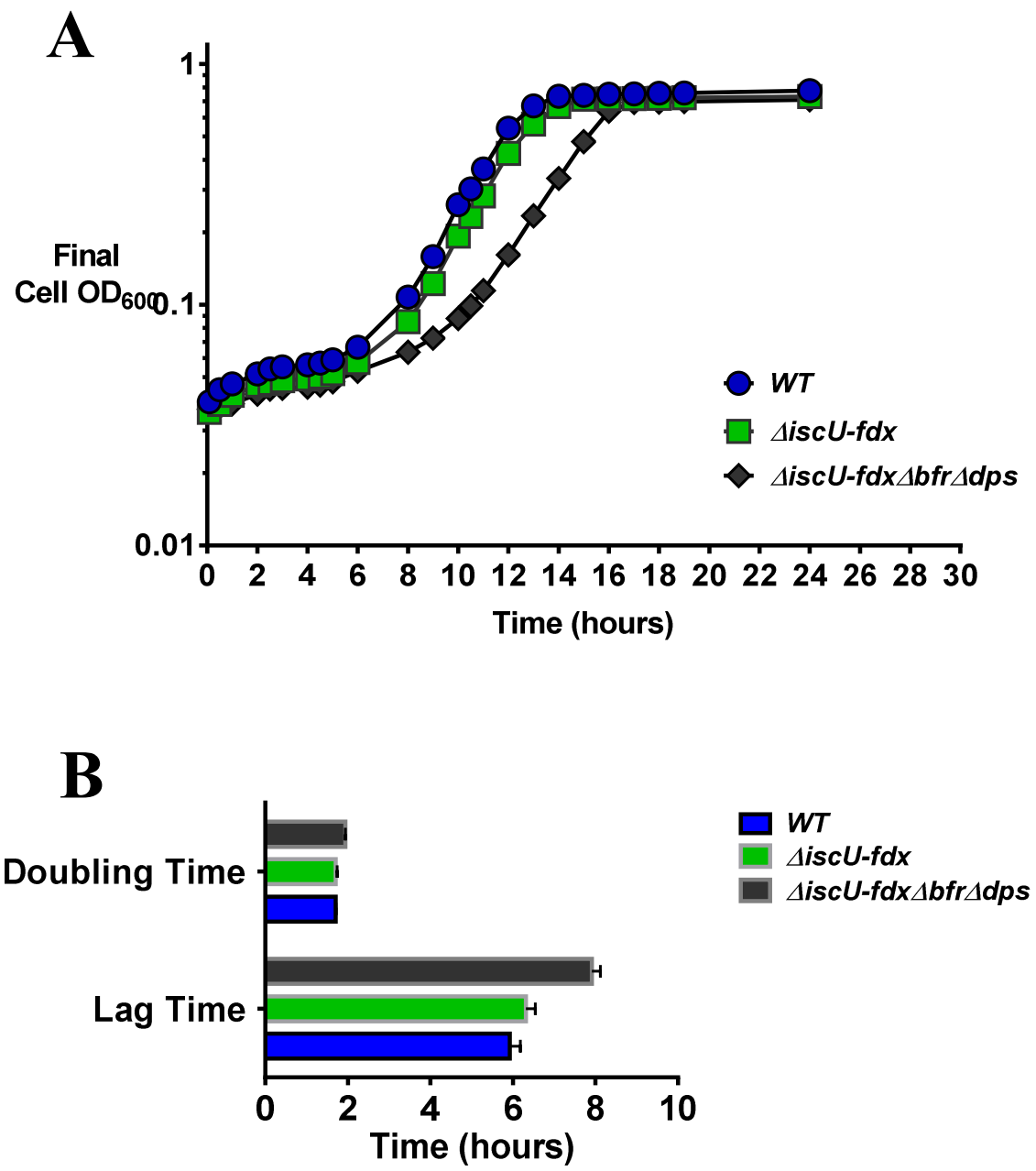

Figure 2.3. The Δ*iscU-fdx*Δ*bfr*Δ*dps* strain shows an extended increase in lag phase duration when pre-grown in LB media with no stress. (A) All strains were grown in LB for 18 hours and then washed and normalized to the same starting OD_{600} in fresh M9 glucose minimal media for 24 hours. Cell density was measured initially every 30 mins until they exited lag phase, and then hourly. All growths were repeated in triplicate (n=3) and error bars indicate one standard deviation from the mean value. (B) Lag phase and doubling time calculated from growth curve in (A)

We then conducted an iron starvation stress assay when cells were pre-grown in the nutrient and iron rich media (LB media) before being transferred to an iron limiting stress media (gluconate media with dipyridyl). This growth assay revealed a marked sensitivity in the Δ*iscU-fdx*Δ*bfr*Δ*dps* strain with this strain being as sensitive to the iron chelator as the Δ*sufA-E* strain (Figure 2.5). This same effect was observed when the strains were stressed with the use of phenazine methosulfate (PMS) to induce oxidative stress (Figure 2.6).

To confirm if this phenotype was specific to the Suf system, we did a growth assay on a Δ*bfr* Δ*dps* mutant that still contains a functional Isc pathway (Figure 2.7). We observed that mutant wasn't sensitive to the iron starvation indicating a specific genetic connection between Bfr, Dps and Suf. This result seems to indicate that in the Δ*iscU-fdx*Δ*bfr*Δ*dps* strain, the Suf system cannot efficiently perform Fe-S cluster biogenesis under stress conditions.

When the strains were grown first in M9 glucose minimal media before being shifted to M9 gluconate minimal media with varying concentrations of 2,2-bipyridyl, the Δ*iscU-fdx*Δ*bfr*Δ*dps* strain showed no sensitivity and grew to a final cell density slightly higher than the wild-type control strain (Figure 2.8). This result shows that when those strains are pre-adapted to minimal media, they are able to withstand the stress effects caused by the presence of the iron-chelator, BIPY. This result was consistent with the improved lag phase seen under non-stress growth conditions when the strains were pre adapted to minimal media (2.3, 2.4). When iron in the form of ferric citrate was added to the sensitive Δ*iscU-fdx*Δ*bfr*Δ*dps* mutant strain in range of concentrations from 1-10 μM concentrations, the pre-incubation of Δ*iscU-fdx* Δ*bfr* Δ*dps* mutant strain with iron caused

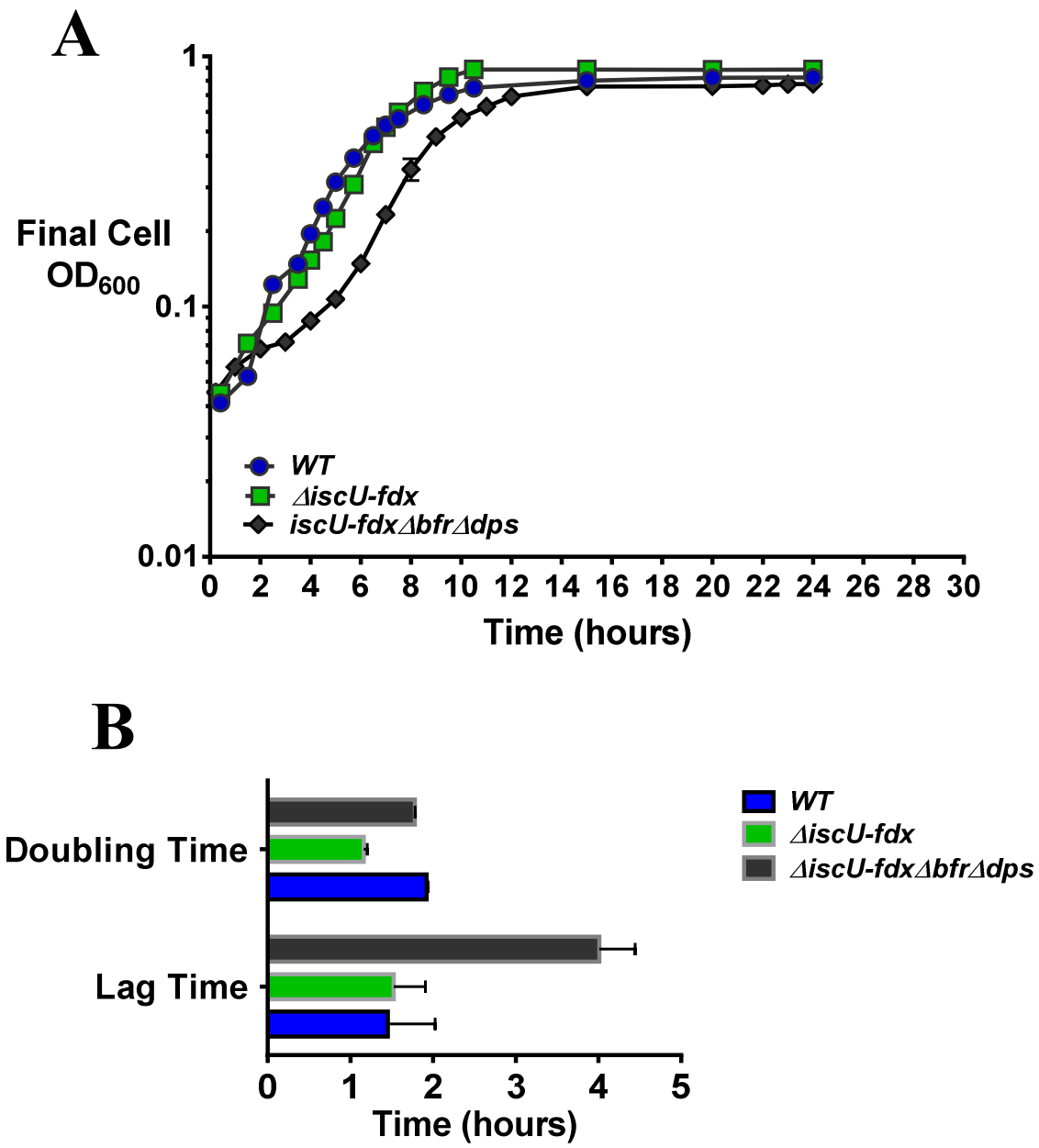

Figure 2.4. The Δ*iscU-fdx*Δ*bfr*Δ*dps* strain to shows a less severe lag phase duration when pre-grown in minimal media with no stress. (A) All strains were grown in M9 glucose minimal media for 24 hours and then washed and normalized to same starting OD_{600} in fresh M9 glucose minimal media for 24 hours. Cell density was measured hourly. All growths were repeated in triplicate (n=3) and error bars indicate one standard deviation from the mean value. (B) Lag phase and doubling time calculated from growth curve in (A).

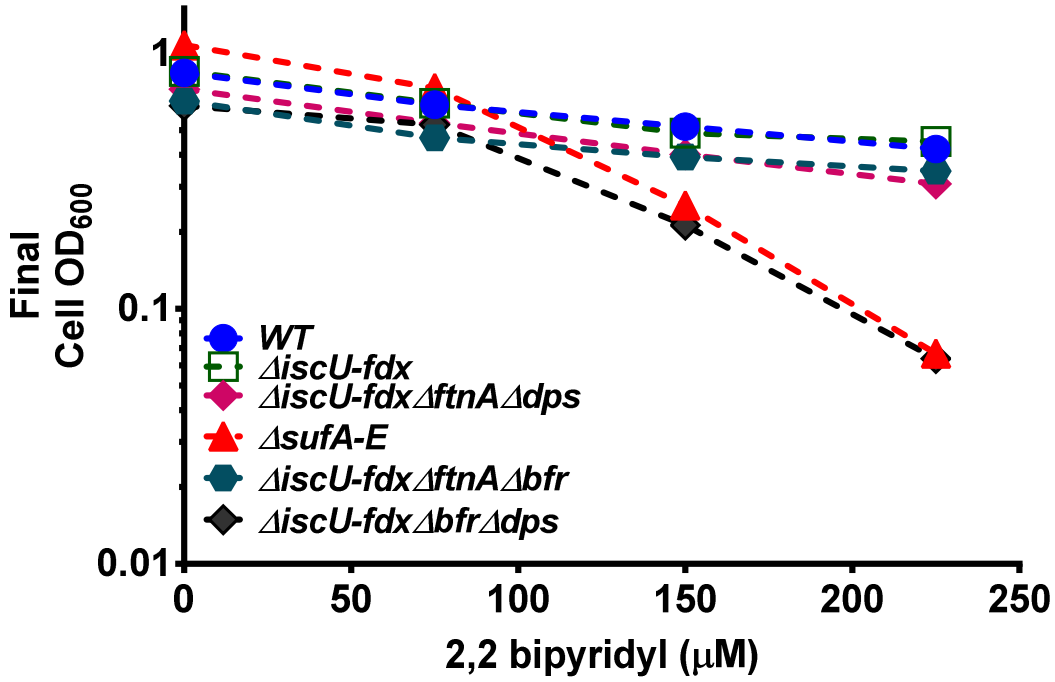

Figure 2.5. The deletion of both *bfr* and *dps* sensitizes the Δ*iscU-fdx* strain to bipyridyl stress. All strains were grown in LB for 18 hours. After this, they were washed and inoculated into fresh M9 gluconate minimal media with varying concentrations of BIPY. The final cell density was measured after 24 hours. All growths were repeated in triplicate (n=3) and error bars indicate one standard deviation from the mean value.

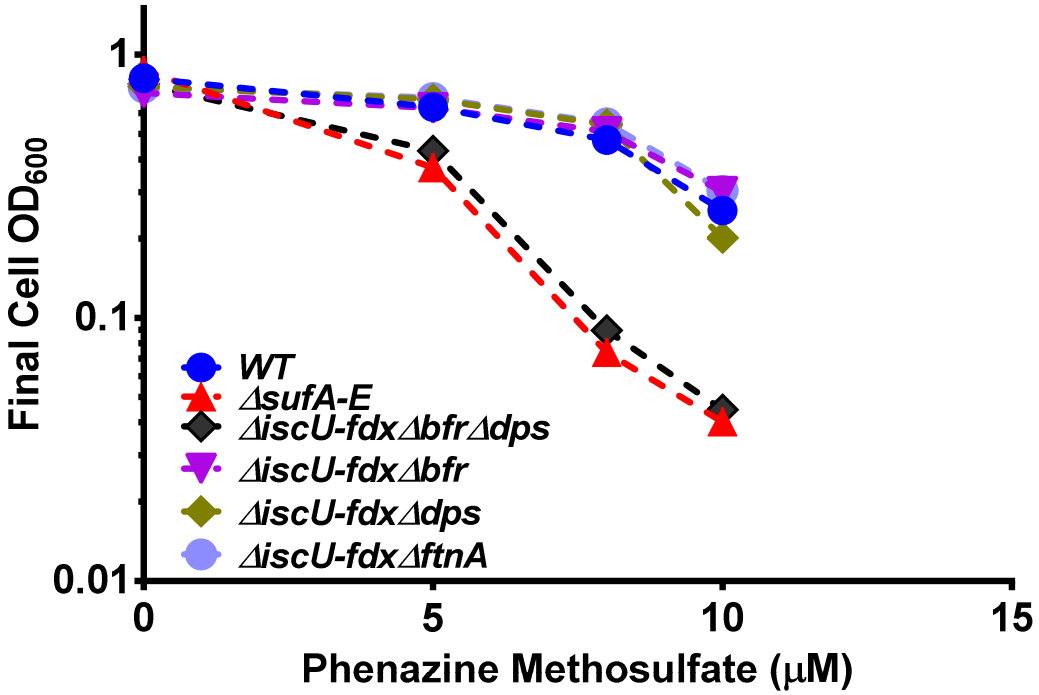

Figure 2.6. The deletion of both *bfr* and *dps* sensitizes the Δ*iscU-fdx* strain to oxidative stress. All strains were grown in LB for 18 hours. After this, they were washed and inoculated into fresh M9 gluconate minimal media with varying concentrations of BIPY. The final cell density was measured after 24 hours. All growths were repeated in triplicate (n=3) and error bars indicate one standard deviation from the mean value.

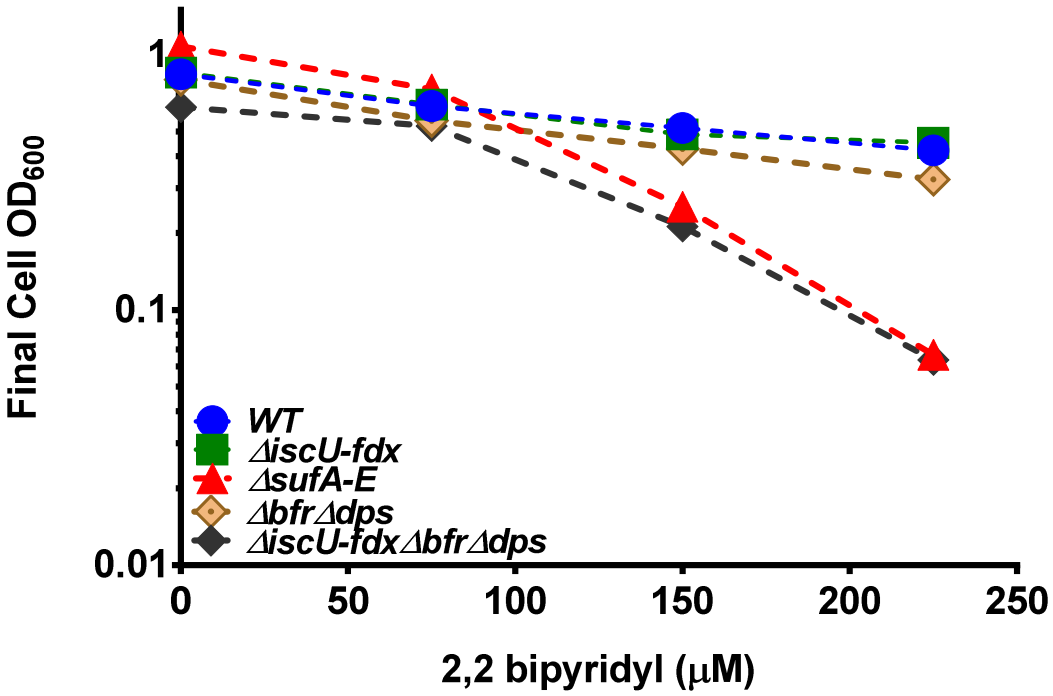

Figure 2.7. Deletion of Bfr and Dps in the presence of a functional Isc pathway rescues sensitive to iron starvation stress. All strains were grown in LB for 18 hours. After this, they were washed and inoculated into fresh M9 gluconate minimal media with varying concentrations of BIPY. The final cell density was measured after 24 hours. All growths were repeated in triplicate (n=3) and error bars indicate one standard deviation from the mean value.

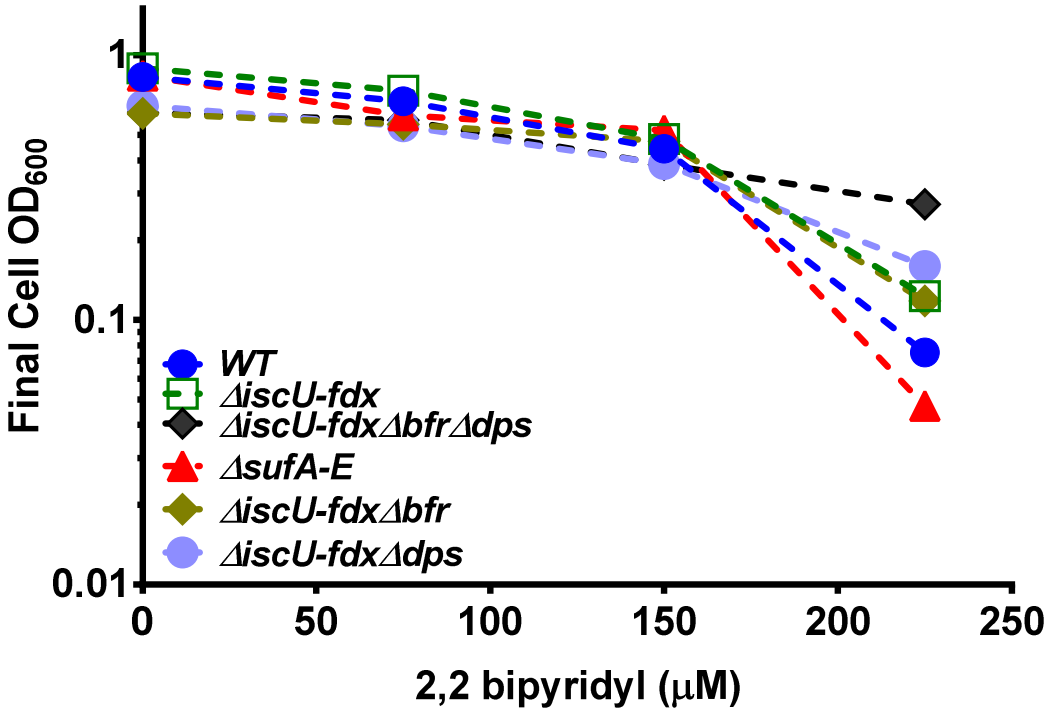

Figure 2.8 Pre-adaptation to low iron media rescues the sensitivity of the Δ*iscU-fdx*Δ*bfr*Δ*dps* strain to bipyridyl. All strains were grown in M9 glucose minimal media for 24 hours. After this, they were washed and inoculated into fresh M9 gluconate minimal media with varying concentrations of BIPY. The final cell density was measured after 24 hours. All growths were repeated in triplicate (n=3) and error bars indicate one standard deviation from the mean value

it to become more sensitive to the iron starvation stress (Figure 2.9). In *E. coli*, FtnA is the main iron storage protein during excess iron conditions. Since the Δ*iscU-fdx* Δ*bfr* Δ*dps* strain with the highest concentration of added iron (10 μM) became the most sensitive under stress conditions, our results suggest that the iron in stored FtnA cannot be assessed by the *suf* pathway.

The Δ*iscU-fdx*Δ*bfr*Δ*dps* strain has impaired Fe-S cluster function

Since growth of the Δ*iscU-fdx* Δ*bfr* Δ*dps* strain is sensitive to 2,2 bipyridyl, we tested if this was due to an inability to form Fe-S clusters *in vivo*. Therefore, cellular iron speciation in the mutant and parental strains was examined by whole-cell Mössbauer spectroscopy. The strains were grown to mid-log phase (OD_{600} 0.5) in glucose (0.2%) M9- salts medium containing 100 μM ^{57}Fe citrate. The cells were washed, cooled rapidly to 469 K, and analyzed by Mössbauer spectroscopy at 60 K. The spectrum of the Δ*iscU-fdx* parent strain (Figure 2.10) shows a diminished central doublet representing decreased $[4Fe\text{-}4S]^{2+}$ clusters and/or Low Spin Heme (LSH) compared to the wild-type strain (from about 20% to 5% of total Fe) but is otherwise similar to the wild-type strain. This result is consistent with previous reports that Suf does not fully restore Fe-S cluster biogenesis under non-stress conditions when *isc* is deleted. In the Δ*iscU-fdx*Δ*bfr*Δ*dps* mutant strain, the central doublet mostly representing $[4Fe\text{-}4S]^{2+}$ or LSH is nearly undetectable compared to the other strains indicating that those strains have increased difficulty with making iron sulfur clusters (Table 2.2).

In the strains, it was observed that there existed 2 NHHS Fe-(II) pools. One coordinated to oxygen/nitrogen ligands and denoted Fe-(II)A and the other coordinated to sulfur ligands and denoted Fe-(II)B. Both pools together make the combined NHHS

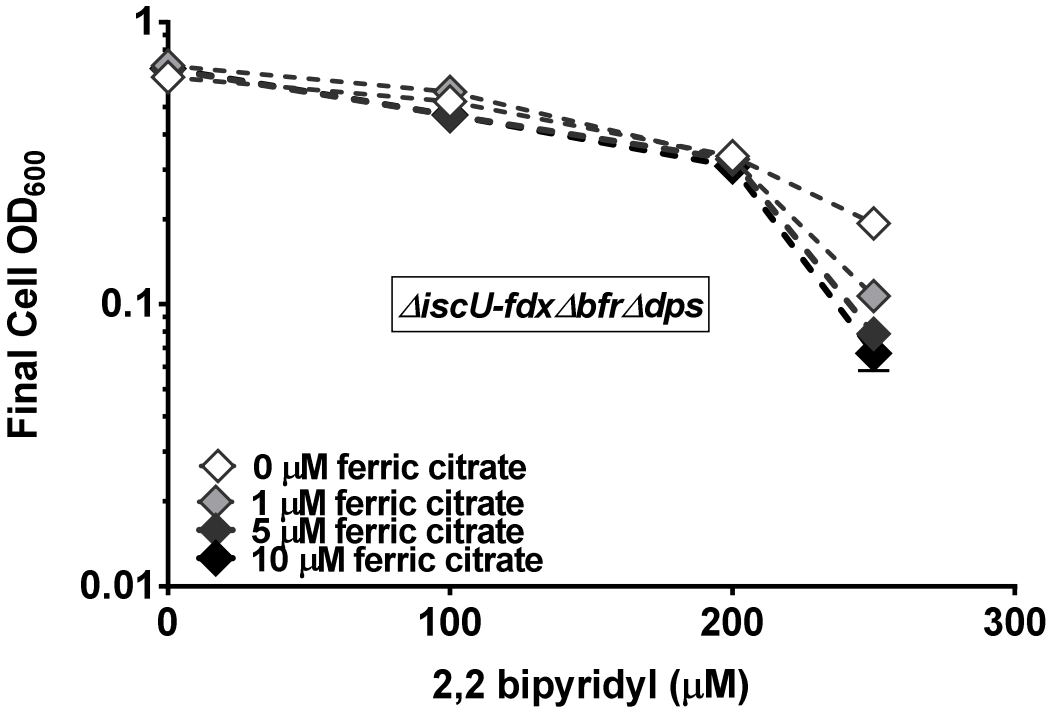

Figure 2.9 Addition of iron to the pre-stress growth media likely enhances the sensitivity of the Δ*iscU-fdx*Δ*bfr*Δ*dps* strain. Δ*iscU-fdx*Δ*bfr*Δ*dps* mutant strain was pre-grown in M9 glucose minimal media with varying concentrations of ferric citrate added to its pre-growth. Cells were grown for 24 hours, subsequently washed and inoculated into fresh M9 gluconate minimal media with BIPY.

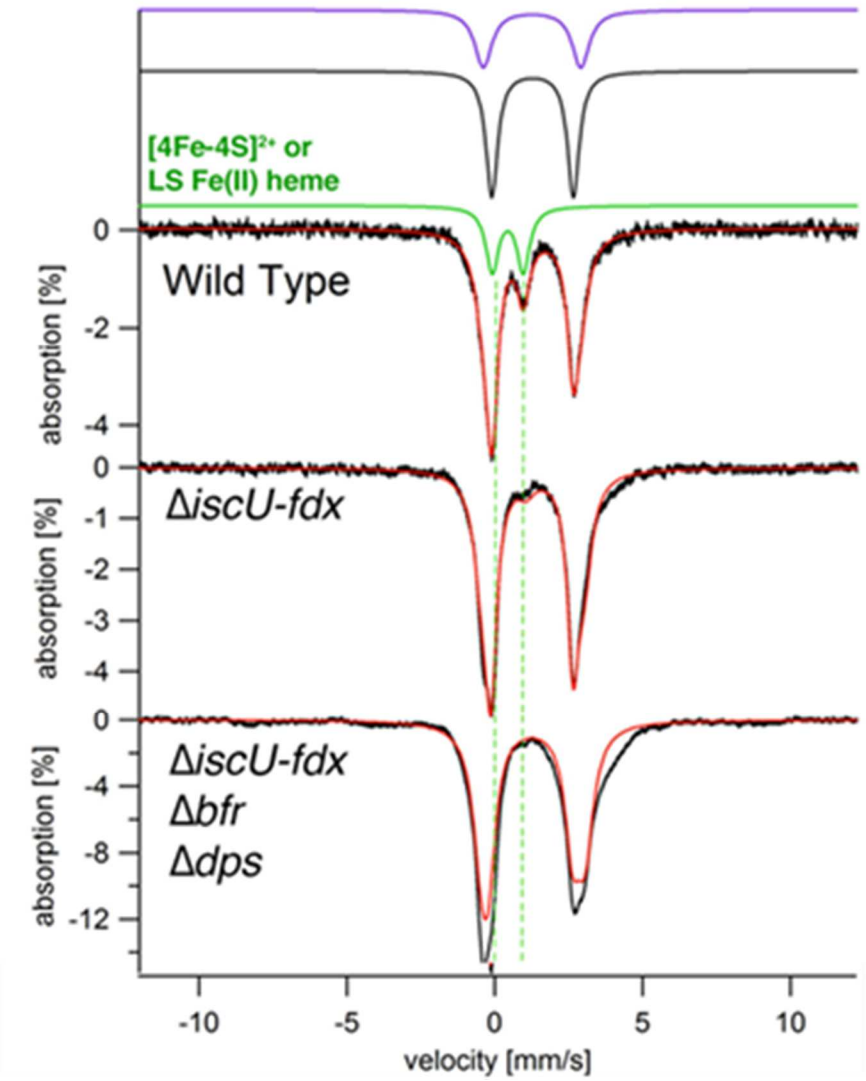

Figure 2.10 The Δ*iscU-fdx* Δ*bfr* Δ*dps* strain has virtually no Fe-S cluster assembly function. Whole-cell Mössbauer spectroscopy of *E. coli* strains grown in M9 glucose media with 100 μM ^{57}Fe (III)-citrate. Spectra were collected at 5 K, 0.05 T. The purple, black, and green lines above the spectrum are simulations of the various spectrum components assuming δ=1.28 mm/s, ΔE_Q = 2.76 mm/s, 45% area (purple); δ=1.26 mm/s, ΔE_Q = 3.3 mm/s, 30% area (black); and δ = 0.44 mm/s, ΔE_Q = 1.05 mm/s, 25% area (green). The Fe-S/heme "central doublet" is shown in green. Green dashed lines are used to indicate positioning of that doublet in all traces. The red line over the black trace of the raw data is the best fit simulation of the spectrum. Strains were initially grown in M9 glucose minimal media for 24 hours and then used to inoculate a 1 L M9 glucose minimal media culture with added 100 μM ^{57}Fe(III)-citrate. The cells were harvested at mid-log phase.

Fe -(II) content. Results show that though the overall NHHS Fe-(II) content of the wild-type strain and the sensitive Δ*iscU-fdx*Δ*bfr*Δ*dps* strain were similar at 70-75%, there were changes in the different Fe(II) pools (Table 2.2). While the parent Δ*iscU-fdx* strain and the sensitive Δ*iscU-fdx*Δ*bfr*Δ*dps* mutant strain had similar concentrations of Fe(II)B pools, they had different Fe(II)A pools. Results also showed that in the Δ*iscU-fdx*Δ*bfr*Δ*dps* strain, the NHHS Fe(II)B pool was doubled and its Fe(II)A pool reduced by almost a third compared to the wild-type strain.

It was observed that the Δ*iscU-fdx*Δ*bfr*Δ*dps* stain also showed a higher non-heme high spin (NHHS) Fe-(III) content: 20% compared to both the wild-type and parent Δ*iscU-fdx* strains. This form of iron is the iron stored in ferritins such as Ferritin A. Total intracellular iron content of the strains showed that the sensitive Δ*iscU-fdx*Δ*bfr*Δ*dps* strain had almost double the wild-type iron content (Figure 2.11).

To further prove that the sensitivity in the Δ*iscU-fdx*Δ*bfr*Δ*dps* strain is caused by impaired Fe-S cluster function, we tested the strains in another growth assay in M9 minimal media using sodium acetate as the carbon source. Cells grown on acetate by-pass glycolysis to go through the glycoxylate shunt and tricarboxylic acid (TCA) cycle for metabolism. The TCA cycle has enzymes that contain Fe-S cluster, such as succinate dehydrogenase and aconitase. Acetate growth requires respiration for all synthesis of molecules. The respiratory complexes I and II contain many Fe-S clusters.[20, 21] Any strain that has difficulty assembling Fe-S clusters will therefore show a dramatic growth phenotype in this media. The Δ*iscU-fdx* strain did grow poorly in this media but the sensitive Δ*iscU-fdx*Δ*bfr*Δ*dps* strain had the biggest growth defect (Figure 2.12) suggesting that this strain had difficulty making Fe-S clusters.

Table 2.2 Mössbauer iron speciation and percentages

	MG1655	Δ*iscU-fdx*	Δ*iscU-fdx*Δ*bfr*Δ*dps*
Non-heme High Spin Fe(II) A	50%	51%	35%
Non-heme High Spin Fe(II) B	23%	39%	40%
Central Doublet / Low Spin Heme	20%	3-5%	-
Non-Heme High Spin Fe(III)	10%	5%	20%
Iron adsorption percent effect	4%	4%	14%

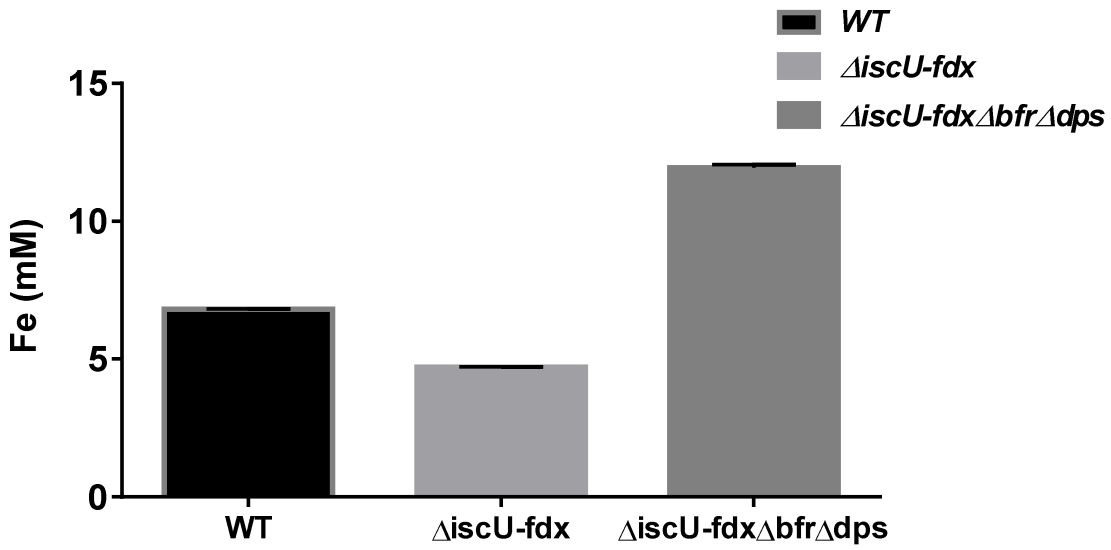

Figure 2.11. The Δ*iscU-fdx* Δ*bfr* Δ*dps* mutant strain accumulates more iron than the WT when pre-grown in 100 µM ^{57}Fe (III)-citrate. Atomic absorption spectroscopy of exponential phase cells grown in 100 µM ^{57}Fe (III)-citrate.

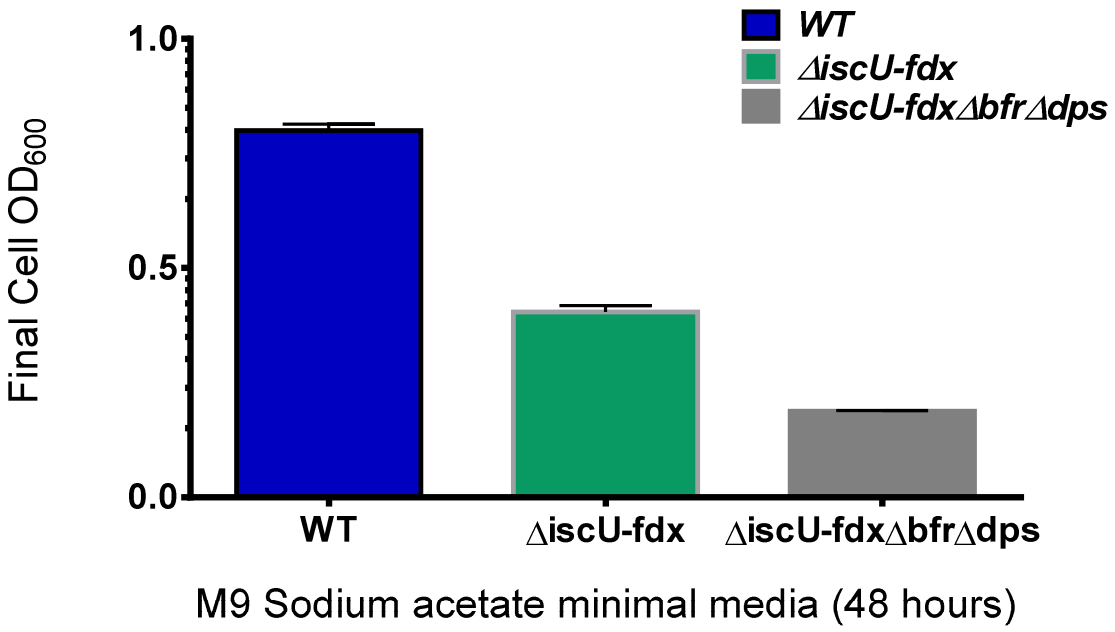

Figure 2.12. The Δ*iscU-fdx*Δ*bfr*Δ*dps* strain shows a defective growth phenotype in M9 acetate growth without stress. All strains were grown in M9 glucose minimal media for 24 hours for 18 hours and then washed and normalized to same starting OD_{600} in fresh M9 sodium acetate minimal media for 24 hours. Cell density was measured after 48 hours. All growths were repeated in triplicate (n=3) and error bars indicate one standard deviation from the mean value.

FtnA is inaccessible by the Suf Pathway

The delayed lag phase in the sensitive Δ*iscU-fdx*Δ*bfr*Δ*dps* strain is abolished with the added *ftnA* deletion when pre-grown in both LB (Figure 2.13) and M9 minimal media (Figure 2.14). In the Δ*iscU-fdx*Δ*bfr*Δ*dps* double mutant strain, additional deletion of *ftnA* (Δ*iscU-fdx*Δ*ftnA*Δ*dps*Δ*bfr*) rescued the sensitivity of the strain to both iron starvation (Figure 2.15) and oxidative stress (Figure 2.16). This seems to suggest that the iron stored in FtnA is not easily accessed by Suf and became more available to the *suf* pathway when FtnA was deleted. This suggests that Fe-S cluster formation had been restored in this Δ*iscU-fdx*Δ*ftnA*Δ*bfr*Δ*dps* mutant. When pre-grown in iron-limiting media and stressed with BIPY, the Δ*iscU-fdx*Δ*ftnA*Δ*bfr*Δ*dps* grew similar to the wild-type strain (Figure 2.17).

FtnA is expressed during the log phase and functions as the main iron storage protein under Fe replete conditions. Its expression is upregulated when the Fur-Fe^{2+} derepresses its transcription by directly competing with the H-NS repressor binding at its promoter site. This suggests that when iron is abundant in the cell, its mainly stored in the protein. When iron in the form of ferric citrate was added to the sensitive Δ*iscU-fdx*Δ*bfr*Δ*dps* mutant strain in a range of concentrations (1-10 μM), the strain pre-incubated with 10 μM was the most sensitive to the BIPY stress (Figure 2.9). This result suggests that the addition of the iron resulted in an up-regulated FtnA expression. This means that in excess iron environments, more iron is sequestered in the FtnA ferritin and this iron is inaccessible to the Suf pathway. When ferric citrate was added to the wild-type and Δ*iscU-fdx*Δ*ftnA*Δ*bfr*Δ*dps* strains, both the strains grew more resistant to BIPY stress (Figure 2.18). This suggests that in the Δ*iscU-fdx*Δ*ftnA*Δ*bfr*Δ*dps* strain, the absence

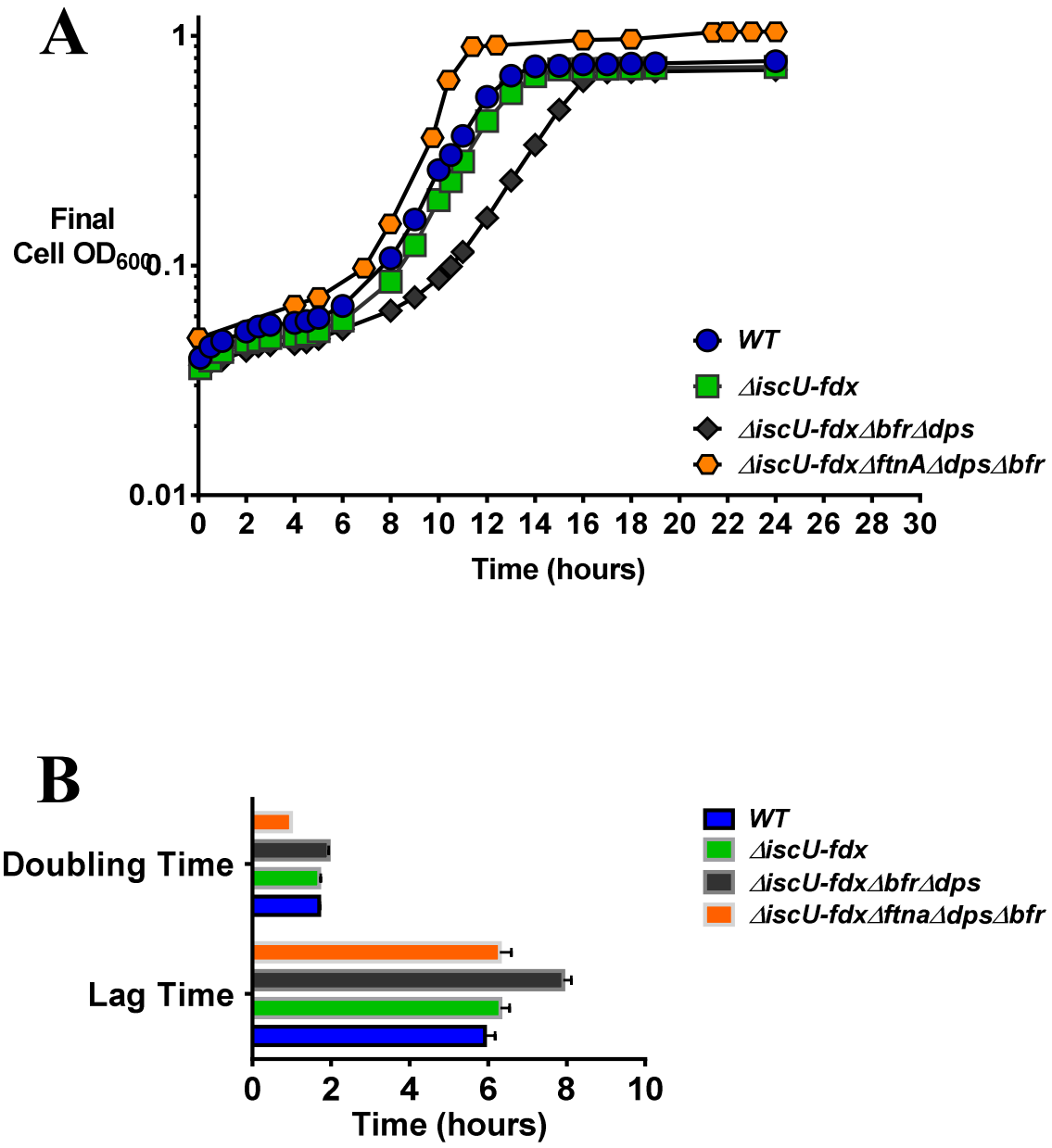

Figure 2.13. Additional deletion of *ftnA* rescues the mild increase in lag phase duration in LB media with no stress of the Δ*iscU-fdx*Δ*bfr*Δ*dps* strain (A) All strains were grown in LB media for 18 hours. After, they were washed and inoculated into fresh 0.2% glucose minimal media and optical cell density was measured initially every 30 mins until they exited lag phase, and then hourly. All cell growths were repeated in triplicate (n=3) and error bars indicate one standard deviation from the mean value. (B) Lag phase and doubling time were calculated from the timed growth curve obtained in (A).

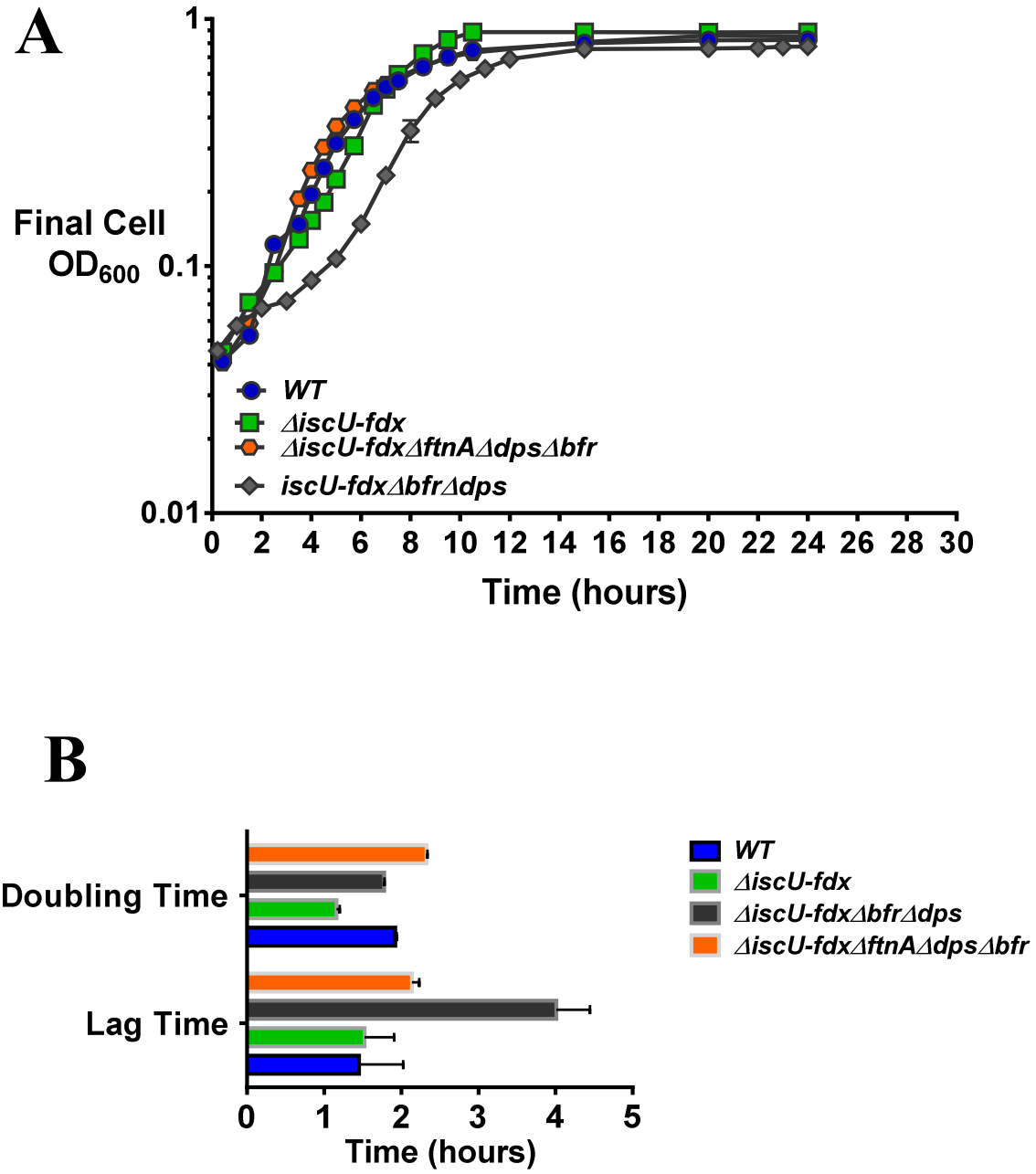

Figure 2.14. Additional deletion of *ftnA* rescues the mild increase in lag phase duration in minimal media with no stress of the Δ*iscU-fdx*Δ*bfr*Δ*dps* strain. (A) All strains were grown in M9 glucose minimal media for 24 hours. After this, they were washed and inoculated into fresh M9 gluconate minimal media and density was measured initially every 30 mins until they exited lag phase, and then hourly. All growths were repeated in triplicate (n=3) and error bars indicate one standard deviation from the mean value. (B) Lag phase and doubling time calculated from growth curve in (A).

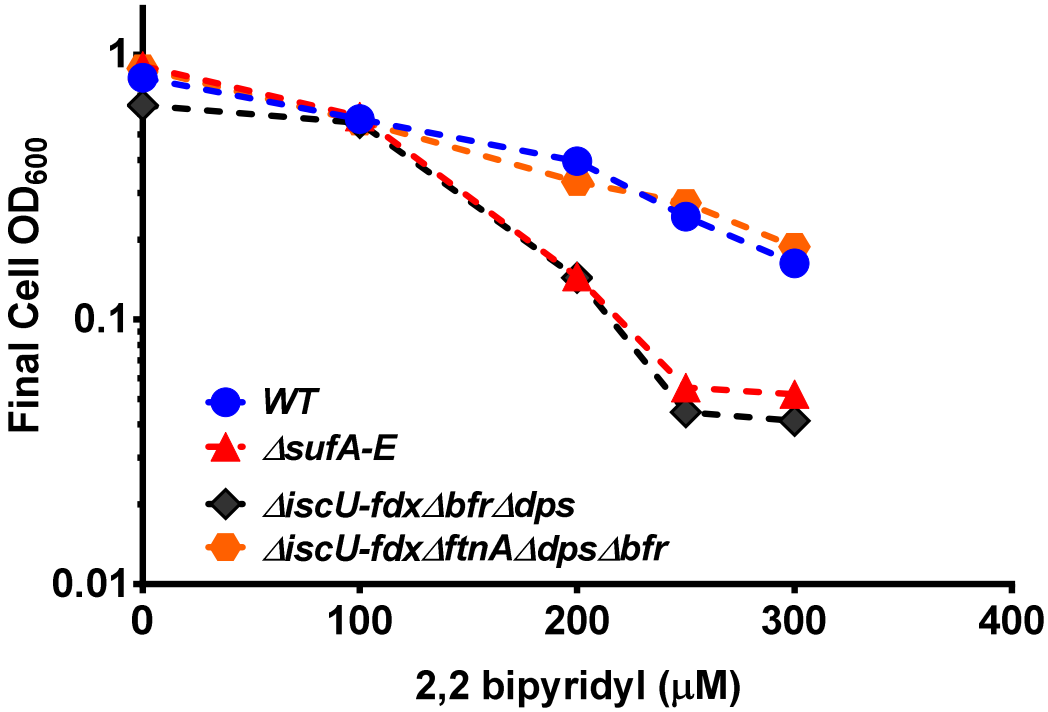

Figure 2.15. Additional deletion of *ftnA* rescues the sensitivity of the Δ*iscU-fdx*Δ*bfr*Δ*dps* strain to bipyridyl. All strains were grown in LB for 18 hours. After this, they were washed and inoculated into fresh 0.2% gluconate minimal media with varying concentrations of BIPY. The final cell density was measured after 24 hours. All growths were repeated in triplicate (n=3) and error bars indicate one standard deviation from the mean value.

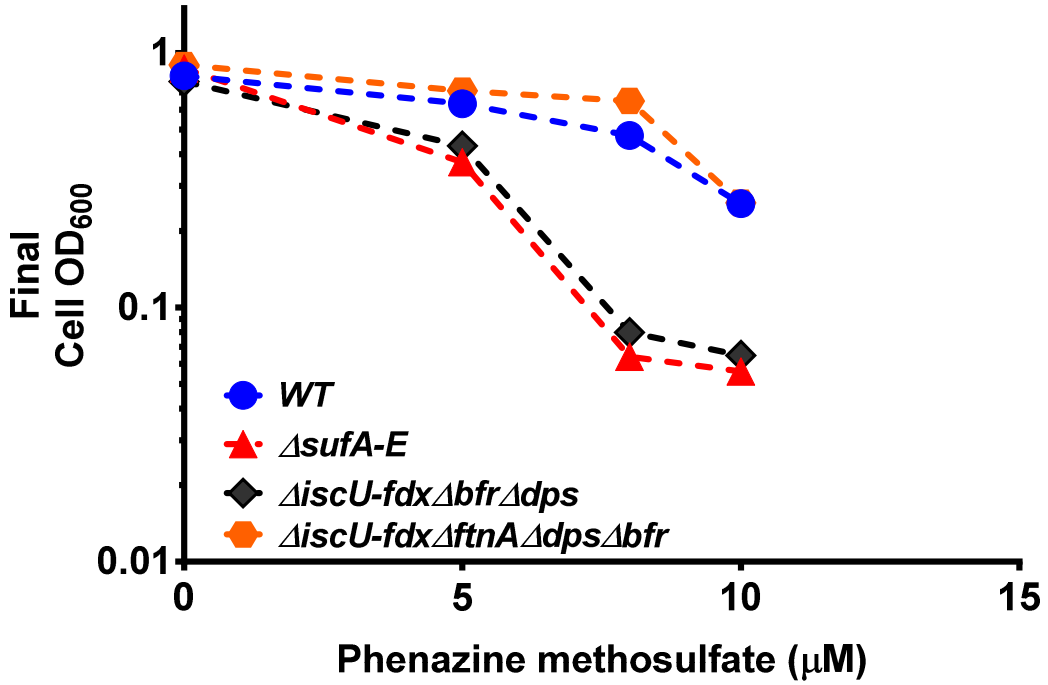

Figure **2.16 Additional deletion of *ftnA* rescues the sensitivity of the Δ*iscU-fdx*Δ*bfr*Δ*dps* strain to oxidative stress.** All strains were grown in LB for 18 hours. After this, they were washed and inoculated into fresh 0.2% gluconate minimal media with varying concentrations of PMS. The final cell density was measured after 24 hours. All growths were repeated in triplicate (n=3) and error bars indicate one standard deviation from the mean value.

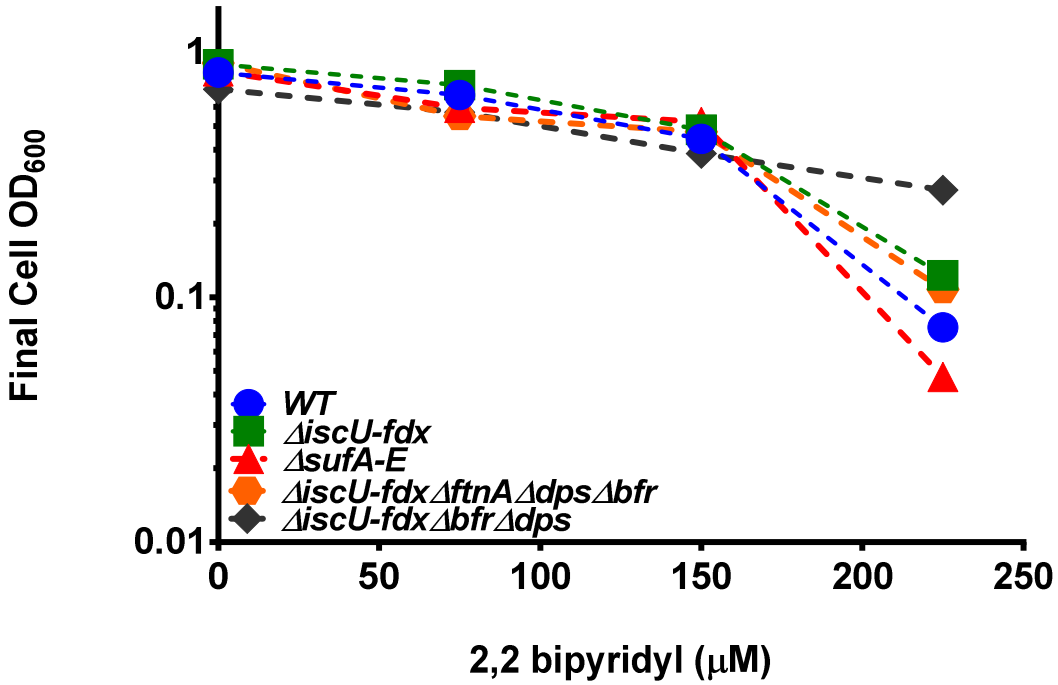

Figure 2.17. Additional deletion of *ftnA* increases the sensitivity of the Δ*iscU-fdx*Δ*bfr*Δ*dps* strain to bipyridyl when pre-grown in M9 minimal media. All strains were grown in M9 glucose minimal media for 24 hours. After this, they were washed and inoculated into fresh 0.2% gluconate minimal media with varying concentrations of BIPY. The final cell density was measured after 24 hours. All growths were repeated in triplicate (n=3) and error bars indicate one standard deviation from the mean value.

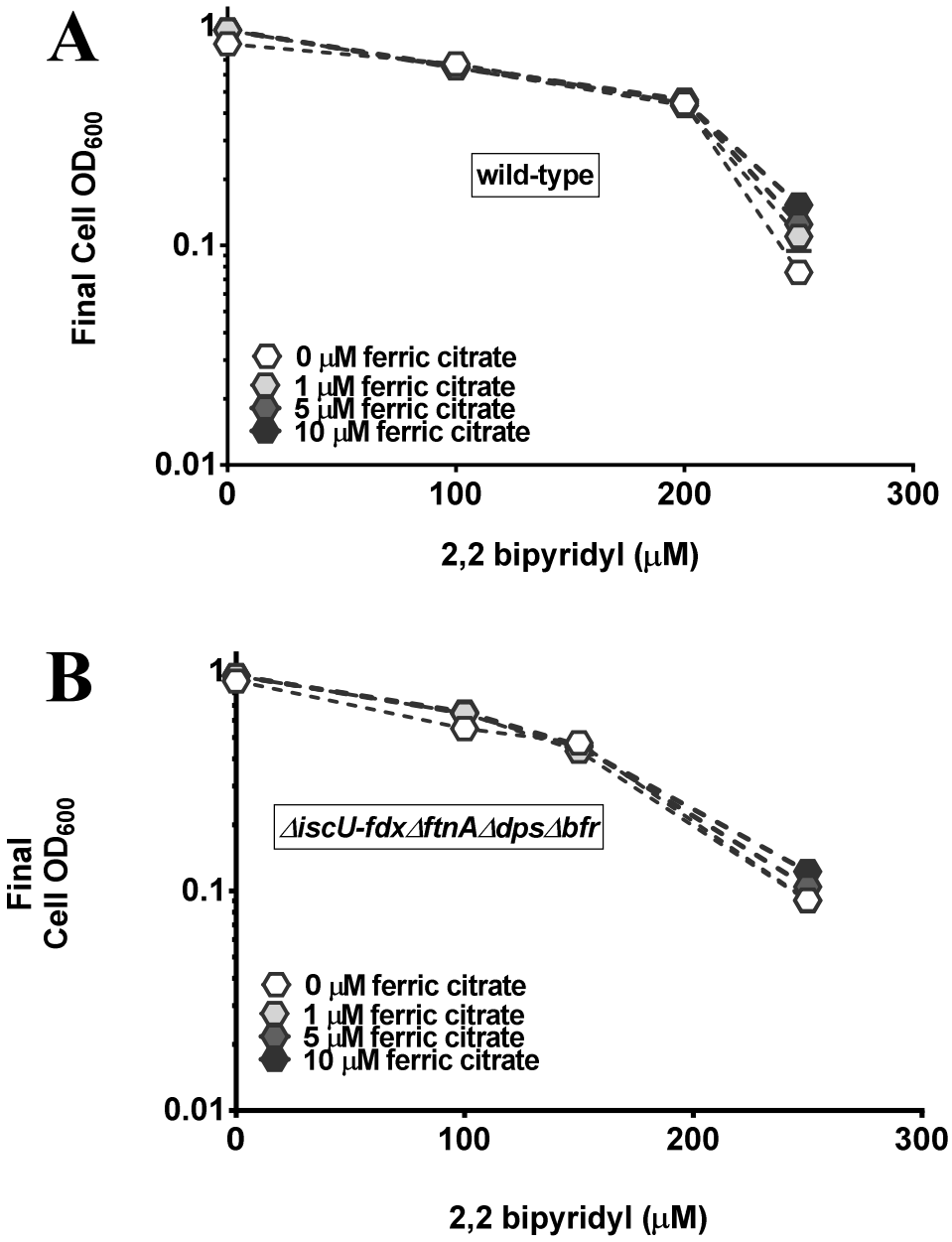

Figure 2.18. Addition of iron to the pre-stress growth media does not alter the sensitivity of the Δ*iscU-fdx*Δ*ftnA*Δ*bfr*Δ*dps* to BIPY (A) and (B) were pre- grown in M9 glucose minimal media with varying concentrations of ferric citrate added. Cells were grown for 24 hours, subsequently washed and inoculated into fresh M9 gluconate minimal media with BIPY.

of FtnA made the extra iron create or increase an iron that is available to Suf for its utilization.

Mössbauer analysis also showed that the additional deletion of FtnA restored Fe-S cluster assembly compared to the sensitive Δ*iscU-fdx*Δ*bfr*Δ*dps* mutant strain (Figure 2.19). The spectra also showed no iron in the baseline. This iron is in form of Non Heme High Spin Fe (III) and it is the iron stored in ferritins usually ferritin A. The Δ*iscU-fdx*Δ*ftnA*Δ*dps*Δ*bfr* strain two NHHS Fe (II) pols were also comparable to the wild-type strain although its NHHS Fe (II)B pool was slightly higher compared to it (Table 2.3).

Total intracellular iron content of the strains showed that the Δ*iscU-fdx*Δ*ftnA*Δ*dps*Δ*bfr* strain with restored Fe-S cluster functions also had the least amount of total intracellular iron (Figure 2.20). To further confirm that Fe-S cluster function had been restored, we tested the strains in another growth assay in M9 sodium acetate minimal media. We observed that the cells grew to a level comparable to the wild-type (Figure 2.21) indicating that it had un-impaired Fe-S cluster function and ability to respire.

The expression of the *sufABCDSE* operon is normally repressed by Fur under iron-replete conditions[22] and this repression is lost, leading to *suf* expression, under iron starvation conditions. It is possible that the various iron storage mutations increase the level of Fe^{2+} -Fur leading to decreased Suf expression which would explain the observed deficiencies in Fe-S cluster biogenesis in a Δ*iscU-fdx* mutant. To test this we directly monitored SufD protein expression by Western blot (Figure 2.22). SufD is translated from a polycistronic mRNA containing the *sufABCDSE* genes and is required for Suf

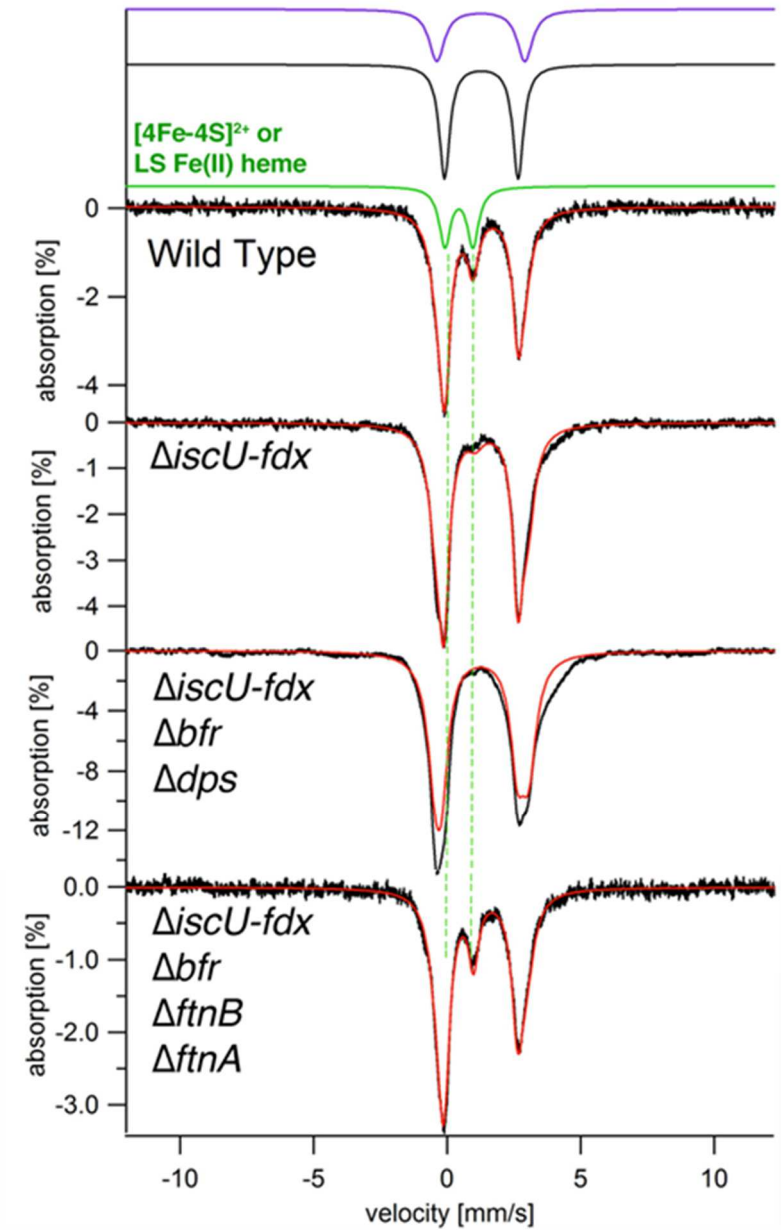

Figure 2.19. The Δ*iscU-fdx*Δ*ftnA*Δ*dp*Δ*bfr* strain has restored Fe-S cluster assembly function. Whole-cell Mössbauer spectroscopy of indicated strains of *E. coli* grown in M9 glucose media with 100 μM ^{57}Fe(III)-citrate. Spectra were collected at 5 K, 0.05 T. The purple, black, and green lines above the spectrum are simulations of the various spectrum components assuming δ=1.28 mm/s, ΔE_Q = 2.76 mm/s, 45% area (purple); δ=1.26 mm/s, 30% area (black); and δ=0.44 mm/s, ΔE_Q = 1.05 mm/s, 25% area (green). The Fe-S/heme "central doublet" is shown in green. The red line over the black trace of the raw data is the best fit simulation of the spectrum. Strains were initially grown in M9 glucose minimal media for 24 hours and then used to inoculate a 1L M9 glucose minimal media culture with added 100 μM ^{57}Fe(III)-citrate. The cells were harvested at mid-log phase, washed and frozen in liquid Nitrogen for Mössbauer analysis.

.

Table 2.3 Mössbauer iron speciation and percentages

	MG1655	**Δ*iscU-fdx***	**Δ*iscU-fdx*Δ*bfr*Δ*dps***	**Δ*iscU-fdx*Δ*ftnA*Δ*dps*Δ*bfr***
Non-heme High Spin Fe (II) A	50%	51%	35%	50%
Non-heme High Spin Fe (II) B	23%	39%	40%	28%
Central Doublet / Low Spin Heme	20%	3-5%	-	22%
Non-Heme High Spin Fe (III)	10%	5%	20%	3%
Iron adsorption percent effect	4%	4%	14%	-

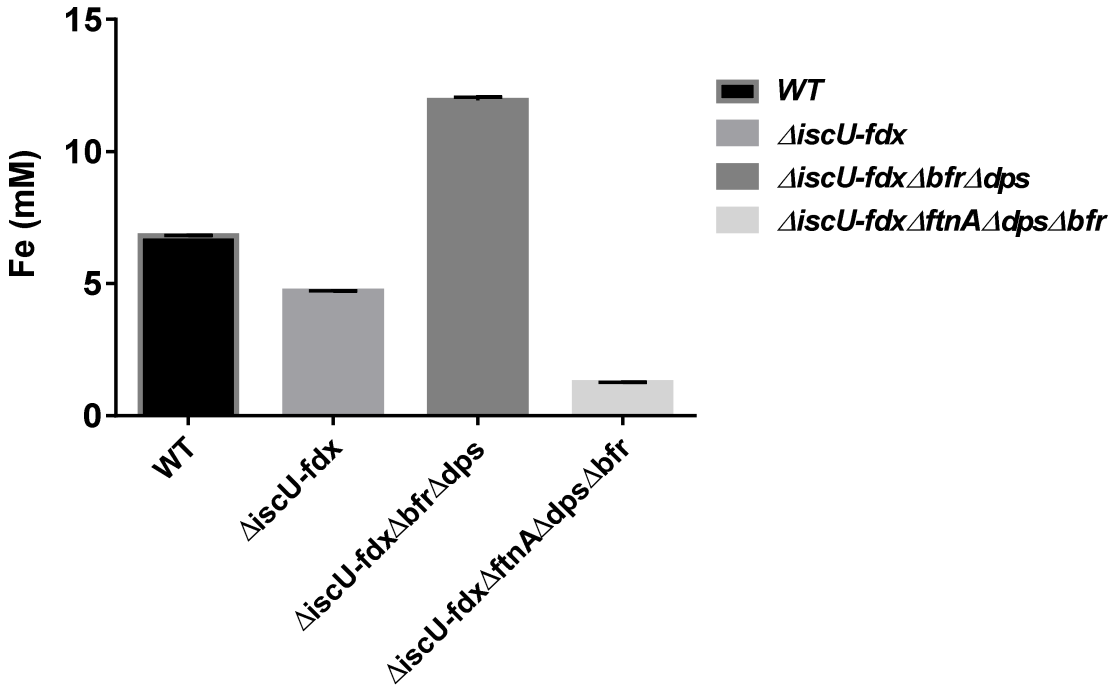

Figure 2.20. The Δ*iscU-fdx*Δ*ftnA*Δ*dps*Δ*bfr* mutant strain accumulates less iron than the WT when pre-grown in 100 µM ^{57}ferric citrate though it has restored Fe-S cluster function. Atomic Absorption Spectroscopy of exponential phase cells grown in 100 µM ^{57}ferric citrate.

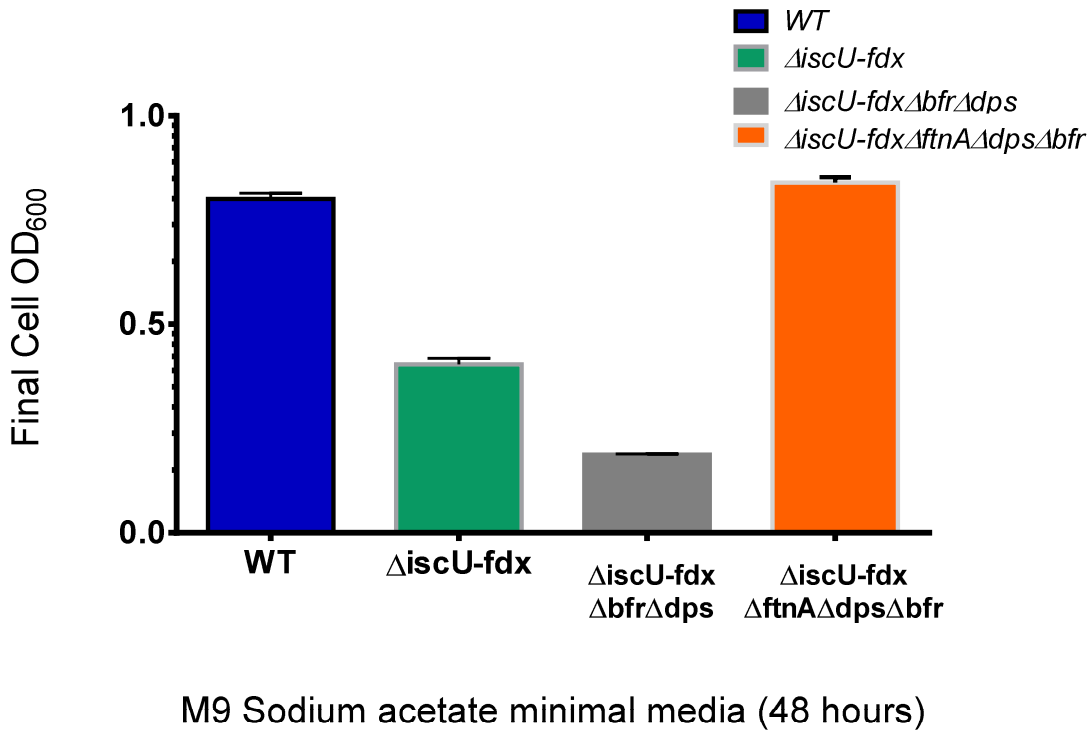

Figure 2.21. The Δ*iscU-fdx*Δ*ftnA*Δ*dps*Δ*bfr* strain shows no defective growth phenotype in M9 acetate growth without stress. All strains were grown in M9 glucose minimal media for 24 hours for 18 hours and then washed and normalized to same starting OD_{600} in fresh M9 sodium acetate minimal media for 24 hours. Cell density was measured after 48 hours. All growths were repeated in triplicate (n=3) and error bars indicate one standard deviation from the mean value.

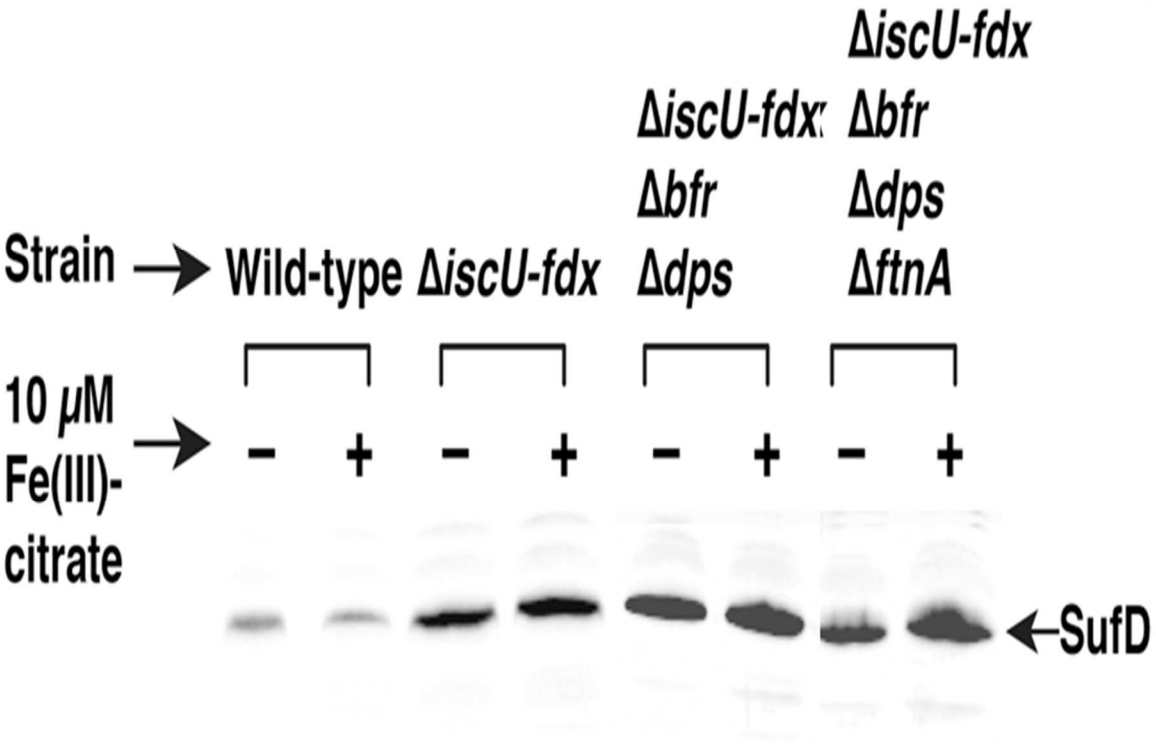

Figure 2.22. Suf expression upregulated in the mutants with the Δ*iscU-fdx* background. Western blot analysis of equal amounts of total protein from *E. coli* strains grown in M9 glucose minimal media with or without 10 μM Fe (III)-citrate addition using α-SufD antibodies.

function. We found that SufD is weakly expressed in M9 glucose minimal media in the wild-type strain (which still contains a functional Isc pathway). This expression is lowered when ferric citrate is added, indicating iron-responsive repression by Fur. In contrast (in the Δ*iscU-fdx* parent strain), SufD expression is constitutively upregulated and in the iron storage mutant strains in the Δ*iscU-fdx* background. Surprisingly, when 10 μM ferric citrate was added SufD expression is further increased in the Δ*iscU-fdx* strain as well as in all of the iron storage mutants constructed in that genetic background (Figure 2.22).

To further assess the regulation in these mutants we decided to assess the transcript levels of another Fur-regulated target gene. FepA is an integral bacterial outer membrane porin protein, which is involved in the active transport of iron bound by the siderophore enterobactin from the extracellular space.[24] To assess whether FepA is differentially regulated in different strains, we carried out primer extension assays to measure *fepA* transcript levels in cells exposed to high BIPY(250 μM). We measured these levels in both nutrient rich (LB) and M9 glucose minimal media. The transcript levels for all the strains were practically undetectable in LB media without BIPY added (Figure 2.23A). That result indicates the iron demand was negligible in LB as they had adequate iron in the cells. When stressed with 250 μM BIPY, the *fepA* transcript was upregulated as the cells needed to increase the iron supply to match the increased cellular demands.

The observed phenotypes are not attributed to changes in total intercellular levels

In order to assess impact of deleting the ferritins on the total cellular Fe levels, wild type and ferritin-deficient mutant strains were analyzed for total Fe content by inductively

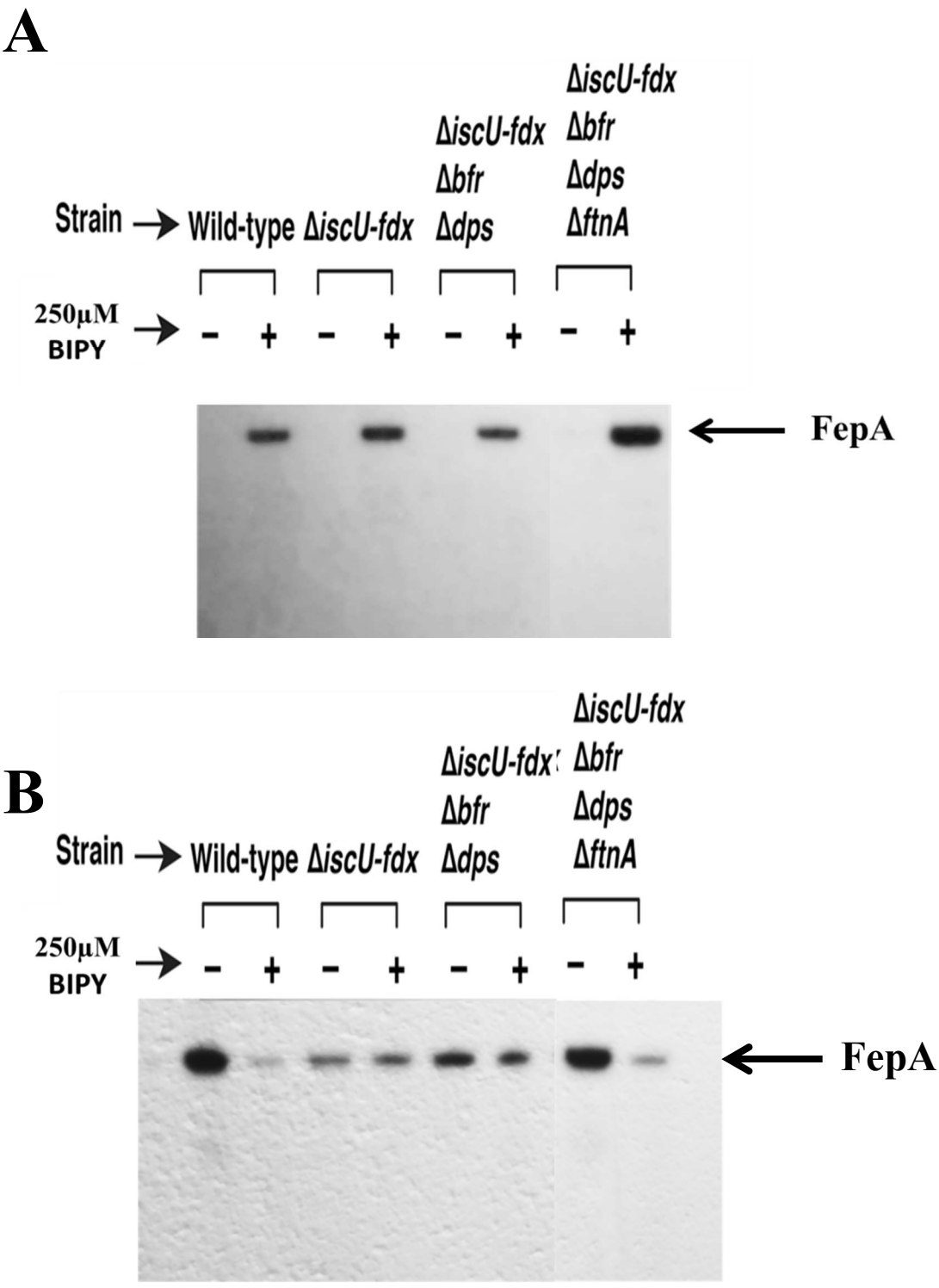

Figure 2.23. Transcriptional activity of FepA. Cells were grown in (A) LB or (B) M9 Glucose minimal media to mid-log phase (0.5), some harvested as the control probe and the remaining induced for 1 hour with 250 μm BIPY for 1 hour.

coupled plasma atomic mass spectroscopy (ICP-MS). Total Fe content was lower in the Δ*iscU-fdx*Δ*bfr*Δ*dps* strain compared to the WT and the parent Δ*iscU-fdx* strain when grown in LB media and up till mid-log in 0.2% glucose minimal media. Strains in stationary phase in the 0.2% glucose minimal media all showed the same approximate total cellular iron content (Figure 2.24). Deletion of the FtnA from the Δ*iscU-fdx*Δ*bfr*Δ*dps* double mutant did not increase the total cellular iron level of the strain indicating increased Fe uptake does not explain the growth rescue (Figure 2.24).

Inactivation of bfr and dps raises the intracellular free Fe concentration

` Chelatable cellular iron pools were measured in LB-cultured stationary phase cells by formation of a desferrioxamine-Fe by EPR spectroscopy. The intracellular labile Fe pools exist predominantly in the Fe^{2+} form, which exists as S = 0 or S = 2 and lacks an EPR signal. However, the cell-permeable Fe chelator desferrioxamine facilitates oxidation of the Fe^{2+}, and the resulting Fe^{3+}-desferrioxamine chelate exhibits a prominent EPR signal at g = 4.3. Moreover, protein-bound Fe does not resonate at this g-value and DFO does not appear to remove iron from metalloproteins. A Δ*fur* strain, which served as a positive control, showed free Fe levels more than twice as high as wild type (Figure 2.25A). This increase in free Fe is presumably a consequence of constitutive Fe assimilation in this strain where iron uptake systems are constitutively expressed. The parent Δ*iscU-fdx* strain had the least amount of DFO-detectable of all the strains. Labile (DFO-chelatable) iron is highest in the Δ*iscU-fdx*Δ*bfr*Δ*dps* mutant strain. The additional deletion of *ftnA* decreases the DFO-detectable iron pool even though total cellular iron levels are comparable with the wild-type and parent Δ*iscU-fdx* strains. This deletion

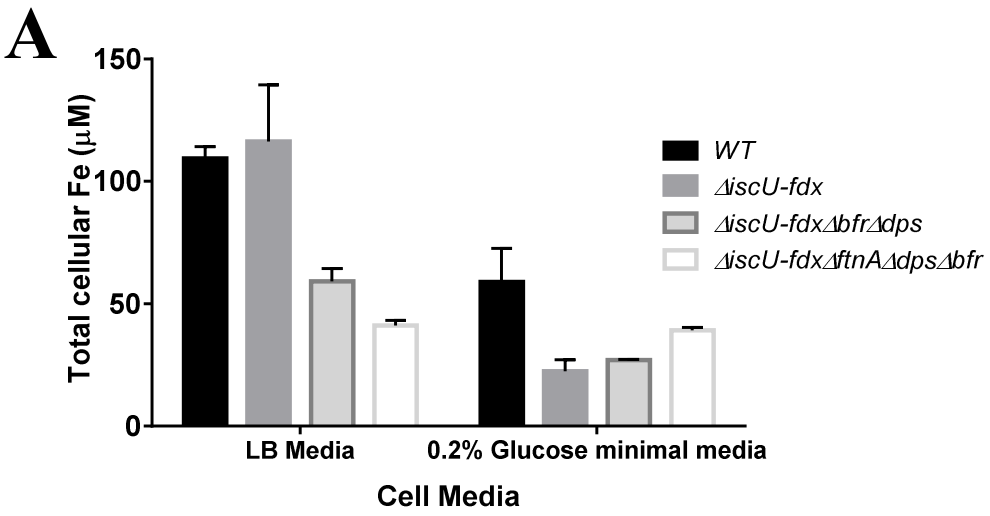

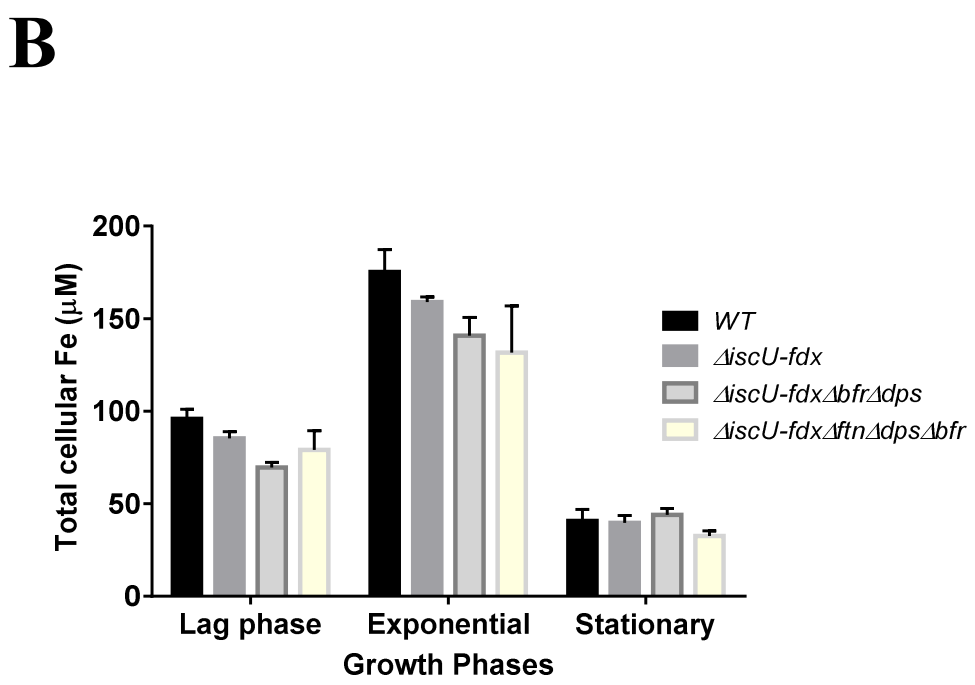

Figure 2.24. The additional deletion of *ftnA* does not alter the low iron content of the Δ*iscU-fdx*Δ*bfr*Δ*dps* strain (so doesn't explain the rescue effect of deletion *ftnA*. (A) Cells analyzed after 18 hours (in LB) and 24 hours (in M9 glucose minimal media) respectively. (B) Cells analyzed at different growth phases in M9 glucose minimal media after initial 18 hours growth in LB media. All growths were repeated in triplicate (n=3) and error bars indicate one standard deviation from the mean value.

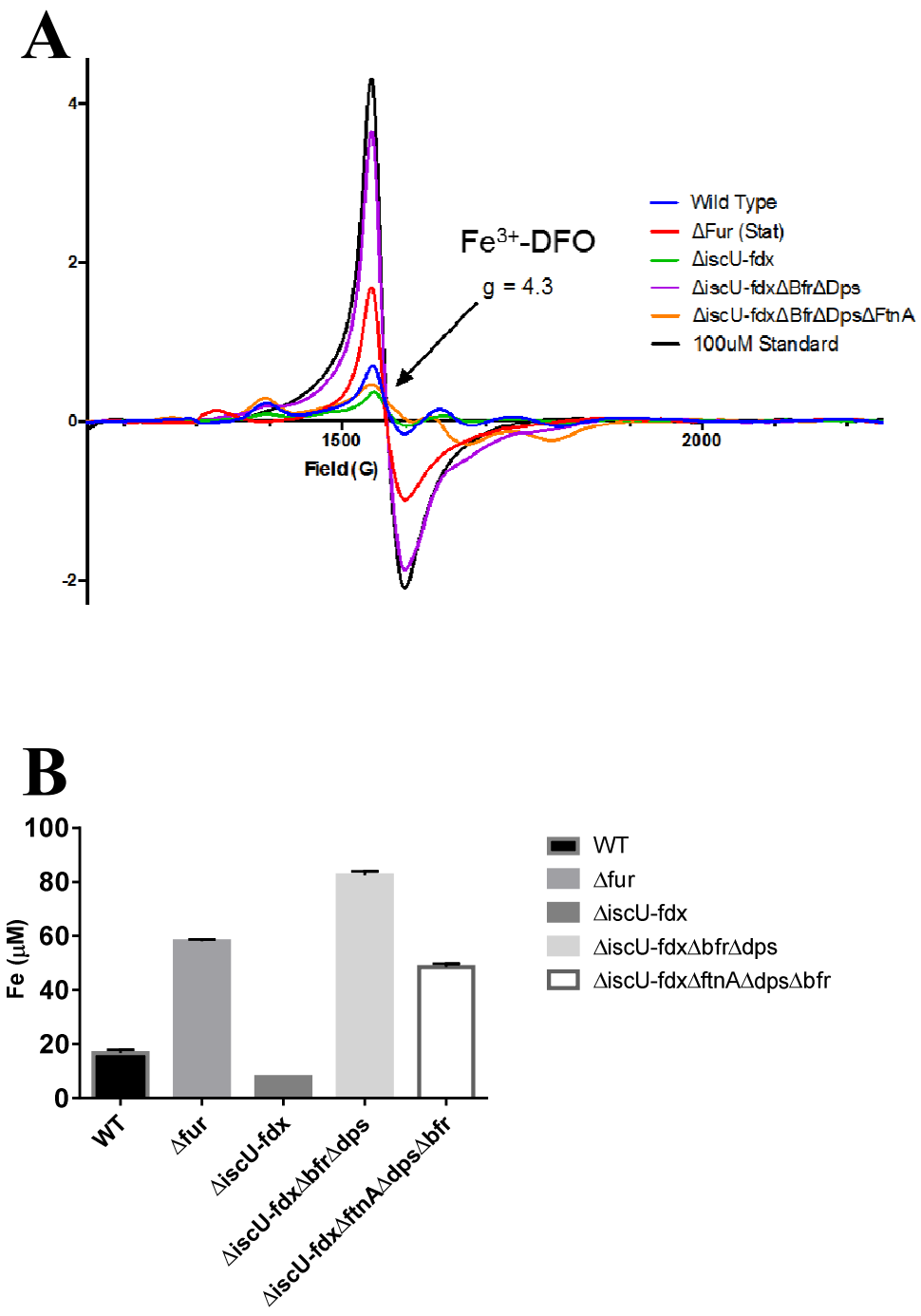

Figure 2.25. Labile iron pools are highest in the Δ*iscU-fdx*Δ*bfr*Δ*dps* strain. (A) Individual EPR spectra of the Fe(III)-DFO complex, showing an EPR signal with a calculated g-value of 4.3 from cells grown in LB. (B) Intracellular, DFO-labile iron concentrations quantified from (A) and normalized to cell volume and number.

releases iron into a novel iron pool when FtnA is deleted. This new pool can be accessed by the Suf pathway but is not DFO-detectable.

Mössbauer analysis on the different strains showed that the while the wild-type strain had 70% of its iron in Non Heme High Spin Fe (II) state, it had about 20% in Fe-S clusters and the remaining in ferritins (Table 2.2, 2.3). The parent Δ*iscU-fdx* in contrast had 90% of its iron in the NHHS Fe (II) state with 5% in Fe-S clusters with 5% in baseline as ferritins. The sensitive Δ*iscU-fdx*Δ*bfr*Δ*dps* mutant strain had no detectable iron in form of Fe-S clusters, 75% in NHHS Fe (II) and 20% in the baseline in form of iron stored in ferritin A. The rescued Δ*iscU-fdx*Δ*ftnA*Δ*dps*Δ*bfr* mutant strain however has a similar iron profile to the wild-type except it had no Fe (III) baseline signal.

2.4 Discussion

We have deleted the Isc system in *E. coli* thereby creating a mutant parent strain (annotated as Δ*iscU-fdx*) that is entirely dependent on the Suf pathway for viability. This mutant still retains both the IscS cysteine desulfurase (it serves as substrate for other metabolism in cell) and the IscR metalloregulatory proteins (regulator to the *suf* pathway).

Our results indicate that in the Δ*iscU-fdx* Δ*bfr* Δ*dps* iron storage mutant the Suf system cannot efficiently perform Fe-S cluster biogenesis under stress conditions even though the Suf system is highly expressed (Figure 2.22), indicating that the changes in intracellular iron pools may prevent Suf access to iron in those backgrounds (Figure 2.3). The Δ*iscU-fdx* Δ*bfr* Δ*dps* had a growth deficiency when 150μM or higher of 2,2-bipyridyl was introduced into the media. This strain didn't show this same growth

deficiency when it had functional *isc* pathway (Figure 2.7). This phenotype was also observed when the strain was exposed to by oxidative stress by PMS (Figure 2.6). This result indicates that the *bfr* and *dps* are both directly or indirectly influencing iron availability to the Suf pathway and have some redundancy between them since individual deletions didn't give a growth phenotype in the Δ*iscU-fdx* background.

Our results suggest that the FtnA iron storage protein, which plays a predominate role in iron storage under iron excess conditions, may inhibit the ability of the Suf system to construct Fe-S clusters under stress. We observed that the growth phenotype occurred when the strains were initially pre-grown in an iron rich media and then stressed with either oxidative stress (PMS) or iron starvation conditions (2,2-bipyridyl). When initially pre-grown in minimal media (iron poor) and then stressed, the Δ*iscU-fdx* Δ*bfr* Δ*dps* and strain grew better than the MG1655 strain. FtnA has been experimentally proven to be the main iron storage protein in *E.coli* and it's been shown to be up-regulated in iron rich environments. In the Δ*iscU-fdx* Δ*bfr* Δ*dps* mutant strain grown in the LB media, we postulate that the FtnA is upregulated and stores most of the available iron in a form that is not easily assessed by the Suf pathway. In the minimal media however, the FtnA expression will be repressed and there would be therefore be more available iron that can be accessed by the Suf pathway. This hypothesis is further supported by the fact that additional deletion of the *ftnA* gene actually rescues the BIPY and PMS sensitivity of the Δ*iscU-fdx* Δ*bfr* Δ*dps* strain.

Our results indicated that total cellular iron content did not necessarily correlate with sensitivity to stress. While the total cellular iron in Δ*iscU-fdx* Δ*bfr* Δ*dps* strain is lower than the wild-type and parent Δ*iscU-fdx* strains, the Δ*iscU-fdx*Δ*ftnA*Δ*bfr*Δ*dps* strain

had the lowest total cellular iron despite the fact it grew well under stress conditions. Further characterization of the iron pools in these mutants using the DFO chelator showed that the Δ*iscU-fdx* Δ*bfr* Δ*dps* had the highest free iron pool. However, the Δ*iscU-fdx* ΔftnA Δ*bfr* Δ*dps* strain (which shows no sensitivity to stress conditions) also had about a 4fold increase in labile iron pool compared to the wild-type or Δ*iscU-fdx* strains. This result indicates that the speciation of these labile iron pools is likely changing in the organism as opposed to total cellular or labile iron levels.

We characterized the mutant strains using whole-cell Mössbauer spectroscopy to determine if deletion of the iron storage proteins affects specific iron pools (Figures 2.9, 2.19). In the case of the stress-sensitive iron storage mutant strains Δ*iscU-fdx* Δ*bfr* Δ*dps*, we found that the signal from [4Fe-4S] $^{2+}$ clusters is nearly undetectable. This result indicates that Suf is further impaired in these mutant backgrounds. Surprisingly this BIPY and PMS sensitive strain showed increased total iron accumulation compared to wild-type and Δ*iscU-fdx* strains at high Fe levels (100μM). Cell-normalized total iron measurements using atomic absorption spectroscopy showed that total iron content in the Δ*iscU-fdx* Δ*bfr* Δ*dps* increased by approximately 2-fold compared to the parent Δ*iscU-fdx* strain (under high Fe growth). Along with this increase in total iron, there also is an increase in the baseline absorption representing NHHS Fe (III) (to about 20% of the total Fe). This signal indicates a likely increase in the amount of Fe (III) in FtnA which is still present. Thus the mutant is sensitive to BIPY and PMS despite the fact it has elevated total iron, indicating that the redistribution of iron into different pools likely accounts for the sensitivity rather than a decrease in total iron.

Whole-cell Mössbauer spectroscopy analysis of the Δ*iscU-fdx*Δ*ftn*AΔ*dps*Δ*bfr* a strain that was rescued for growth in BIPY and PMS showed a spectrum markedly similar to the WT strain (Fig. 2.19). In fact the amount of the Fe-S cluster central doublet/ Low Spin heme was nearly to the levels observed in the WT strain and was actually greater than that of the Δ*iscU-fdx* parent strain. This result suggests that at least part of the reason that Suf cannot fully complement the loss of Isc in the Δ*iscU-fdx* parent strain is because of the presence of FtnA. In addition to restoring Fe-S cluster biogenesis by Suf, the additional deletion of *ftnA* in the Δ*iscU-fdx* Δ*bfr* Δ*dps* strain reverses the iron over-accumulation phenotype and restored normal Fur regulation in M9 media under high iron conditions. The *iscU-fdx*Δ*ftnA*Δ*dps*Δ*bfr* spectrum also showed a much reduced NHHS Fe (III) signal compared to that of the Δ*iscU-fdx* Δ*bfr* Δ*dps* strain, possibly due to lack of iron incorporation into FtnA.

SufD levels were actually further increased by ferric citrate addition to the Δ*iscU-fdx*Δ*bfr*Δ*dps* strain. These results were quite surprising given that the strain has elevated total intracellular iron levels compared to the WT and Δ*iscU-fdx* strains and one would expect that SufD expression would actually be strongly repressed by Fe^{2+}-Fur under those conditions.[23] Suf expression may also be altered due to elevated oxidative stress. The OxyR regulon is activated in oxidative stress and induces *suf* expression.[25] This may have been potentiated by excess iron in the cell.

Clearly the exact speciation of that additional iron is key to its interaction with Fur and effects on iron-dependent regulation. Together the gene expression studies monitoring Suf expression and the Mössbauer spectroscopy analysis support the hypothesis that the iron storage proteins themselves represent distinct iron "pools" within

the cell that may not interface similarly with the Suf Fe-S cluster biogenesis pathway or the Fur iron regulatory network. Suf expression may also be altered due to elevated oxidative stress. The OxyR regulon is activated in oxidative stress and induces *suf* expression. This may have been potentiated by excess iron in the cell.

References

[1] Andrews, S.C., Robinson, A.K. and Rodriguez-Quinones, F. (2003). Bacterial iron homeostasis. *FEMS Microbiol Rev* 27, 215-37.

[2] Touati, D. (2000) iron and oxidative stress in bacteria. *Arch Biochem Biophys* 373, 1-6

[3] Winterbourn, C. C. (1995) Toxicity of iron and hydrogen peroxide: the Fenton reaction. *Toxicol Lett* 82-83, 969-974.

[4] Bradley, J. M., Le Brun, N. E. and Moore, G. (2016). Ferritins, furnishing the cells with iron. *J Biol Inorg Chem* 21, 13-28.

[5] Andrews, S. C. (2010) The Ferritin-like superfamily: Evolution of the biological iron storeman from a rubrerythrin-like ancestor, *Biochim Biophys Acta 1800*, 691-705

[6] Andrews, S.C. (1998). Iron storage in bacteria. *Adv Microb Physiol* 40, 281-351.

[7] Le Brun, N. E., Crow, A., Murphy, M. E. P., Mauk, A. G. and Moore, G. R. (2010). Iron core mineralization in prokaryotes. *Biochim Biophys Acta 1800*, 732-744

[8] Abdul-Tehrani, H. et al. (1999). Ferritin mutants of Escherichia coli are iron deficient and growth impaired, and fur mutants are iron deficient. *J Bacteriol* 181, 1415-28.

[9] Frolow, F., Kalb, A.J. and Yariv, J. (1993). Location of haem in bacterioferritin of *E. coli*. *Acta Crystallogr D Biol Crystallogr* 49, 597-600

[10] Yao, H., Wang, Y., Lovell, S., Kumar, R., Ruvinsky, A. M., Battaile, K. P., Vakser, I. and Rivera, M. (2012) The structure of the Bfr-Bfd complex reveals protein-protein interactions enabling iron release from bacterioferritin. *J Am Chem Soc* 134, 13470-13481.

[11] Grant, R.A., Filman, D.J., Finkel, S.E., Kolter, R. and Hogle, J.M. (1998). The crystal structure of Dps, a ferritin homolog that binds and protects DNA. *Nat Struct Biol* 5, 294- 303.

[12] Trefrey, A., Zhao, Z., Quail, M. A., Guest, J. and Harrison, P. (2009). How the presence of three iron binding sites affects the iron storage function of the ferritin (EcFtnA) of *Escherichia coli*. *FEBS Lett* 432, 231-218

[13] Johnson, M.K. (1998). Iron-sulfur proteins: new roles for old clusters. *Curr*

Opin Chem Biol 2, 173-181.

[14] ImLay, J.A. (2006). Iron-sulfur clusters and the problem with oxygen. *Mol Microbiol* 59, 1073-82.

[15] Agar, J.N., Krebs, C., Frazzon, J., Huynh, B.H., Dean, D.R. and Johnson, M.K. (2000). IscU as a scaffold for iron-sulfur cluster biosynthesis: sequential assembly of [2Fe-2S] and [4Fe-4S] clusters in IscU. *Biochem* 39, 7856-62.

[16] Zheng, L., Cash, V.L., Flint, D.H. and Dean, D.R. (1998). Assembly of iron-sulfur clusters. Identification of an *iscSUA-hscBA-fdx* gene cluster from *Azotobacter vinelandii*. *J Biol Chem* 273, 13264-72.

[17] Outten, F.W., Djaman, O. and Storz, G. (2004). A suf operon requirement for Fe-S cluster assembly during iron starvation in *Escherichia coli*. *Mol Microbiol* 52, 861-72.

[18] Dai, Y., and Outten, F. W. (2012) The *E. coli* SufS-SufE sulfur transfer system is more resistant to oxidative stress than IscS-IscU, *FEBS Lett 586*, 4016-4022.

[19] Woodmansee, A. L. and ImLay, J. A. (2002). Quantitation of intracellular free iron by electron paramagnetic resonance spectroscopy. *Meth Enzymol* 349, 3–9.

[20] Sezonov, G., Joseleau-Petit, D. and d'Ari, R. (2007). *Escherichia coli* Physiology in Luria-Bertani Broth. *J Bacteriol* 189,8746-8749.

[21] Eiseberg, R. C. and Dobrogoz, W. J. (1967). Gluconate metabolism in *Escherichia coli. J Bacteriol* 93,941-949.

[22] Cozzone, A. J. (1998). Regulation of acetate metabolism by protein phosphorylation In enteric bacteria. *Ann Rev Microbiol* 52, 127-16

[23] McHugh, J.P., Rodriguez-Quinones, F., Abdul-Tehrani, H., Svistunenko, D.A., Poole, R.K., Cooper, C.E. and Andrews, S.C. (2003). Global iron-dependent gene regulation in *Escherichia coli*. A new mechanism for iron homeostasis. *J Biol Chem* 278, 29478-86.

[24] Salvail, H., Boubannais, P., Sobota, J. M., Caza, M., Benjamin, J. M., Medieta, M. E. S., Lepine, F., Dozois, C., ImLay, J. and Masse, E. (2010). A small RNA promotes siderophore production through transcriptional and metabolic remodeling. *PNAS* 107, 15223-15228.

[25] Jang, S., and ImLay, J. A. (2010) Hydrogen peroxide inactivates the *Escherichia coli* Isc iron-sulfur assembly system, and OxyR induces the Suf system to compensate, *Mol Microbiol 78*, 1448-1467.

CHAPTER THREE
FtnB may pay a role in iron donation to the Suf pathway

Abstract

The *Escherichia coli* genome encodes at least four putative ferritins: Ferritin A (FtnA), Bacterioferritin (Bfr), DNA binding protein of starved cells (Dps) and a ferritin-like protein designated Ferritin B (FtnB). The coexistence of multiple ferritins within *E. coli* suggests that they may fulfill disparate physiological roles and/or are expressed under different conditions. FtnB, which lacks the conserved ferroxidase site conserved in other ferritins has not been characterized in *E.coli.* In this study, we characterize the possible role of FtnB for Suf Fe-S cluster assembly in *E. coli.* We found that the deletion of the FtnB and Bacterioferritin proteins caused an inability for the strain to make Fe-S clusters. Our studies therefore indicate that the FtnB protein plays a role in iron donation to the *suf* pathway.

3.1 Introduction

The *Escherichia coli* genome encodes at least four putative ferritins: Ferritin A (FtnA), Bacterioferritin (Bfr), DNA binding protein of starved cells (Dps) and a ferritin-like protein designated Ferritin B (FtnB). The coexistence of multiple ferritins within *E. coli* suggests that they may fulfill disparate physiological roles and/or are expressed under different conditions.[1] FtnB, sometimes annotated as YecI, has not been characterized in *E.coli.* It's been shown to lack several of the key amino acid residues comprising the ferroxidase centre of other ferritins (Figure 3.1). It shares the highest peptide percent identity with FtnA (32.335%) compared to Bfr (14%) and Dps (10.4%).[2] Transcriptional expression of FtnB is upregulated by Fe^{2+}-Fur binding at the Pribnow box upstream to prevent binding of other repressors[3] (Figure 1.2). A recent study in *Salmonella Typhimurium* however suggests it plays an important role in Fe-S cluster repair and virulence. The protein characterized for the first time was shown to exacerbate oxidative stress in absence of other ferritins and be required for full Salmonella virulence and efficient repair of Fe-S cluster containing enzymes. However, in contrast to its regulation in *E.coli,* it was expressed during iron-restricted conditions and repressed by Fur.[4] It has been proposed that FtnB might not function as a real ferritin but rather function as a store of Fe^{2+} that can be readily mobilized for the repair of damaged Fe-S clusters.[5]

In this study, we characterize the possible role of FtnB for Suf Fe-S cluster assembly in *E. coli.* We examine its possible contribution on intracellular free iron, susceptibility to oxidative stress and possible iron donation to the Suf Fe-S cluster pathway. To test whether the Suf system directly or indirectly accesses iron from one or more iron storage proteins *in vivo*, we constructed a mutant strain with the Iron Sulfur

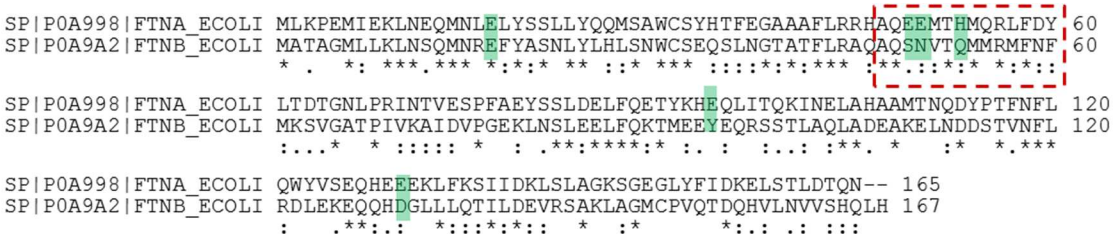

Figure 3.1. Sequence comparisons of FtnA and FtnB. The areas shaded in green are the binding iron binding sites in FtnA Sequence generated using ClustalW

Cluster (Isc) housekeeping pathway inactivated in the background (Δ*iscU-fdx)*.

This ensured that the strain was completely dependent on the Suf pathway for its Fe-S cluster biogenesis. Various mutants were then constructed by further deleting FtnB singly and in combination with other iron storage proteins in this Isc inactivated background

3.2 Materials and Methods

Recombineering. *E.coli* wild-type strain mG1655 was the parent strain for all studies. The gene deletions were constructed as described previously. Briefly, a kanamycin resistance cassette was amplified from pKD4 primer pairs containing approximately 35bp of sequence homologous to regions upstream and downstream of the target genes. The PCR products were transformed into NM400 expressing the **λ-** Red recombinase system, resulting in placement of the target gene with the Kan^R cassette. Mutations were moved by P1 transduction into wild-type MG1655. In some cases, the Kan cassette was removed from a single mutant strain after transformation with the pCP20 plasmid so that the double mutant strains could be conducted by P1 transduction. Colonies will be selected and screened for positive recombinants by colony PCR using the primers designed to detect each point mutation. Mutations will be confirmed by sequencing.

Growth medium and conditions. For bacterial growth, an individual colony was transferred from fresh Lennox Broth (LB) agar plates into either LB media or M9 glucose minimal media containing 1X M9 minimal salts (Sigma-Aldrich), 0.2% (w/v) glucose (Acros Organics), 0.2% (w/v) magnesium chloride (Sigma-Aldrich) and 0.1mM calcium chloride (Sigma-Aldrich). Cultures were grown in LB or M9 minimal media for 18hours and 24 hours respectively at 37°C and 200rpm. When necessary, kanamycin (30μg/mL)

or chloramphenicol (25µg/mL) was added to the media. For cells grown under various iron conditions, different concentrations of ferric citrate were added to the 0.2% glucose M9 minimal media. For cell growth curves, the cell growth was monitored by UV-Vis absorption at 600nm and plotted versus time in hours. For sensitivity assays, the cells were collected, washed in sterile 1 X M9 minimal salts and normalized to a final OD_{600} of 0.04 in M9 minimal media with 0.2% (w/v) gluconate (Alfa Aesar) containing varying amounts of 2,2-bipyridyl (BIPY) or Phenazine Methosulfate (PMS). Cell density (final optical density at 600nm) was measured after 24-hr growth at 37°C and assays were performed in triplicate.

Whole cell EPR spectroscopy: A protocol was adapted from the ImLay and Kiley Labs. Cells were grown overnight aerobically in 250 mL of LB before harvesting by centrifugation. Cells were collected by centrifugation at 8,000 x g for 20min at 4°C. The pellet was re-suspended using 10mL of pre-warmed M9 gluconate media supplemented with 10mM diethylenetriaminepentaacetic acid (DTPA) (Sigma-Aldrich), 20 mM desferrioxamine mesylate salt (DFO) (CalBiochem) and incubated for 10 min at 37°C at 200rpm in a 250mL flask for proper oxygenation. The cells were then centrifuged, washed with cold 20 mM Tris-HCl, pH 7.4and re-suspended in a final volume of 0.5 volumes (relative to the pellet volume) of 20 mM Tris-HCl, pH 7.4, 30% glycerol to give a final glycerol concentration of approximately 10-15%. A 300µL volume of the re-suspended cells was loaded into a 3-mm quartz EPR tube (Norell Incorporated, NC) and immediately frozen in liquid N_2. A sample of each cell suspension was diluted 200x to obtain a final OD_{600}. Samples were stored in liquid N_2 until EPR measurements were performed. Ferric-DFO standards were prepared over a range from 0µm to 100µm $FeCl_3$

Table 3.1 Bacterial Strains

Strain	Relevant Genotype Or Phenotype	**Reference or Source**
Primers	Sequence 5' to 3'	
FtnB_PS1	ATCTTGCACCTCTCCACTTCTGGATATAAGG ATATTAGGTGTAGGCTGGAGCTGCTTC CAAAACCTTCATCGGCGCAATGCATTAGCGC	This Study
FtnB_PS2	CGATGATGACATATGAATATCCTCCTTAG	This Study
FtnB_up	ACATTTCGGACCGGCAGAAAGG	This Study
FtnB_down	CCGCTGCTTCAAACAGATGAG	This Study
E.coli Strains		
MG1655	Wild Type. *E. coli,* K12	Laboratory Strain
Δ*iscU-fdx*	Δ*iscU-fdx*	Laboratory Strain
BN001	Δ*iscU-fdx*_Δ*bfr::kan*^{R}_Δ*dps::cm*^{R}	This Study
BN006	Δ*ftnB::cm*^{R}	This Study
BN007	Δ*iscU-fdx*_Δ*ftnB::cm*^{R}	This Study
BN008	Δ*iscU-fdx*_Δ*bfr::kan*^{R}_Δ*ftnB::cm*^{R}	This Study
BN009	Δ*iscU-fdx*_Δ*ftnA::kan*^{R}_Δ*ftnB::cm*^{R}	This Study
BN010	Δ*iscU-fdx*_Δ*dps::kan*^{R}_Δ*ftnB::cm*	This Study
Δ*fur::kan*^{R}	Δ*fur::kan*^{R}	Laboratory Strain

in 20 mM Tris-HCl, 1mM DFO, 10% glycerol, pH 7.4. The EPR signals were measured with a Bruker EMX X-band spectrometer (Rheinstetten, Germany). EPR parameters used were as follows: centerfield: 1564 G; sweep width: 500 G; Temp: 110K, Modulation frequency: 100KHz, Modulation amplitude: 12.5 Gauss, Modulation phase: 0, Harmonic: 1, Receiver gain: 60, Time constant: 20.4 ms, Field: 301.25-2801.25 Gauss, g factor: 4.3, Attenuation: 16, Power: 5mW, number of scans, 10. Fe levels were quantified by normalizing the amplitude of the Fe signal of the samples to the Fe-DFO standards, and internal concentrations were calculated using the cell density and intracellular volume.

Western Blot Analysis: Cells were prepared as described above and pelleted at 6,000 x g for 20 mins. The pellets were lysed by sonication or Bacterial Protein Extraction Reagent (B-PER) (ThermoScientific) and the protein concentration checked using the Bradford assay. Equal total protein amounts were electrophoresed on a 15% SDS PAGE gel. Proteins were transferred to nitrocellulose membrane and blocked overnight with 80% Odyssey blocking buffer (Li-Cor) in 1 X TBS (50 mM Tris-HCl pH 8.0, 150 mM NaCl) at 4□C. Primary antibody incubations with α-SufD (1:5000), α-Bfr (1:1000), or α-FtnA (1:2000) were performed in 40% blocking buffer in 1 X TBST (TBS + 0.001% Tween-20). After 2 hours incubation at room temperature with shaking, membranes were washed 5 times (10 min each) with copious amounts of 1 X TBST. Then they were incubated with goat α-rabbit secondary antibody (1:20,000) at room temperature with shaking for 45 min. Membranes were washed with 1 X TBS and scanned using an Odyssey Infrared Imager (Li-Cor).

Primer extension assay: RNA was extracted from MG1655 and the mutant strains by using the acid phenol method. The *fepA* primer was labeled by [γ-^{32}P] ATP using T4

polynucleotide kinase (NEB). Primer extension with Superscript II reverse transcriptase (Invitrogen) was carried out according to manufacturer instructions. 8µg of total RNA was used as a template for cDNA synthesis. The cDNA products were separated on an 8% polyacrimide gel. The gel was dried and exposed to CL-XPosure film (ThermoScientific).

Atomic Absorption Spectroscopy. Intracellular iron content was calculated using the atomic absorption spectroscopy (AAS). Cells were grown to desired growth phase in M9 minimal media and harvested, centrifuged at 4000 x g for 20 mins and then pelleted three times at 16,000 x g with intermediate washing in ICP-MS wash solution consisting of 50 mM EDTA tetrasodium salt, 100 mM Sodium Oxalate, 300 mM NaCl and 10 mM KCl to remove any cell surface associated metal ions. Washed cell pellets were re-suspended in 1 mL 3% NaCl. The OD_{600} and volume of the cell suspension after the last wash was recorded. Cells digested in 300 µL concentrated nitric acid for 10 hours at 70ºC and diluted to get an avid matrix of 3.5% in MilliQ water. Iron standards were prepared in MilliQ water. Iron analysis of fractions was performed on a PerkinElmer PinAACle 900T graphite furnace atomic absorption spectrometer using the manufacturer's recommended conditions.

Mössbauer Analysis: Cells were initially grown in 35mL M9 glucose minimal media for 24 hours at 37□C at 200rpm. The overnight culture was then used to inoculate a 1L M9 glucose minimal media supplemented with 10 µM and 100 µM ^{57}Fe(III) citrate. 10 mM ^{57}Fe(III) citrate stock solution was prepared by dissolving 100mg ^{57}Fe metal powder (IsoFlex USA) in 2 mL minimal amount aqua regia which is a 3:1 mixture of trace metal grade nitric acid (TMG) to trace metal grade hydrochloric acid (Fischer Scientific) while

stirring. Once dissolved, the solution was further diluted to a final volume of 100 mL. This stock was then treated with a 3-fold molar excess of sodium citrate (Fisher Scientific) while stirring. The solution was adjusted to pH 5 with 1 M NaOH (EMD Chemicals) resulting in a final ^{57}Fe concentration of 10 mM. Cells were grown to desired growth phase, harvested and centrifuged at 6,000 x g for 20min. The pellet was washed in 40 mL wash solution comprising 50 mM EDTA tetrasodium salt, 100 mM Sodium Oxalate, 300 mM NaCl, 10 mM KCl and centrifuged for at 4,000 x g for 20min. The wash solution was fully removed from the pellet and it was packed into Mössbauer cups and immediately frozen in liquid nitrogen prior to analysis.

Mössbauer spectra were collected at the Texas A&M and analyzed in the Dr. Paul Lindahl lab by Joshua Wofford. Mössbauer spectra were recorded on MS4 WRC 4.5 to 300 K closed-cycle Helium-refrigerated system and a W106 temperature controller) and LHe6T spectrometers (SEE Co., Edina, MN), the latter of which is capable of generating 0–6 T fields. Both were calibrated using α-Fe foil. Spectra was analyzed at 5K and 0.05T and the resulting spectra were fitted over different iron species including Non-Heme Fe (II), Non Heme Fe (III) and Low Heme Fe fits.

3.3 Results

FtnB and Bfr may act as Iron sources to the Suf Pathway during stress conditions.

To test if FtnB could donate iron to the Suf pathway we constructed a strain that was wholly dependent on the Suf pathway both during normal housekeeping and stress conditions. To do this, we selectively deleted part of the Isc pathway to create the Δ*iscU-fdx* strain retaining *iscR,* a global regulator of Fe-S cluster assembly and *iscS* that donates

sulfur to other metabolic pathways. In this parent strain Isc is disrupted. We then deleted FtnB alone or in combination with other iron storage proteins in this background (Table 3.1)

We first checked the growths of the mutants in the absence of stress in two types of media broth, the complex media Lennox Broth (LB) and the chemically defined M9 glucose minimal media. LB is a rich, iron replete complex media containing several carbon sources and optimal levels of small molecule metabolites (i.e. amino acids) required for growth.[6] In contrast, M9 minimal media is limited for most nutrients and metals as compared to LB and only provides a single, controlled carbon source to support growth. Minimal media therefore allows a greater control over which nutrients and metals the cells are exposed to.

To test whether disruption of iron storage proteins affects sensitivity to iron deprivation, varying concentrations of the cell permeable iron chelator 2,2-bipyridyl (BIPY) were added to the growth media and the final optical density measured after 24 hours of growth in M9 gluconate minimal media. Growth on M9 gluconate minimal media occurs via the Entner-Duodoroff pathway that requires Phosphogluconate dehydratase (Edd) which contains a [4Fe-4S] cluster.[7] Disruption of Suf Fe-S cluster biogenesis in the Δ*iscU-fdx* strains will therefore result in that mutant being sensitive to environmental stress in M9 gluconate media. None of the mutations were lethal.

A timed growth assay with no stress showed that the Δ*iscU-fdx*Δ*ftnB*Δ*bfr* mutant strain had an extended lag phase compared to both the parent Δ*iscU-fdx* strain and WT strain in M9 minimal media. This lag phase was exacerbated when 10μM iron was added to the minimal media (Figure 3.2).

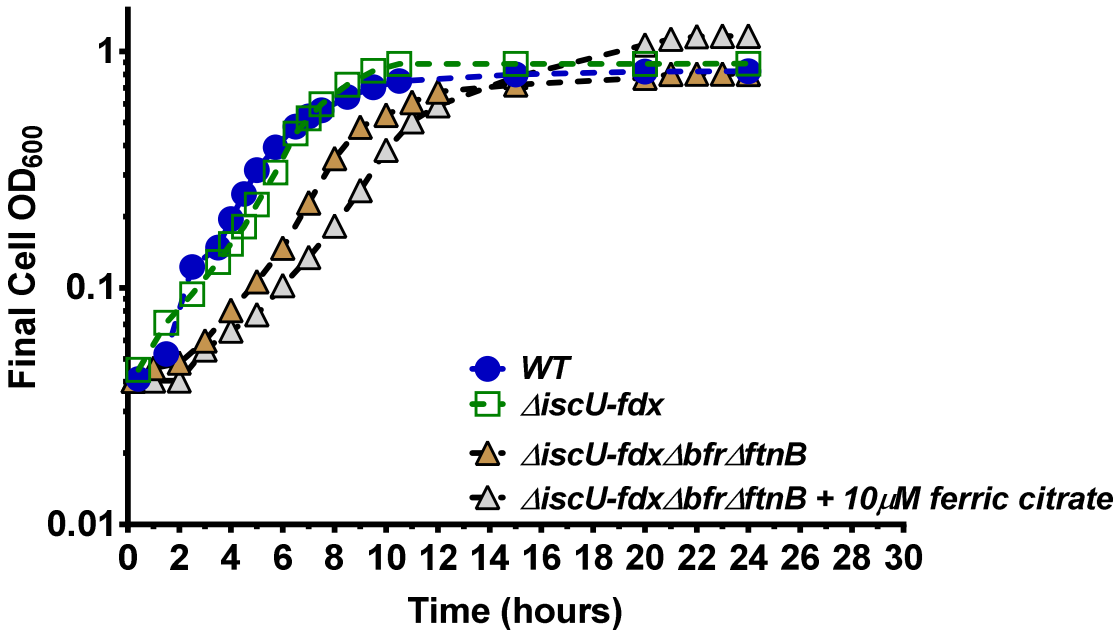

Figure 3.2. The Δ*iscU-fdx*Δ*ftnB*Δ*bfr* strain shows an extended lag phase duration when pre-grown in minimal media with no stress which becomes more severe with addition of iron. All strains were grown in M9 glucose minimal media for 24 hours and then washed and normalized to same starting OD_{600} in fresh M9 glucose minimal media for 24 hours. Cell density was measured initially every 30 mins until they exited lag phase, and then hourly. All growths were repeated in triplicate (n=3) and error bars indicate one standard deviation from the mean value.

We observed that while individual deletion of FtnB didn't make the parent Δ*iscU-fdx* sensitive to oxidative and iron starvation stress, the double mutant Δ*iscU-fdx*Δ*ftnB*Δ*bfr* strain showed a marked sensitivity to the stress conditions when pre-grown in the nutrient and iron rich media LB media before being transferred to an iron limiting stress media (gluconate media with dipyridyl) (Figure 3.3). The sensitive growth phenotype was also observed when strains were stressed with phenazine methosulfate to induce oxidative stress.

When the strains were initially grown in a somewhat iron limited media (M9 glucose minimal media) before being shifted to M9 gluconate minimal media with varying concentrations of 2,2-bipyridyl, the Δ*iscU-fdx*Δ*ftnB*Δ*bfr* strain showed no sensitivity and grew to a final cell density slightly higher than the wild-type control strain (Figure 3.5). This phenotype is similar to the Δ*iscU-fdx*Δ*bfr*Δ*dps* mutant strain. This shows that when the strain is a pre-adapted to low iron conditions, they are able to withstand the stress effects caused by the presence of the iron-chelator, BIPY. These results together indicate that in the Δ*iscU-fdx*Δ*ftnB*Δ*bfr* strain, the Suf system cannot efficiently perform Fe-S cluster biogenesis under stress conditions.

The Δ*iscU-fdx*Δ*ftnB*Δ*bfr* strain has impaired Fe-S cluster function

Since growth of the Δ*iscU-fdx* Δ*ftnB* Δ*bfr* strain is sensitive to 2,2 bipyridyl, we tested if this was indeed due to an inability to form iron sulfur clusters. Therefore, cellular iron speciation in the mutant and parent strains was analyzed by Mossbauer Spectroscopy. The cells of interest were initially pre-grown in M9 glucose minimal media to stationary phase. These were then used to inoculate fresh media at a cell optical density of 0.04 and grown to mid-log phase (OD_{600} 0.5) in glucose (0.2%) M9- salts

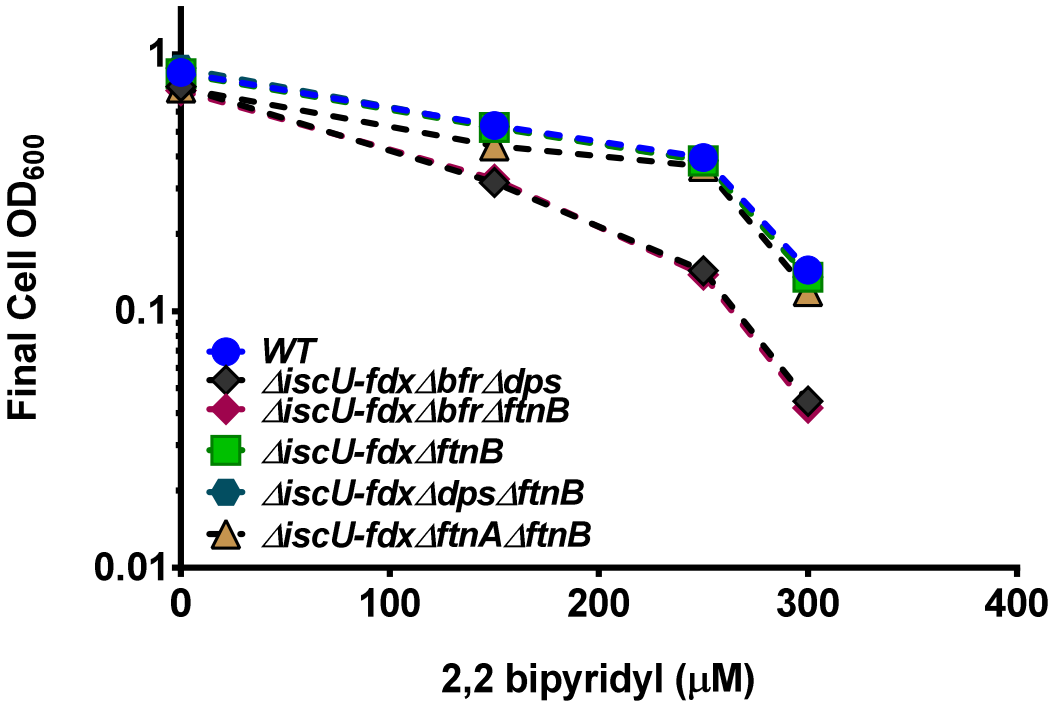

Figure 3.3. The deletion of both *ftnB* and *bfr* sensitizes the Δ*iscU-fdx* strain to bipyridyl stress. All strains were grown in LB for 18 hours. After this, they were washed and inoculated into fresh 0.2% gluconate minimal media with varying concentrations of BIPY. The final cell density was measured after 24 hours. All growths were repeated in triplicate (n=3) and error bars indicate one standard deviation from the mean value.

medium containing 100 μM ^{57}Fe citrate. The cells were washed, cooled in liquid nitrogen and then analyzed by Mossbauer spectroscopy at 60K. In the spectrum of the Δ*iscU-fdx*Δ*ftnB*Δ*bfr,* the central doublet mostly representing $[4Fe\text{-}4S]^{2+}$ / Low Spin Heme (LSH) is nearly undetectable indicating that those strains have increased difficulty with making iron sulfur clusters (Figure 3.6). This spectra was similar to the parent Δ*iscU-fdx* strain in lack of detectable Fe-S clusters, but it also had a much less Non High Heme Spin Fe (III) content compared to it. This is the iron in baseline which is stored in ferritins especially ferritin A.

In the stains, it was observed that there existed 2 NHHS Fe (II) pools. One coordinated to oxygen/nitrogen ligands and denoted Fe (II)A and the other coordinated to sulfur ligands and denoted Fe (II)B. Both pools together make the combined NHHS Fe (II) content. Results show that the sensitive Δ*iscU-fdx*Δ*ft*n*B*Δ*bfr* mutant strain had similar NHHS Fe (II)B iron content to the parent Δ*iscU-fdx* but different NHHS Fe (II)A pools. The Δ*iscU-fdx*Δ*ft*n*B*Δ*bfr* mutant strain had 2 completely different NHHS Fe (II) A and NHHS Fe(II)B concentrations compared to the wild-type.

To further prove that the sensitivity in the Δ*iscU-fdx*Δ*bfr*Δ*dps* strain is caused by impaired Fe-S cluster function, we tested the strains in another growth assay in M9 minimal media using Sodium acetate as the carbon source. Cells grown on acetate by-pass glycolysis to go through the glycoxylate shunt and Tri-Carboxylic Acid (TCA) cycle for all cellular metabolism. The TCA cycle has enzymes that contain Fe-S cluster e.g. aconitase. Acetate growth requires respiration for all cellular synthesis. The respiratory complexes I and II contain many Fe-S clusters.[8] Any mutant strain that has difficulty assembling Fe-S clusters will therefore show a dramatic growth phenotype in this media.

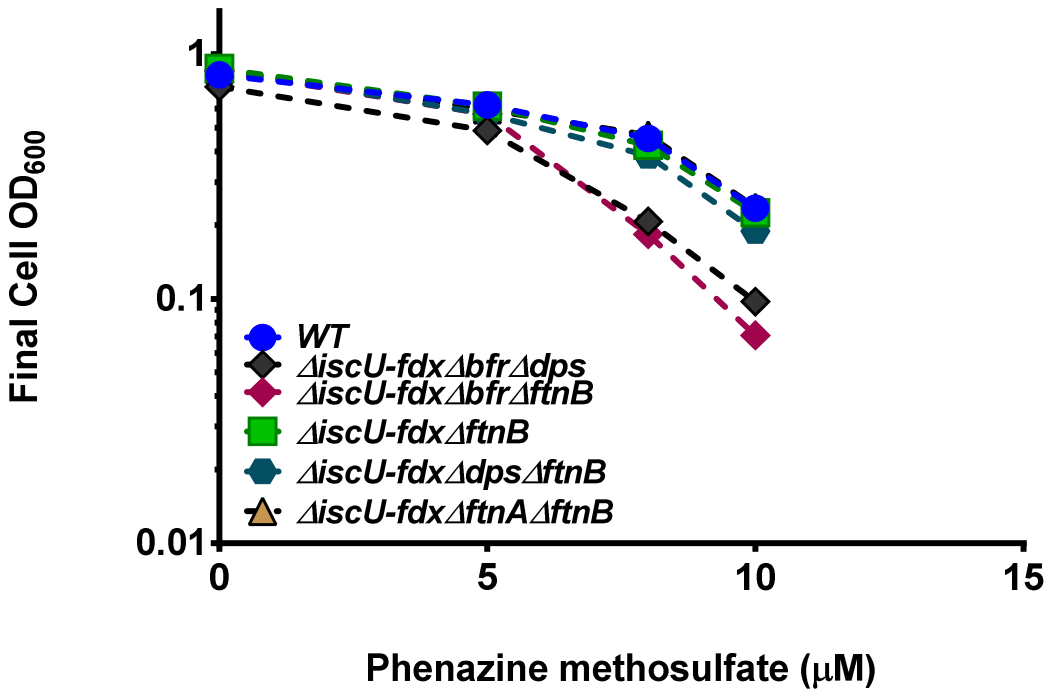

Figure 3.4. The deletion of both *ftnB* and *bfr* sensitizes the Δ*iscU-fdx* strain to Oxidative stress. All strains were grown in LB for 18 hours. After this, they were washed and inoculated into fresh 0.2% gluconate minimal media with varying concentrations of BIPY. The final cell density was measured after 24 hours. All growths were repeated in triplicate (n=3) and error bars indicate one standard deviation from the mean value.

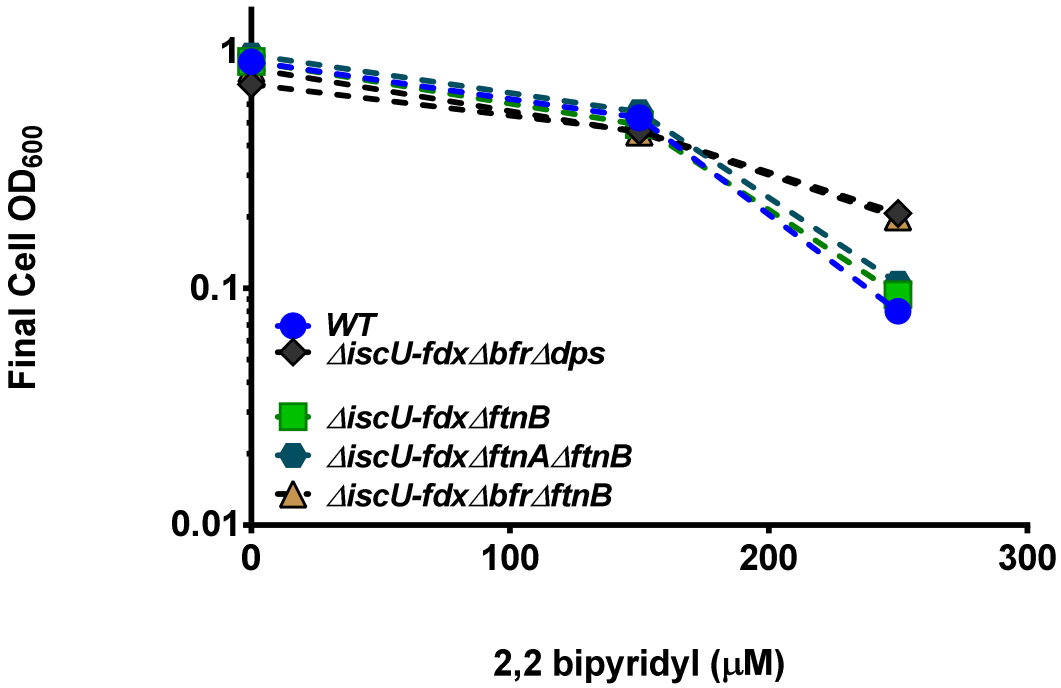

Figure 3.5. Pre-adaptation to low iron media rescues the sensitivity of the Δ*iscU-fdx* Δ*ftnB*Δ*bfr* strain to dipyridyl. All strains were grown in 0.2% glucose minimal media for 24 hours. After this, they were washed and inoculated into fresh 0.2% gluconate minimal media with varying concentrations of BIPY. The final cell density was measured after 24 hours. All growths were repeated in triplicate (n=3) and error bars indicate one standard deviation from the mean value.

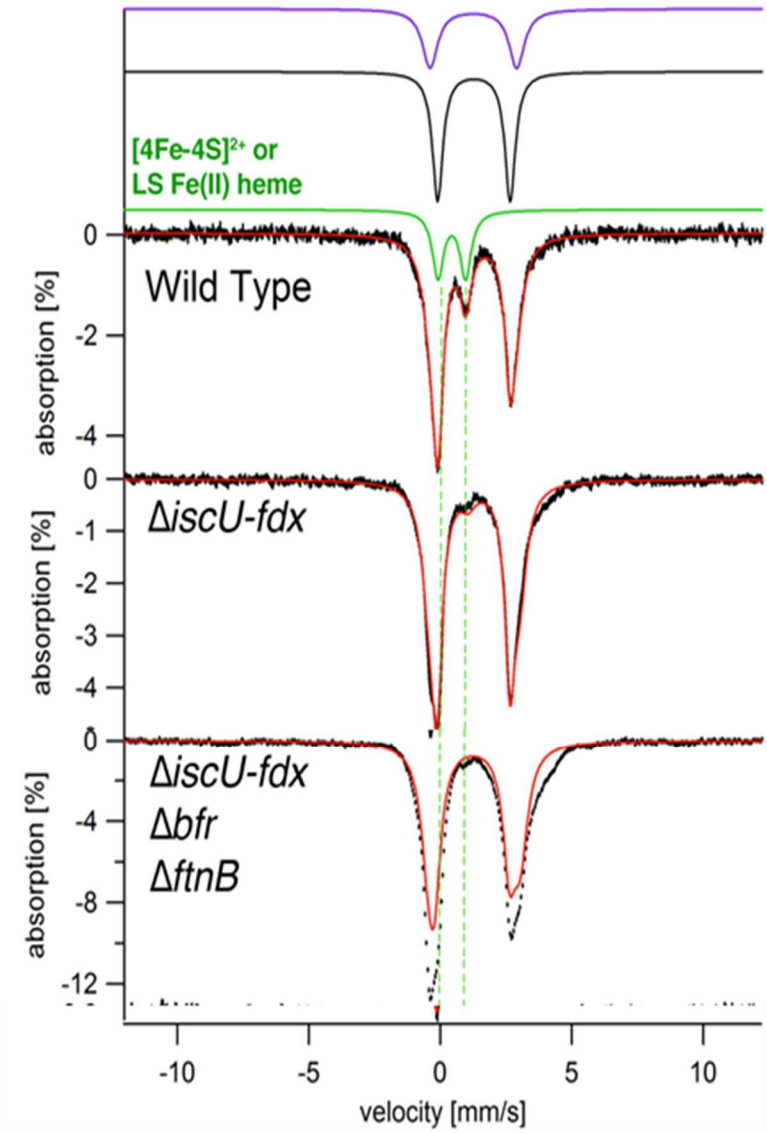

Figure 3.6. The Δ*iscU-fdx*Δ*ftnB*Δ*bfr* strain has virtually no Fe-S cluster assembly function. Whole-cell Mössbauer spectroscopy of indicated strains of *E. coli* grown in M9 glucose media with 100 μM ^{57}Fe(III)-citrate. Spectra were collected at 5 K, 0.05 T. The purple, black, and green lines above the spectrum are simulations of the various spectrum components assuming δ=1.28 mm/s, ΔE_Q = 2.76 mm/s, 45% area (purple); δ=1.26 mm/s, ΔE_Q = 3.3 mm/s, 30% area (black); and δ=0.44 mm/s, ΔE_Q = 1.05 mm/s, 25% area (green). The Fe-S/heme "central doublet" is shown in green. Green dashed lines are used to indicate positioning of that doublet in all traces. The red line over the black trace of the raw data is the best fit simulation of the spectrum. strains were initially grown in 0.2% glucose minimal media for 24 hours and then used to inoculate a 1L 0.2% glucose minimal media culture with added 100 um ^{57}Fe(III)-citrate. The cells were harvested at mid-log phase, washed and frozen in liquid Nitrogen for Mossbauer analysis.

Table 3.2 Mössbauer iron speciation and percentages

	MG1655	**Δ*iscU-fdx***	**Δ*iscU-fdx*Δ*ftnB*Δ*bfr***
Non-heme High Spin Fe (II)A	50%	51%	35%
Non-heme High Spin Fe (II)B	23%	39%	40%
Central Doublet / Low Spin Heme	20%	3-5%	-
Non-Heme High Spin Fe(II)I	10%	5%	25%
Iron adsorption percent effect	4%	4%	11%

The Δ*iscU-fdx* had a slight growth phenotype in this media but the sensitive Δ*iscU-fdx*Δ*ftnB*Δ*bfr* strain was even more sensitive in this media (Figure 3.7) indicating that this strain had more difficulty than the parent Δ*iscU-fdx* in Fe-S cluster assembly.

Since we tested that the Δ*iscU-fdx*Δ*ftnB*Δ*bfr* strain had impaired Fe-S cluster assembly functions, we wanted to check if it was due to the Suf system not being properly expressed, or if iron importers in the strain had been affected. The α-SufD (Figure 3.8) showed that the Δ*iscU-fdx*Δ*ftnB*Δ*bfr* strain expressed the Suf pathway adequately in minimal media and also that which was supplemented with 10 μM ferric citrate. This indicates that the impairment is not due to an abnormal function of the Suf pathway. It had elevated SufD expression compared to the Δ*iscU-fdx* parent strain. We checked the transcription levels of FepA, an iron importer[9] both with and without iron starvation in form of 250 μM BIPY. Transcript levels for all the strains were practically undetectable in LB media without BIPY added. That indicates the iron demand was negligible as they had adequate iron in the cells.

When stressed with 250 μM BIPY, the *fepA* transcript was upregulated in all the strains as the cells needed to increase the iron supply to match the increased cellular demands. However, in the Δ*iscU-fdx*Δ*ftnB*Δ*bfr* mutant it wasn't as expressed as in the wild-type or parent Δ*iscU-fdx* strain (Figure 3.9A). In the cells initially grown on 0.2% glucose minimal media (iron-limited), the transcript level was repressed in the wild-type when it was stressed in the 250 μM BIPY.

In both the Δ*iscU-fdx*Δ*ftnB*Δ*bfr* and the Δ*iscU-fdx* parent strains, the expression levels remained fairly equal in both control and stressed conditions although the Δ*iscU-fdx*Δ*ftnB*Δ*bfr* had the lowest expression (Figure 3.9B).

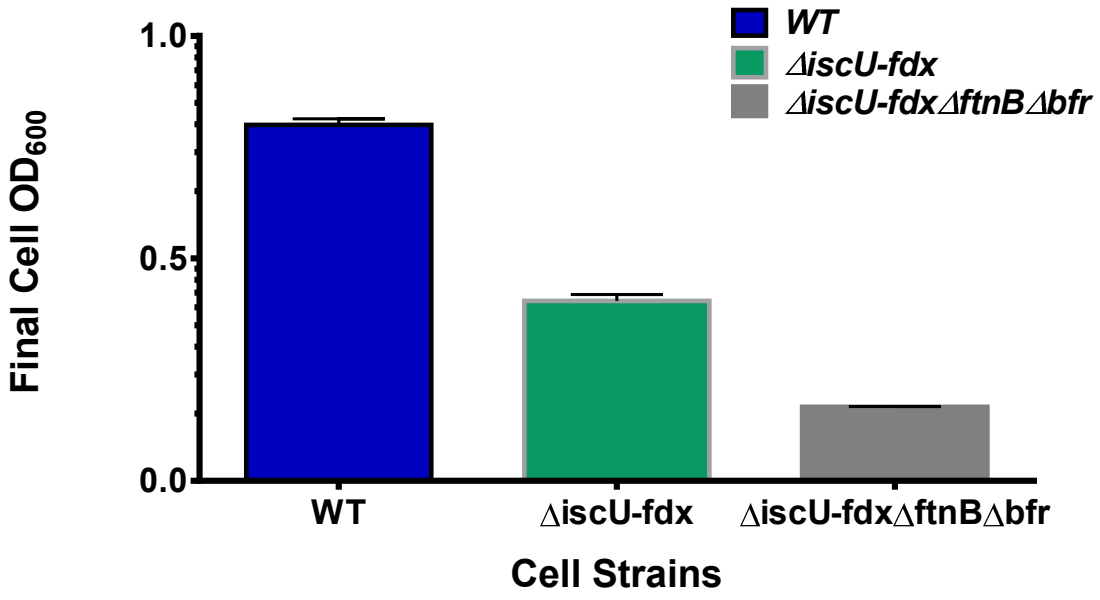

Figure 3.7. The Δ*iscU-fdx*Δ*ftnB*Δ*bfr* strain shows a growth phenotype in M9 acetate growth.. All strains were grown in M9 glucose minimal media for 24 hours for 18 hours and then washed and normalized to same starting OD_{600} in fresh M9 sodium acetate minimal media for 24 hours. Cell density was measured after 48 hours. All growths were repeated in triplicate (n=3) and error bars indicate one standard deviation from the mean value.

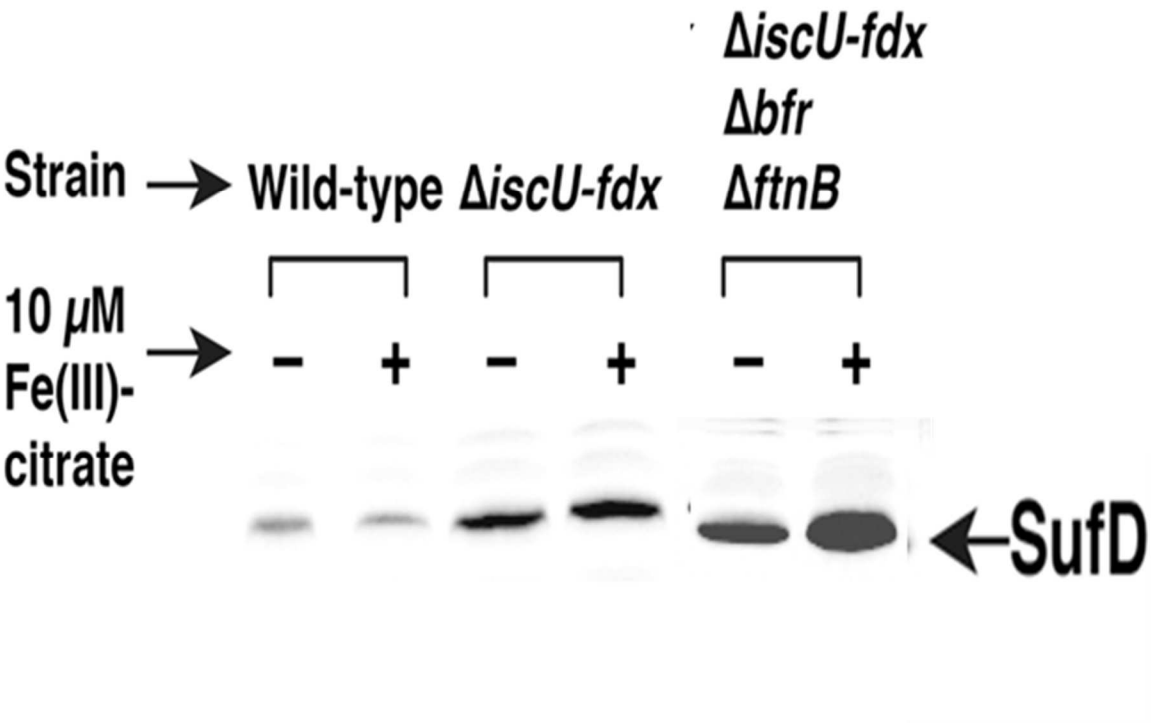

Figure 3.8. Suf expression upregulated in the Δ*iscU-fdx*Δ*ftnB*Δ*bfr* mutant strain. Western blot analysis of equal amounts of total protein from *E. coli* strains grown in M9 glucose minimal media with or without 10 μM Fe(III)-citrate using α-SufD antibodies.

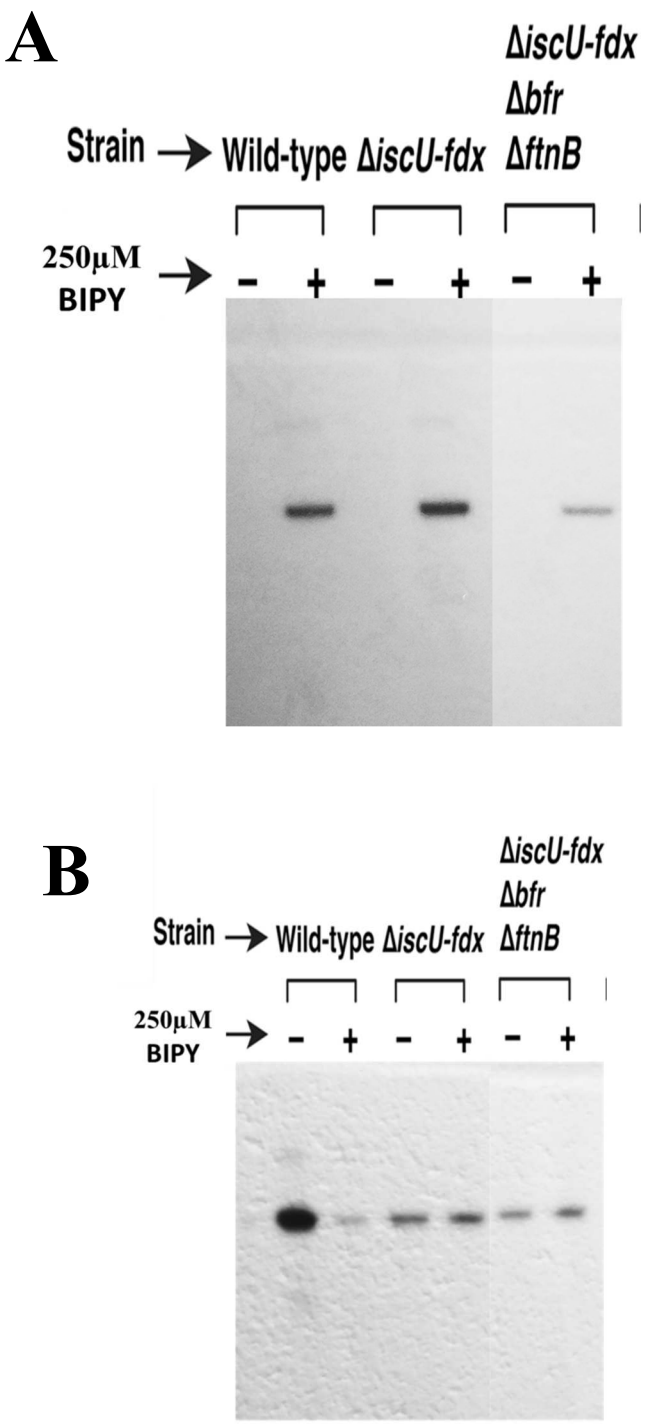

Figure 3.9. Transcriptional activity of FepA. Cells were grown in (A) LB and (B) M9 Glucose minimal media to mid-log phase (0.5), some harvested as the control probe and the remaining induced for 1 hour with 250μm BIPY for 1

Inactivation of bfr and ftnB raises the intracellular free Fe concentration

Free Fe concentrations in LB-cultured stationary phase cells were measured as desferrioxamine-chelatable Fe by EPR spectroscopy. The intracellular free Fe pool exists predominantly in the Fe^{2+} form, the EPR signal of which is non-existent. However, the cell-permeable Fe chelator desferrioxamine facilitates oxidation of the Fe^{2+}, and the resulting Fe^{3+}-desferrioxamine chelate exhibits a sharp EPR signal at g = 4.3. Moreover, protein-bound Fe does not resonate at this g-value. A Δ*fur* strain, which served as a positive control, showed free Fe levels more than twice as high as wild type (Figure 3.10). This increase in free Fe is presumably a consequence of constitutive Fe assimilation in this strain. Labile (DFO-chelatable) iron is higher in the Δ*iscU-fdx*Δ*ftnB*Δ*bfr* mutant strain compared to the wild-type and the parent *iscU-fdx* parent strain. It was also higher than the un-sensitive Δ*iscU-fdx*Δ*ftnB*Δ*ftnA* strain (Figure 3.9).

3.4 Discussion

We have deleted the Isc system in E. coli thereby creating a mutant parent strain (annotated as ΔiscU-fdx) that is entirely dependent on the Suf pathway for viability. This mutant still retains both the IscS cysteine desulfurase (it serves as substrate for other metabolism in cell) and the IscR metalloregulatory proteins (regulator to the suf pathway).

Surprisingly, our results indicate that the FtnB protein may play a role in possible iron donation to the Suf pathway. The FtnB protein has been thought to be redundant or lack true ferritin activities since it lacks all the conserved residues for ferroxidase activity. Our results however indicate that it may serve a functional redundancy with the Bfr

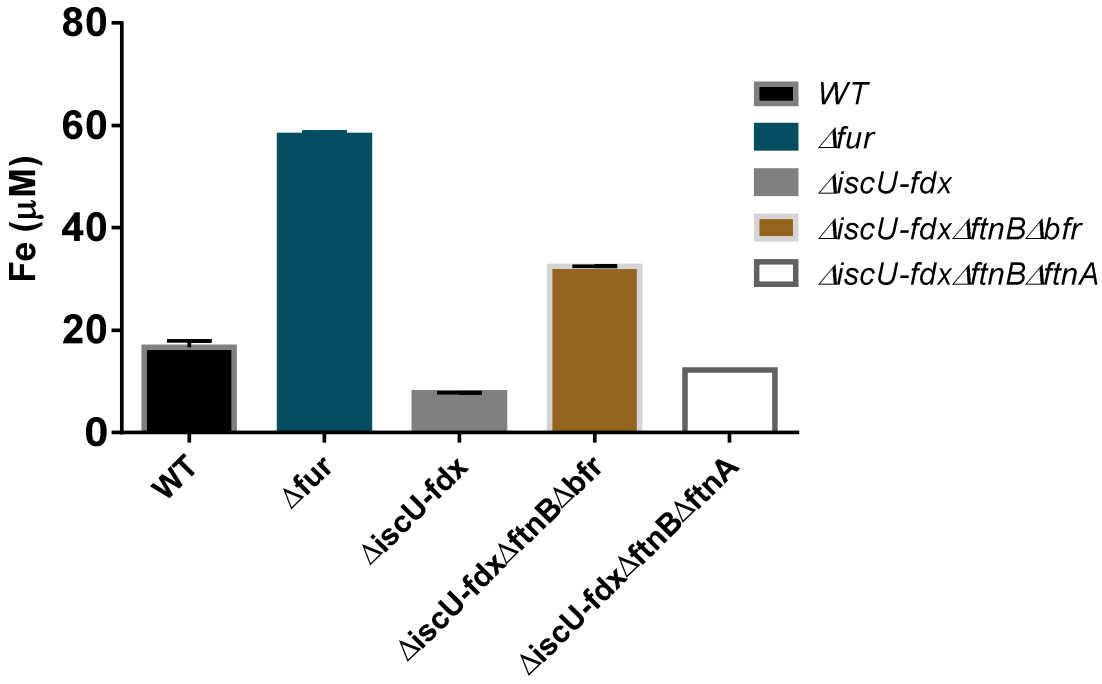

Figure 3.10. Labile iron pools are higher in the Δ*iscU*Δ*ftnB*Δ*bfr* strain. Intracellular, DFO-labile iron concentrations normalized to cell volume and number.

protein in possible iron donation to the Suf pathway. We showed that in the Δ*iscU-fdx*Δ*ftnB*Δ*bfr* iron storage mutant the Suf system cannot efficiently perform Fe-S cluster biogenesis under iron starvation (Figure 3.3) conditions even though the Suf system is highly expressed (Figure 3.8) and iron import systems are fully expressed (Figure 3.9) indicating that the changes in intracellular iron pools may prevent Suf access to iron in those backgrounds. The Δ*iscU-fdx*Δ*ftnB*Δ*bfr* had a growth deficiency when 150μM or higher of 2,2-bipyridyl was introduced into the media. This strain didn't show this same growth deficiency when it was just the individual *ftnB* deleted, or when it was deleted in combination with either *ftnA* or *dps* in the Δ*iscU-fdx* background (Figure 3.3). This phenotype was also observed when the strain was induced by oxidative stress by PMS (Figure 3.4). This indicates that the *bfr and ftnB* are both directly or indirectly influencing iron availability to the Suf pathway.

Our results indicated that characterization of the iron pools in these mutants using the DFO chelator showed that the Δ*iscU-fdx*Δ*ftn*BΔ*bfr* mutant had a higher labile iron pool compared to the wild type and the parent Δ*iscU-fdx* strain. This might contribute to the increase sensitivity of the strain.

We characterized the mutant strains using whole-cell Mössbauer spectroscopy to determine if deletion of the iron storage proteins affects specific iron pools. The reasons for the lack of full complementation partially stem from the transcriptional repression of the *suf* operon by the Fur metalloregulatory protein. There is evidence Suf does not fully mature all Fe-S proteins as well as Isc and this accounts for the lower Fe-S cluster content as shown by Mossbauer analysis.

In the case of the stress-sensitive iron storage mutant strains Δ*iscU-fdx*Δ*ftnB*Δ*bfr*,

we found that the signal from [4Fe-4S] $^{2+}$clusters is nearly undetectable. This result indicates that Suf is further impaired in these mutant backgrounds. Surprisingly Δ*iscU-fdx*Δ*ftnB*Δ*bfr* mutant strain accumulated about 2-fold more iron than the wild-type strain when grown under high iron conditions. The strain had less baseline absorption representing NHHS Fe (III) compared to them also. It also had more NHHS Fe (II)B compared to the wild-type strain. Our results suggest that one of these pools may not be DFO-chelatable.

We characterized the possible function and regulation of FtnB in the *E. coli* Suf pathway. Our results revealed surprisingly that although the FtnB protein lacks a true ferroxidase centre, it plays a part in the iron donation to the Suf pathway like the other ferritins: Bacterioferritin and DNA binding protein of starved cells. This results suggests that the FtnB might not function as a real ferritin but rather function as a store of Fe^{2+} that can be readily mobilized for Fe-S clusters in *E.* coli.

References

[1] Abdul-Tehrani, H. et al. (1999). Ferritin mutants of *Escherichia coli* are iron deficient and growth impaired, and fur mutants are iron deficient. *J Bacteriol* 181, 1415-28.

[2] Treffry, A., Zhao, Z., Quail, M.A., Guest, J.R. and Harrison, P.M. (1995). Iron(II) oxidation by H chain ferritin: evidence from site-directed mutagenesis that a transient blue species is formed at the dinuclear iron center. *Biochem* 34, 15204-13.

[3] McHugh, J.P., Rodriguez-Quinones, F., Abdul-Tehrani, H., Svistunenko, D.A., Poole, R.K., Cooper, C.E. and Andrews, S.C. (2003). Global iron-dependent gene regulation in *Escherichia coli*. A new mechanism for iron homeostasis. *J Biol Chem* 278, 29478-86.

[4] Velayudhan, J., Castor, M., Richardson, A., Main-Hester, K.L. and Fang, F.C. (2007). The role of ferritins in the physiology of *Salmonella enterica sv. Typhimurium:* a unique role for Ferritin B in iron-sulfur cluster repair and virulence. *Mol Micro* 63, 1495- 507

[5] Djaman, O., Outten, F.W. and ImLay, J.A. (2004). Repair of oxidized iron-sulfur clusters in *Escherichia coli*. *J Biol Chem* 279, 44590-9.

[6] Sezonov, G., Joseleau-Petit, D. and d'Ari, R. (2007). *Escherichia coli* Physiology in Luria-Bertani Broth. *J Bacteriol* 189,8746-8749.

[7] Eiseberg, R. C. and Dobrogoz, W. J. (1967). Gluconate metabolism in *Escherichia coli. J Bacteriol* 93,941-949.

[8] Cozzone, A. J. (1998). Regulation of acetate metabolism by protein phosphorylation In enteric bacteria. *Ann Rev Microbiol* 52, 127-16

[9] Salvail, H., Boubannais, P., Sobota, J. M., Caza, M., Benjamin, J. M., Medieta, M. E. S., Lepine, F., Dozois, C., ImLay, J. and Masse, E. (2010). A small RNA promotes siderophore production through transcriptional and metabolic remodeling. *PNAS* 107, 15223-15228.

CHAPTER FOUR

Wild-type *Escherichia coli* has multiple Non-Heme High Spin iron species

Abstract

Iron is an essential transition metal for most organisms due to its use in cofactors such as heme and iron-sulfur (Fe-S) clusters. Much is known about iron acquisition from the environment and iron transport into the cell. However, not much is known about its cytoplasmic iron pools. Release of iron from damaged cofactors or accumulation of iron due to misregulation of iron homeostasis can lead to elevated Fenton chemistry, production of $OH^{\bullet}$ radicals, and cell death. We have decided to use Mössbauer spectroscopy to characterize the iron pools in *Escherichia coli*. Whole-cell Mössbauer spectroscopy provides a comprehensive overview of all iron in cells labeled during growth with the nuclear isotope ^{57}Fe, to include iron oxidation state and some information as to likely atomic ligands (S, N, O). Our results indicate that majority of the Fe species in the bacterial cell is non-heme high-spin (NHHS) Fe (II). Our results also show that the NHHS Fe (II) pool has differentially coordinated and Fur regulated species.

4.1 Introduction

Iron an essential transition element, plays vital roles in many important biological processes including gene regulation, protein synthesis, oxygen transport and the TCA cycle.[1] However, despite the indispensability of iron, it is also potentially toxic due to its tendency to catalyze the formation of toxic reactive oxygen species (ROS) which destroy DNA, RNA, cellular membranes, lipids and proteins. To avoid ROS-mediated damage, cells have evolved a complex system to maintain iron homeostasis and tightly regulate the concentration of Fe. Iron acquisition and storage systems therefore have to be strictly regulated in response to iron availability.[2,3] This regulation is mediated by the homodimeric repressor protein, Fur, which employs ferrous iron as co-repressor.[4] After adequate Fe^{2+} levels are reached in cell, it binds to Fur protein and the ensuring Fe-Fur complex activates its repression activity. This activation allows the Fe-Fur complex bind to a 19-bp sequence, designated the "iron box," normally located near the Pribnow box of cognate promoters of iron-uptake genes to repress their transcription (Figure 1.2). 100 Fe^{2+}-Fur-regulated genes have been detected, most of which have not been previously reported. These include unknown genes potentially involved in iron acquisition. A large number of energy metabolism genes, mainly encoding Fe-containing respiratory complexes, were found to be Fe^{2+}-Fur induced.[5]

Fur is thought to directly sense on or more pools of kinetically exchangeable (labile) iron. Due to the reduction potential of the cytoplasm, these irons are likely Ferrous iron (Fe^{2+}).

E. coli had been proposed to have multiple candidate ligands which coordinate

intracellular Fe (II) pools. However, it is difficult to study intracellular iron pools using only *in vitro* biochemical techniques since loss of cell integrity will dilute and mix cell components and potentially expose iron to oxygen or other reactive species. While *in vivo* chemical probes that directly bind iron offer useful information on the concentration of the intracellular iron pools and can be used on intact cells, they may directly perturb iron or may sense only a fraction of the total labile iron pool.[6-9] Whole-cell Mossbauer spectroscopy provides detailed overview of all iron in cells labeled during growth with the nuclear isotope ^{57}Fe, to include iron oxidation state and some information as to likely atomic ligands (S, N, O). It therefore gives an initial picture without cellular fractionation that may disrupt cellular iron pools, thereby preserving the integrity of the pools.

In all previously examined eukaryotic cells grown under Fe-sufficient conditions, the Fe content is dominated by Fe (III) bound to storage proteins (e.g. ferritin) or small molecules (polyphosphate) used for storage (e.g. yeast vacuoles). In yeast, majority of iron in Fe-replete yeast cells is located in its vacuoles. These acidic organelles store Fe for use under Fe-deficient conditions and they sequester it from other parts of the cell to avoid Fe-associated toxicity. This iron has been shown to in the form of Non-Heme High Spin (NHHS) Fe(III) complexes coordinated to polyphosphate-related ligands. In respiring isolated yeast mitochondria, Mössbauer spectra show that the majority of the iron is present in the form of $[Fe_4S_4]^{2+}$ clusters and heme centers - the prosthetic groups of the respiratory complexes with just about ~ 2–3% is present as NHHS Fe (II) iron. The iron speciation of the eukaryotic cells depends on a multitude of factors including cell type, iron content of the media and if the cell is respiring or undergoing fermentation.[10-16]

We have decided to test if intracellular iron speciation is distinct between the Archaea, Bacteria, and Eukaryotes. To test this, we will first characterize cellular iron pools in *E. coli*. We will analyze cells grown in a range of low to excess iron (in form of ferric citrate) concentrations.

4.2 Materials and Methods

Growth medium and conditions. For bacterial growths, an individual colony was transferred from Fresh Lennox Broth (LB) agar plates into M9 glucose minimal media containing 1X M9 minimal salts (Sigma-Aldrich), 0.2% (w/v) glucose (Acros Organics), 0.2% (w/v) magnesium chloride (Sigma-Aldrich), 0.1mM calcium chloride (Sigma-Aldrich) for 24 hours at 37°C and 200rpm. When necessary, kanamycin (30µg/mL) was added to the media. For cell growth curves, the cell growth was monitored by UV-Vis absorption at 600 nm and plotted versus time in hours. For sodium acetate growth assay, the cells were initially pre-grown in M9 glucose minimal media for 24 hours. They were then washed and normalized into fresh M9 sodium acetate minimal media containing 1X M9 minimal salts (Sigma-Aldrich), 0.4% (w/v) glucose (Acros Organics), 0.2% (w/v) magnesium chloride (Sigma-Aldrich), 0.1mM calcium chloride and monitored over 48 hours.

Mössbauer Analysis: Cells were initially grown in 35mL M9 glucose minimal media for 24 hours at 37□C at 200rpm. The overnight culture was then used to inoculate a 1L M9 glucose minimal media supplemented with 10µM and 100µM ^{57}Fe(III) citrate. 10mM ^{57}Fe(III) citrate stock solution was prepared by dissolving 100 mg ^{57}Fe metal powder (IsoFlex USA) in 2 mL minimal amount aqua regia which is a 3:1 mixture of trace metal

grade nitric acid (TMG) to trace metal grade hydrochloric acid (Fischer Scientific) while stirring. Once dissolved, the solution was further diluted to a final volume of 100 mL. This stock was then treated with a 3-fold molar excess of sodium citrate (Fisher Scientific) while stirring. The solution was adjusted to pH 5 with 1 M NaOH (EMD Chemicals) resulting in a final ^{57}Fe concentration of 10 mM. Cells were grown to desired growth phase, harvested and centrifuged at 6,000 x g for 20min. The pellet was washed in 40mL wash solution comprising 50mM EDTA tetrasodium salt, 100 mM Sodium Oxalate, 300 mM NaCl, 10 mM KCl and centrifuged for at 4,000 x g for 20min. The wash solution was fully removed from the pellet by an additional wash in MilliQ water and it was packed into Mössbauer cups and immediately frozen in liquid nitrogen prior to analysis.

Mössbauer spectra were collected at the Texas A&M and analyzed in the Dr. Paul Lindahl lab by Joshua Wofford. Mössbauer spectra were recorded on MS4 WRC 4.5 to 300 K closed-cycle Helium-refrigerated system and a W106 temperature controller) and LHe6T spectrometers (SEE Co., Edina, MN), the latter of which is capable of generating 0–6 T fields. Both were calibrated using α-Fe foil. Spectra was analyzed at 5K and 0.05T and the resulting spectra were fitted over different iron species including Non-Heme Fe (II), Non Heme Fe (III) and Low Heme Fe fits.

Western Blot Analysis. Cells were prepared as described above and pelleted at 6,000 x g for 20 mins. The pellets were lysed by sonicator or Bacterial Protein Extraction Reagent (B-PER) (ThermoScientific) and the protein concentration checked using the Bradford assay. Equal total protein amounts were electrophoresed on a 15% SDS PAGE gel. Proteins were transferred to nitrocellulose membrane and blocked overnight with

80% Odyssey blocking buffer (Li-Cor) in 1 X TBS (50mM Tris-HCl pH 8.0, 150mM NaCl) at 4□C. Primary antibody incubations with α-FtnA (1:2000) incubations were performed in 40% blocking buffer in 1 X TBST (TBS + 0.001% Tween-20). After 2 hours incubation at room temperature with shaking, membranes were washed 5 times (10 min each) with copious amounts of 1 X TBST. Then they were incubated with goat α-rabbit secondary antibody (1:20,000) at room temperature with shaking for 45 min. Membranes were thrice washed with 1 X TBS (10 mins each) and then 1 X TBST twice (10 mins each) and scanned using an Odyssey Infrared Imager (Li-Cor).

4.3 Results

The Wild-type *E. coli* has two differentially Fur regulated Non High Spin Fe(II) (NHHS) species that are primarily ligated by oxygen donor ligands.

We prepared 3 wild-type samples, grown to exponential phase aerobically ($_{OD600}$ approximately 0.5-0.6) with 1μM, 10 μM and 100 μM ^{57}ferric citrate. These are designated WT1, WT10 and WT100 respectively. Mössbauer analysis of the wild-type exponential cells in different iron concentrations showed it contains Non-Heme High Spin (NHHS) Fe (II), Non-Heme High Spin Fe (III) and Low Spin Heme (LSH) Fe (II) / $[4Fe\text{-}4S]^{2+}$ iron species. It also contains iron in the baseline and this is iron in forms stored in iron storage proteins.

Preliminary data from whole-cell Mössbauer spectroscopy of *E. coli* wild-type cells showed that the majority of the Fe species in the bacterial cell is Non-Heme High-spin (NHHS) Fe (II) (black and purple simulations in Figure 4. 1). These isolated *E. coli* cells were grown to early exponential phase in M9 glucose minimal media supplemented

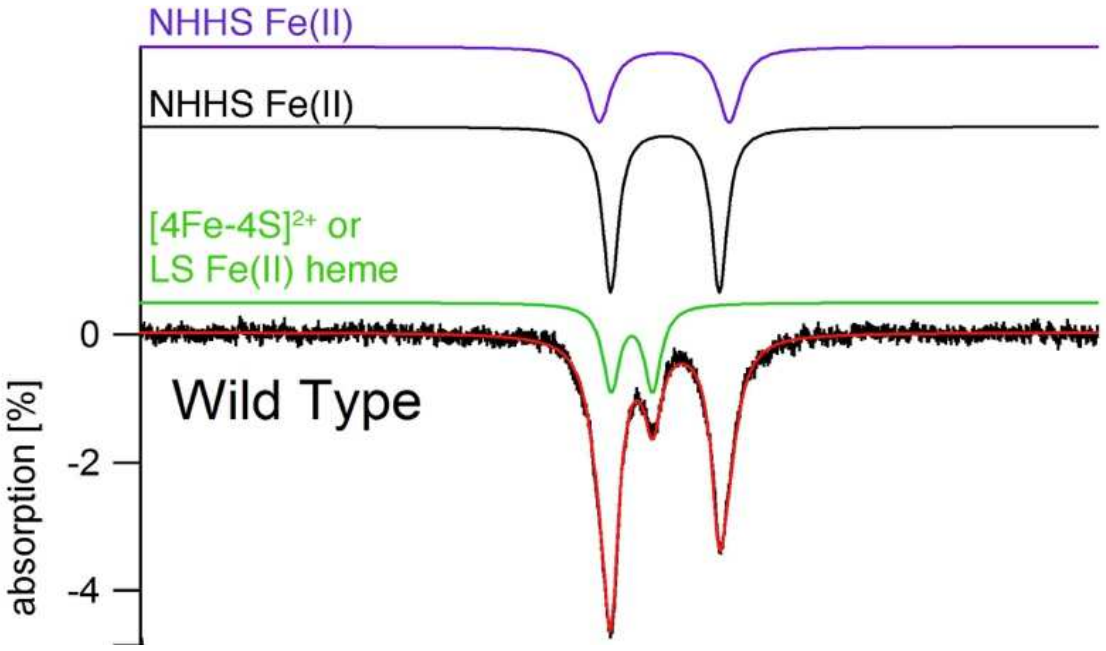

Figure 4.1. Whole-cell Mössbauer spectroscopy of wild-type *E. coli* grown in M9 glucose media with 100 μM ^{57}Fe(III)-citrate. Spectra were collected at 5 K, 0.05 T. The purple, black, and green lines above the spectrum are simulations of the various spectrum components assuming δ=1.28 mm/s, ΔE_Q = 2.76 mm/s, 45% area (purple); δ=1.26 mm/s, ΔE_Q = 3.3 mm/s, 30% area (black); and δ=0.44 mm/s, ΔE_Q = 1.05 mm/s, 25% area (green). The red line is the best fit traced over the raw data (black)

with 100 μM ^{57}Fe (III)-citrate. The concentration of NHHS Fe (II) we observed in *E. coli* is dramatically greater than that present in eukaryotic cells, including yeast and jurkat cells. Mössbauer analysis also showed that the NHHS Fe (II) was in 2 forms based on the ligands the Fe (II) is coordinated to. The NHHS Fe (II) A pool is coordinated to oxygen/nitrogen ligands while the NHS (II)B pool is coordinated to sulfur ligands.

In the *E. coli* wild-type strain, these NHHS Fe (II) species are primarily NHHS Fe (II)A form i.e. ligated by oxygen donor ligands (Figure 4.2). In this species, the NHHS Fe (II) exists in 2 forms. One of these species is Fur-dependent; the other is Fur-independent. The Fur-dependent Fe (II)A changes strongly as the concentration of Fe in the medium changes. It does not seem as well regulated as the other Fe (II)A species. It was observed that the central doublet which accounts for Fe-S clusters and low spin heme varied with the iron concentrations in the media.

In WT1, the NHHS Fe (II) concentration was the lowest but it had the highest, about 70% concentration of central doublets out of the three samples. WT10 had about 10-20% of central doublet, while WT100 had the largest NHHS Fe (II) feature but the smallest Fe-S cluster activity (Figure 4.2). We therefore hypothesize that the non - regulated Fur-dependent Fe (II)A may primarily serve as feedstock for building Fe-S clusters and or heme. The fur-independent Fe (II)A species may be better regulated compared to the fur-dependent Fe (II)A species.

The other main NHHS Fe (II) species is the NHHS Fe (II)B species i.e. coordinated with sulfur donors. This exists as a minority species in the wild-type strain compared to the NHHS Fe (II)A species. This also seems Fur-independent and pretty well regulated (Table 4.1).

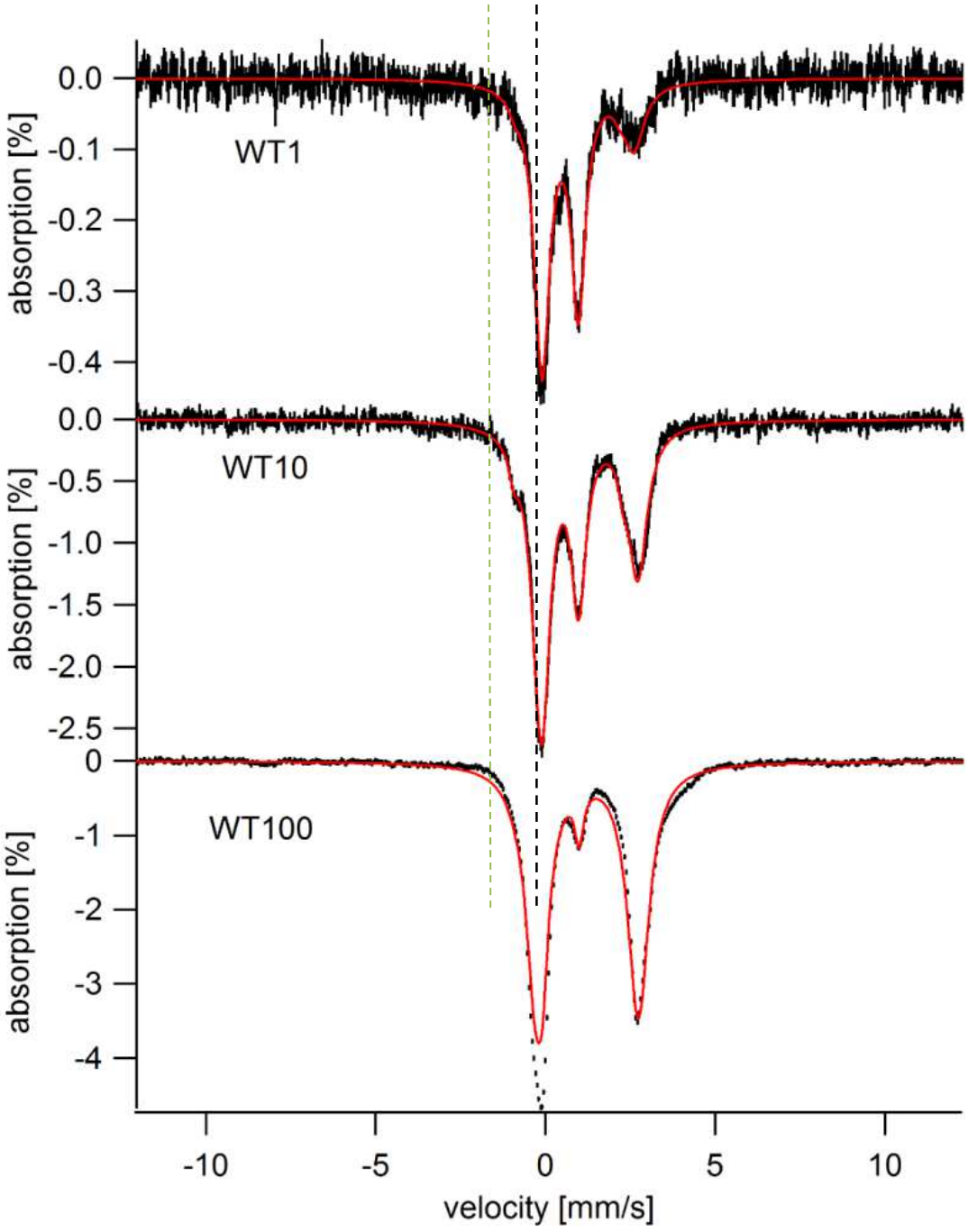

Figure 4.2. Whole-cell Mössbauer spectroscopy of wild-type *E. coli* grown in M9 glucose media with 1, 10 and 100 µM ^{57}Fe(III)-citrate. Spectra were collected at 5 K, 0.05 T. The green and black lines through the spectra indicate the central doublet (Fe-S cluster) and NHHS content respectively. The red line is the best fit traced over the raw data (black). Cells were grown to exponential phase before harvested.

Table 4.1- Offline ICP Metal Concentrations and Mössbauer Percentages

	Central Doublet %; µM	Fe (II)A (O/N) %; µM	Fe (II)B (S4) %; µM
WT 1	69.3	28	3
WT 10	45.6	49.4	5
WT 100	8	90	1

***E.coli* iron accumulation varies from yeast iron accumulation.**

In yeast cells, it has been proven that slower-growing cells accumulate more Fe than the faster growing ones. To compare this with the *E. coli* wild-type cells, we did a timed growth assay with the different ^{57}ferric citrate concentrations in the media (Figure 4.3). In the growth assay, both WT1 and WT10 had identical growth rates while the WT100 grew just a faction faster. The W10 and W100 had a higher final cell density than the W1.This shows that the *E.coli* cells have different iron speciation from yeast cells and different iron accumulation patterns.

The Δ*fur* mutant has only one Fur independent Non High Heme Spin Fe (II) species.

We prepared 3 Δ*fur::kan*^{R} samples, grown to exponential phase aerobically (OD_{600} approximately 0.5-0.6) with 1μM, 10 μM and 100 μM ^{57}ferric citrate . These are designated Fur1, Fur10 and Fur100 respectively. The Δ*fur::kan*^{R} strains contain 2-3 times less iron than WT cells (Table 4.2) for the same concentration of Fe in the growth medium (Figure 4.3). They contain a much smaller percentage change in Fe content as iron concentrations in the media increase. They also central doublet (Fe-S / LSH) signal compared to the WT samples. In contrast to the WT Mössbauer samples (Figure 4.1), the Δ*fur::kan*^{R} strains didn't show such a variability in its NHHS Fe (II) speciation as its iron content increased in the media.

Similar to the WT species, they contain both a NHHS Fe (II) species that is ligated primarily by oxygen donor ligands (majority species) and a NHHS Fe (II) species that is ligated primarily by sulfur donor ligands (minority species). The Δ*fur::kan*^{R} strains also had similar growth rates that didn't change in response to addition of ferric ion

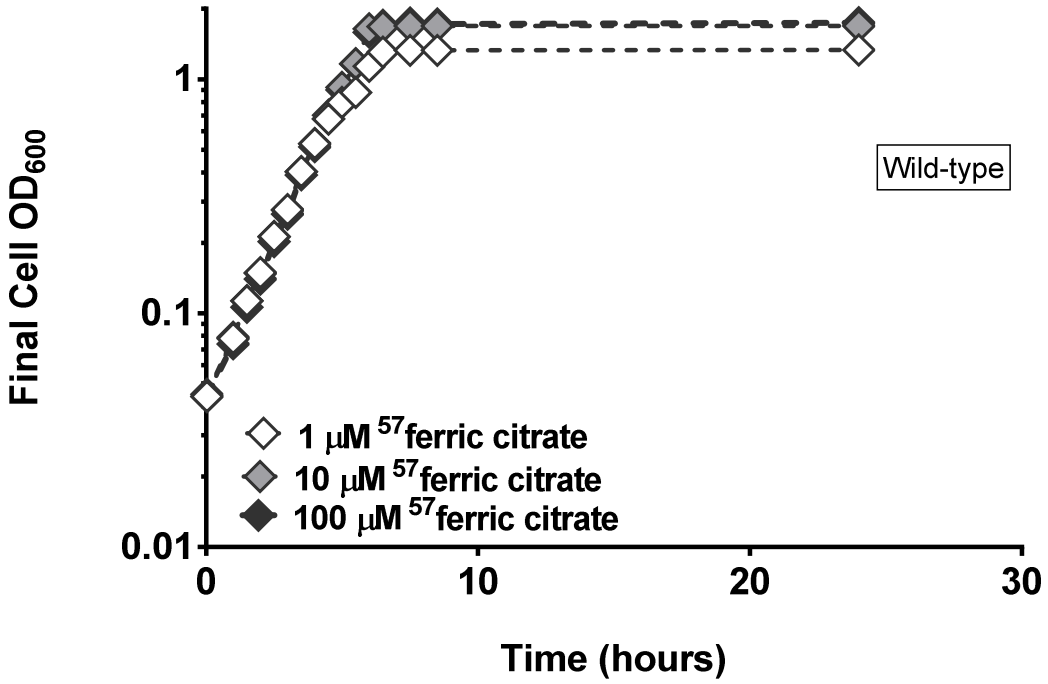

Figure 4.3. Growth curves of the 3 wild-type strains in different iron concentrations were similar. Cells were pre- grown in 0.2% glucose minimal media for 24 hours, and inoculated into fresh 0.2% glucose minimal media with different ^{57}ferric citrate concentrations. Cells OD_{600} were then checked hourly.

in all the samples with the different strains (Figure 4.4)

The Δ*fur* mutant has impaired Fe-S cluster assembly function.

To further investigate if the Δ*fur::kan*^{R} mutant had impaired Fe-S cluster assembly, we conducted a growth assay on the strain in Sodium acetate minimal media. Cells grown on acetate by-pass glycolysis to go through the glycoxylate shunt and Tri-Carboxylic Acid (TCA) cycle for metabolism. The TCA cycle has enzymes that contain Fe-S cluster e.g. aconitase. Acetate growth requires respiration for all cellular metabolic synthesis. The respiratory complexes I and II also contain many Fe-S clusters. Any strain that has difficulty assembling Fe-S clusters will therefore show a dramatic growth phenotype in this media. We grew both the Δ*fur::kan*^{R} mutant and the wild-type as a control. We initially grew the strains in 0.2% glucose minimal media for 24 hours and then transferred to 0.4% sodium acetate minimal media. After 48 hours, the Δ*fur* mutant showed a severe growth defect in this media (Figure 4.5) and didn't grow indicating that the Δ*fur::kan*^{R} mutant strain has difficulty in making Fe-S clusters.

4.4 Discussion

We have attempted to characterize the iron pools Iin *E. coli* in both the wild type and a Δ*fur::kan*^{R} strain. Fur is known as a global regulator of iron so we wanted to observe the effects its deletion would have on the various iron pools in the organism. We tested this using mainly Mossbauer which is a technique that can identify iron speciation *in vivo* and also tell us the ligands they are bound too. We tested by adding a range of ^{57}ferric citrate concentrations to our strains ranging from minimal 1μM, to 10 μM (approximate concentration found in rich media) and 100 μM (excess).

Table 4.2- Offline ICP Metal Concentrations and Mössbauer Percentages

	Central Doublet %; µM	Fe (II)A (O/N) %; µM	Fe (II)B (S4) %; µM
WT 1	69.3	28	3
WT 10	45.6	49.4	5
WT 100	8	90	1
Fur 1	28.4	60.7	9
Fur 10	28.5	64.2	10.6
Fur 100	25.1	58.3	8.7

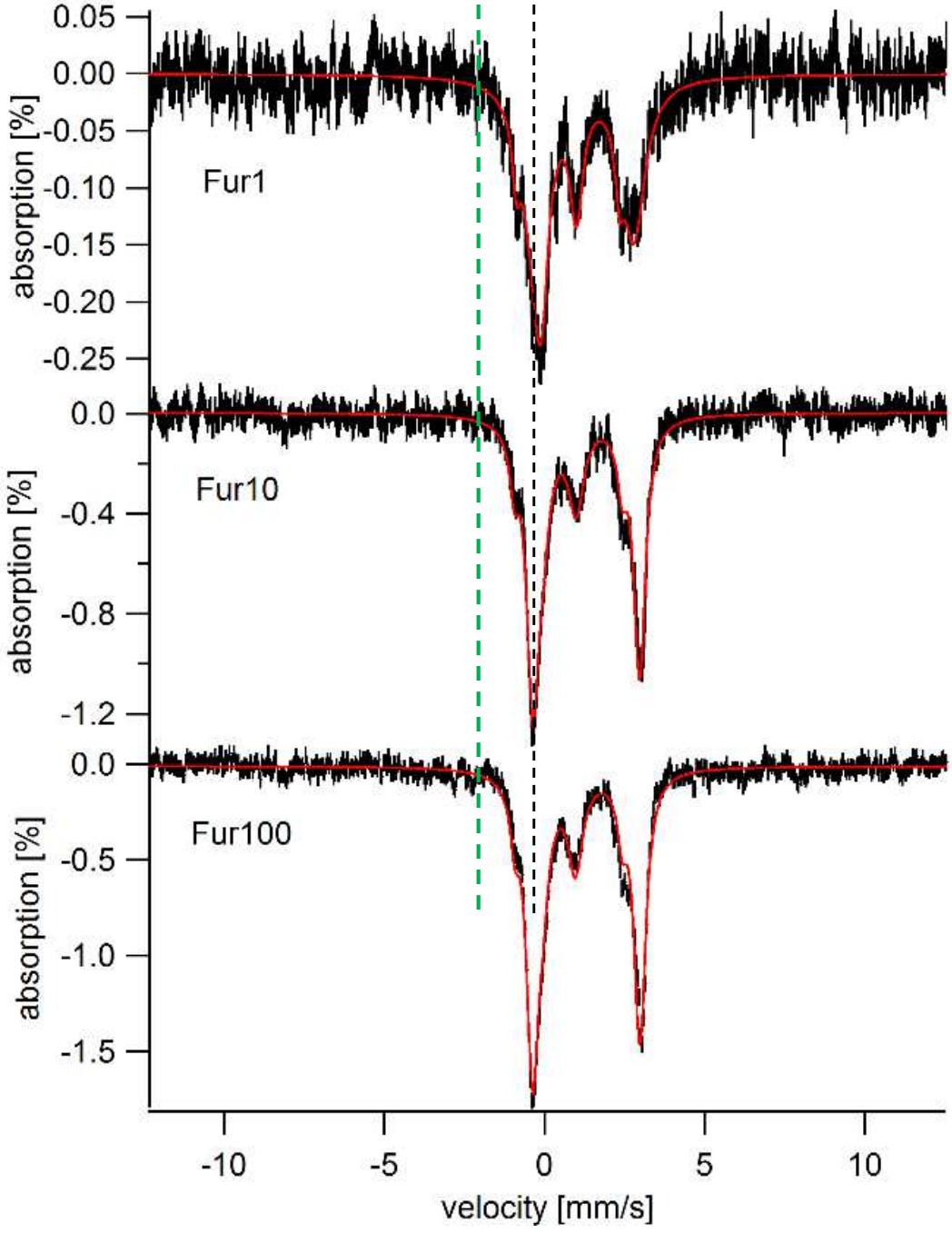

Figure 4.4. Whole-cell Mössbauer spectroscopy of Δ*fur::kan*^{R} grown in M9 glucose media with 1, 10 and 100 µM ^{57}Fe(III)-citrate. Spectra were collected at 5 K, 0.05 T. The green and black lines through the spectra indicate the central doublet (Fe-S cluster) and NHHS content respectively. The red line is the best fit traced over the raw data (black). Cells were grown to exponential phase before harvested.

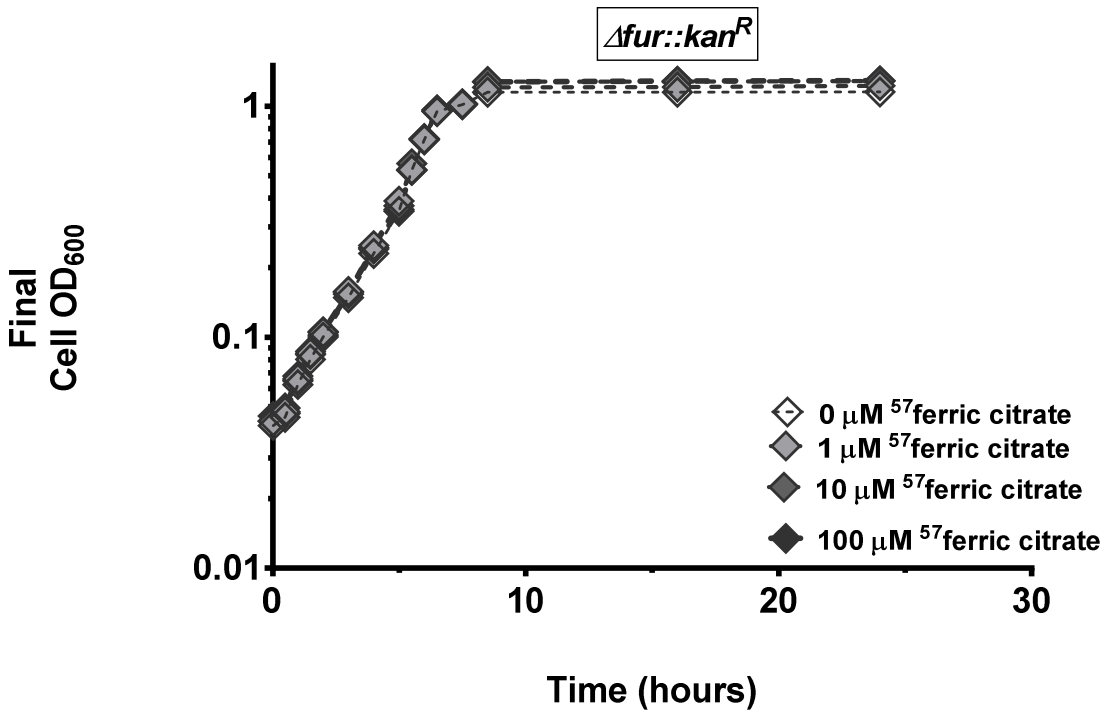

Figure 4.5. Growth curves of the Δ*fur::kan*^{R} strains in different iron concentrations were similar. Cells were pre- grown in 0.2% glucose minimal media for 24 hours, and inoculated into fresh 0.2% glucose minimal media with different ^{57}ferric citrate concentrations. Cells OD_{600} were then checked hourly

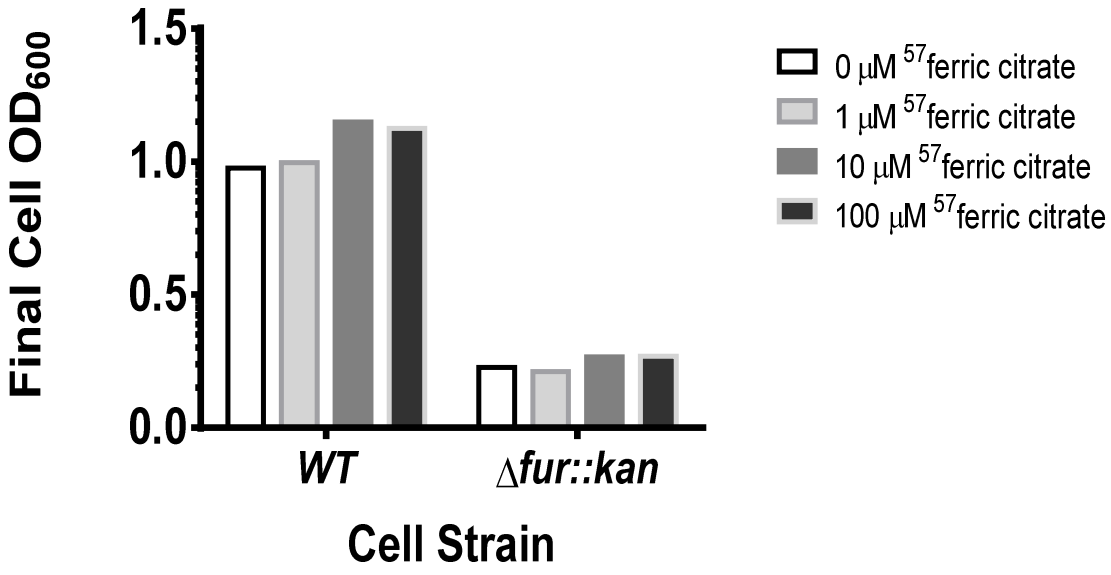

Figure 4.6. The Δ*fur::kan*^{R} strain shows a defective growth phenotype in M9 acetate growth without stress. All strains were grown in M9 glucose minimal media for 24 hours for 18 hours and then washed and normalized to same starting OD_{600} in fresh M9 sodium acetate minimal media for 24 hours. Cell density was measured after 48 hours. All growths were repeated in triplicate (n=3) and error bars indicate one standard deviation from the mean value.

We have identified that wild type has two primary NHHS Fe (II) species: NHHS Fe (II)A pool coordinated to oxygen/nitrogen ligands and the NHS (II)B pool is coordinated to sulfur ligands. In the *E. coli* wild-type strain, the majority species is the NHHS Fe (II)A species, these are the that are primarily ligated by oxygen/nitrogen donor ligands. This NHHS Fe (II)A is also divided into 2; one being fur-dependent and the other is fur-independent. The fur-dependent Fe (II)A changes strongly as the concentration of Fe in the medium changes. The Fur-dependent Fe (II)A species is not well regulated. This species is present at extremely high concentrations in WT cells grown on 100 μM Fe, and weaker in WT cells grown on 10 μM Fe, and very weak in WT cells grown on 1 μM Fe. The Fur-dependent Fe (II)A species may primarily serve as feedstock for building Fe/S clusters and/or heme. The Fur-independent Fe (II)A species may be better regulated. The NHHS Fe (II)B species coordinated with primarily sulfur donors. This is the minority species. It seems Fur-independent and pretty well regulated.

The Δ*fur::kan*^{R} train strain lso has two NHHS Fe (II) pools. Its NHH Fe (II)A pool however has just one Fur indepenedent NHHS Fe(II) species. It has defective Fe-S clusters than the WT. It showed an increase in total Fe as more iron is added to the media although th echange wasn't as dramatic as in the wild-type . Fur is a regulator and but may act as a chaperone in the cell. Fur may positively regulate the ligand for the "Fe dependent Fe(II) species" that is found in wild-type strain. It may do this via the action of RyhB which it represses when bound to its iron promoter box upstream many Fe-S and Fe containg proteins. Therefore in the Δ*fur::kan*^{R} strain it may not be responsive to changes to iron.

We also discovered that the Δ*fur::kan*^{R} strain definitely has an impairment in

forming Fe-S clusters. It showed up on the Mossbauer spectra and they couldn't grow when forced to respire. This is likely explained by constittutive upreegulaion of *ryhB* in the Δ*fur::kan*^{R} strain, leading to targeted degradation of many mRNA for Fe-S enzymes (and also of iscU- iscX mRNA). It mightr also be partialy explained by changes in iron speciation but that is not the only reason.

References

[1] Andrews, S.C., Robinson, A.K. and Rodriguez-Quinones, F. (2003). Bacterial iron homeostasis. *FEMS Microbiol Rev* 27, 215-37.

[2] Touati, D. (2000). iron and oxidative stress in bacteria. *Arch Biochem Biophys* 373, 1-6.

[3] Winterbourn, C. C. (1995). Toxicity of iron and hydrogen peroxide: the Fenton reaction. *Toxicol Lett* 82-83, 969-974.

[4] Hantke, K. (2001). Iron and metal regulation in bacteria. *Curr Opin Microbiol* 4, 172-7.

[5] McHugh, J.P., Rodriguez-Quinones, F., Abdul-Tehrani, H., Svistunenko, D.A., Poole, R.K., Cooper, C.E. and Andrews, S.C. (2003). Global iron-dependent gene regulation in *Escherichia coli*. A new mechanism for iron homeostasis. *J Biol Chem* 278, 29478-86.

[6] Lindahl, P. A., and Holmes-Hampton, G. P. (2011). Biophysical probes of iron metabolism in cells and organelles. *Curr Opin Chem Biol* 15, 342-346.

[7] Carter, K. P., Young, A. M., and Palmer, A. E. (2014). Fluorescent sensors for measuring metal ions in living systems. *Chem Rev* 114, 4564-4601.

[8] Kakhlon, O., and Cabantchik, Z. I. (2002). The labile iron pool: Characterization, measurement, and participation in cellular processes. *Free Radic Biol Med* 33, 1037-1046.

[9] Petrat, F., de Groot, H., Sustmann, R., and Rauen, U. (2002). The chelatable iron pool in living cells: A methodically defined quantity. *Biol Chem* 383, 489-502.

[10] Chakrabarti, M., Cockrell, A. L., Park, J., McCormick, S. P., Lindahl, L. S., and Lindahl, P. A. (2015). Speciation of iron in mouse liver during development, iron deficiency, IRP2 deletion and inflammatory hepatitis. *Metallomics* 7, 88-96.

[11] Cockrell, A., McCormick, S. P., Moore, M. J., Chakrabarti, M., and Lindahl, P. A. (2014). Mossbauer, EPR, and modeling study of iron trafficking and regulation in Δ*ccr1* and *ccc1-up* of *Saccharomyces cerevisiae*. *Biochem* 53, 2926-2940.

[12] Cockrell, A. L., Holmes-Hampton, G. P., McCormick, S. P., Chakrabarti, M., and Lindahl, P. A. (2011) Mossbauer and EPR Study of Iron in vacuoles from fermenting *Saccharomyces cerevisiae*. *Biochem* 50, 10275-10283.

[13] Holmes-Hampton, G. P., Jhurry, N. D., McCormick, S. P., and Lindahl, P. A. (2013) Iron Content of *Saccharomyces cerevisiae* cells grown under iron-deficient and iron-overload conditions. *Biochem* 52, 105-114.

[14] Jhurry, N. D., Chakrabarti, M., McCormick, S. P., Holmes-Hampton, G. P., and Lindahl, P. A. (2012) Biophysical investigation of the ironome of human Jurkat cells and mitochondria. *Biochem* 51, 5276-5284.

[15] McCormick, S. P., Moore, M. J., and Lindahl, P. A. (2015) Detection of labile low-molecular-mass transition metal complexes in mitochondria. *Biochem* 54, 3442-3453.

[16] Wofford, J. D., and Lindahl, P. A. (2015) Mitochondrial iron-sulfur cluster activity and cytosolic iron regulate iron traffic in *Saccharomyces cerevisiae*. *J Biol Chem* 290, 26968-26977.

Appendix A – SUPPLEMENTAL EXPPERIMENTS AND RESULTS

FepA transcripts differ based on carbon source

We decided to assess the transcript levels of FepA (an integral bacterial outer membrane porin protein), with another carbon source: gluconate instead of glucose. To assess whether FepA is differentially regulated in different strains, we carried out primer extension assays to measure *fepA* transcript levels in cells exposed to high BIPY(250 μM) and measured these levels in cells initially grown in nutrient rich (LB) before being transferred to M9 gluconate minimal media (Figure A.1).

Plasmid re-insertion didn't rescue sensitive strain

We re-inserted Bfr (pGS281::amp^R) and FtnA (pGS1096::amp^R) into the sensitive Δ*iscU-fdx*Δ*bfr*Δ*dps* strain by P1 transduction to see if the growth phenotype would be rescued. We also inserted the plasmids into the parent Δ*iscU-fdx* strain to see if there would be any effect on the phenotype. All plasmids were obtained from Dr. Nick LeBrun lab from East Anglia. The Bfr plasmid insertion made both the sensitive Δ*iscU-fdx*Δ*bfr*Δ*dps* and parent Δ*iscU-fdx* strains more sensitive (Figure A2). The FtnA insertion also made the parent Δ*iscU-fdx* strain more sensitive in higher BIPY stress (Figure A.2)

Deletion of all the iron storage proteins shows no sensitivity to iron starvation and oxidative stress

We wanted to check the effect in a strain that had all iron storage proteins deleted.

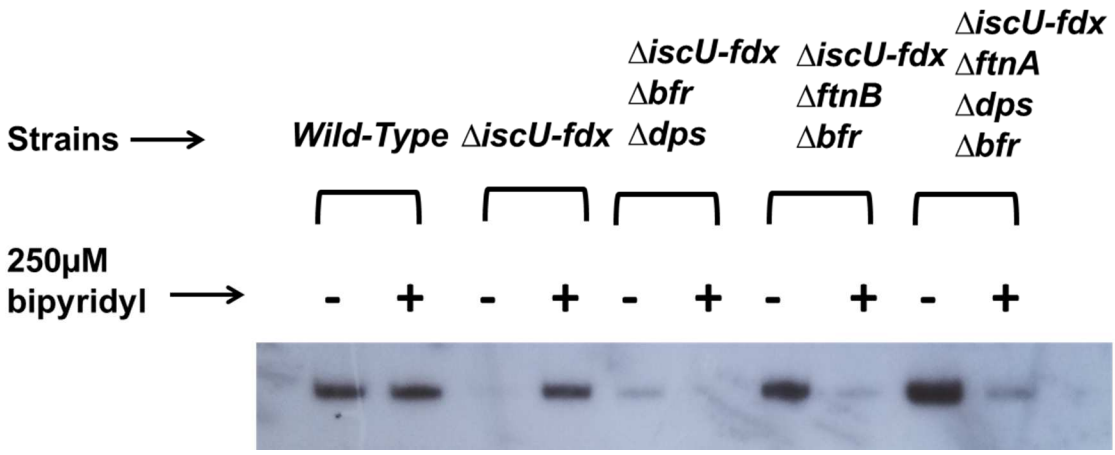

Figure A.1. Transcriptional activity of FepA. Cells were grown in LB for 18 hours, then washed and transferred to M9 Glucoate minimal media to mid-log phase (0.5), some harvested as the control probe and the remaining induced for 1 hour with 250 μm BIPY for 1 hour.

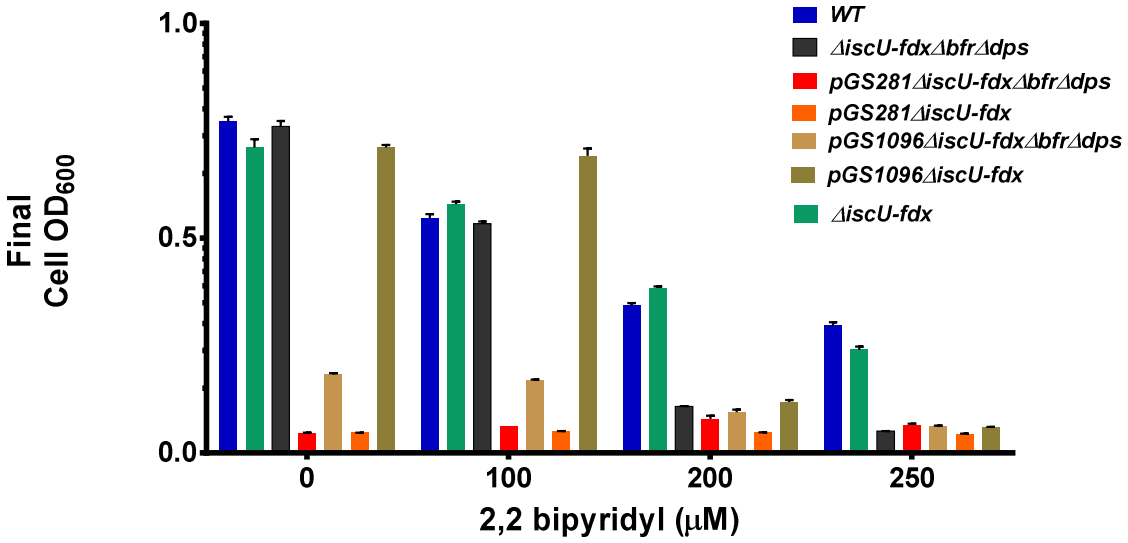

Figure A.2. Bfr and FtnA Plasmid re-insertion didn't rescue the sensitivity of the Δ*iscU-fdx*Δ*bfr*Δ*dps* strain. Cells were grown in LB and then washed and transferred to M9 gluconate minimal media containing varying concentrations of BIPY.

In the Δ*iscU-fdx*Δ*bfr*Δ*dps* double mutant strain, we deleted both *ftnA* and *ftnB* to construct the Δ*iscU-fdx*Δ*ftnA*Δ*dps*Δ*bfr* Δ*ftnB* strain. This strain showed no sensitivity when stressed with iron starvation (Figure A.3). This strain also had rescued lag phase compared to the sensitive Δ*iscU-fdx*Δ*bfr*Δ*dps* phase (Figure A.4). We also checked the transcript levels of FepA in this strain both in LB (Figure A.5.i) and in M9 glucose minimal media (Figure A.5.ii). This Δ*iscU-fdx*Δ*ftnA*Δ*dps*Δ*bfr*Δ*ftnB* strain also had slightly lower DFO-accessible labile iron pool compared to the Wild-type and about 6x less levels compare to the sensitive Δ*iscU-fdx*Δ*bfr*Δ*dps* sensitive strain (Figure A.6).

Mossbauer Analysis of samples shows that concentration of iron critical to iron components in the different strains.

In the wild-type strain, the stationary cells with 100 μM Fe had nanoparticles (Figure A.7). In the Δ*iscU-fdx* strain, the 100 μM exponential spectrum was about twice as intense (Figure A8) About 90% of spectral intensity was due to Sites 1 (50%) and Site 2 (40%) [δ = 1.28 mm/s; ΔE_Q = 3.44 mm/s]. Both Sites 1 and 2 have increased in intensity. In Site 3, the central doublet was only 3% while a Sire 4 cannot be observed. The 100 μM spectrum exhibited the same major species as well as a sextet arising from a NHHS $Fe(II)^I$ species. The sextet was simulated using the following parameters [D = 0.2 cm^{-1}; E/D = 0.30; δ = 0.2 mm/s; ΔE_Q = 1.1 mm/s; eta = 0.27; A = -206 gauss]; it represented 17% of spectral intensity. The spectral intensity also included a CD (19%), a NHHS $Fe(II)(O/N)_{5-6}$ species (38%), the $Fe(II)S_4$ species (3%) and $Fe(II)^I$ nanoparticles [δ = 0.55 mm/s; ΔE_Q = 0.55 mm/s] at 28% spectral intensity. Compared to cells harvested under exponential conditions, some Fe in stationary state cells is present as a NHHS $Fe(II)^I$

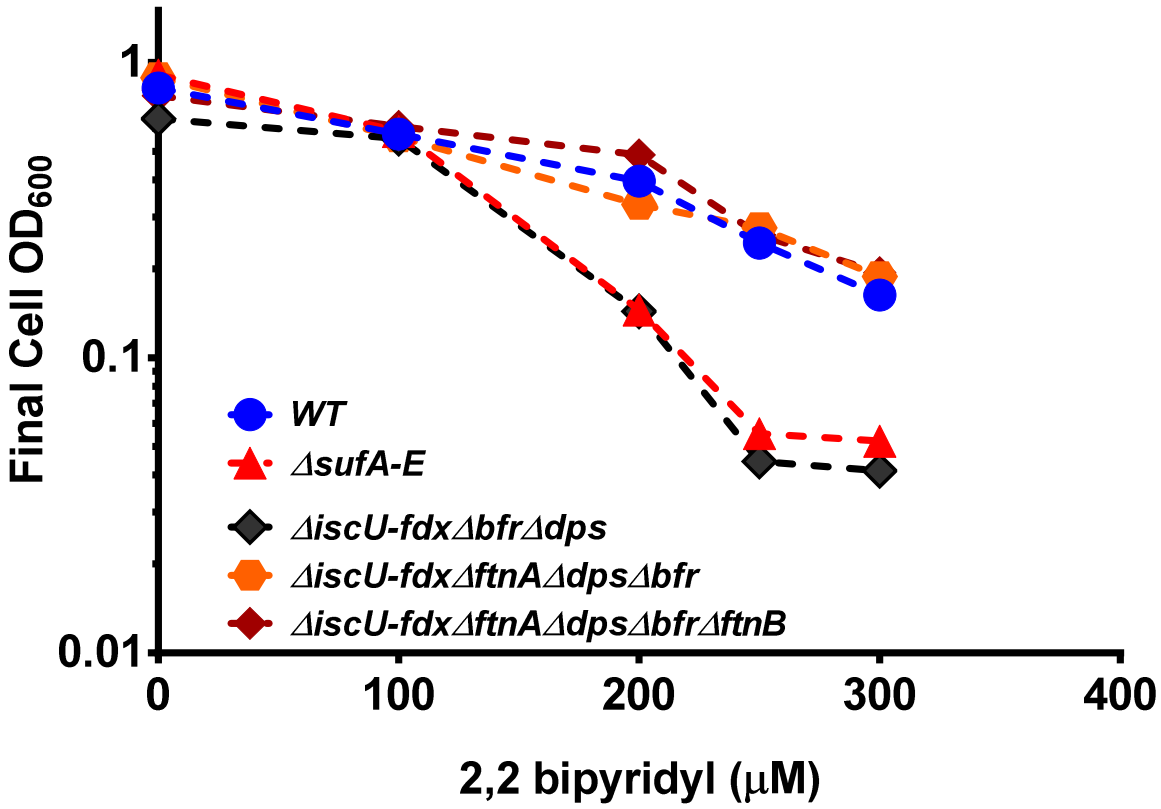

Figure A.3. Additional deletion of *ftnA and ftnB* rescues the sensitivity of the Δ*iscU-fdx*Δ*bfr*Δ*dps* strain to bipyridyl. All strains were grown in LB for 18 hours. After this, they were washed and inoculated into fresh 0.2% gluconate minimal media with varying concentrations of BIPY. The final cell density was measured after 24 hours. All growths were repeated in triplicate (n=3) and error bars indicate one standard deviation from the mean value.

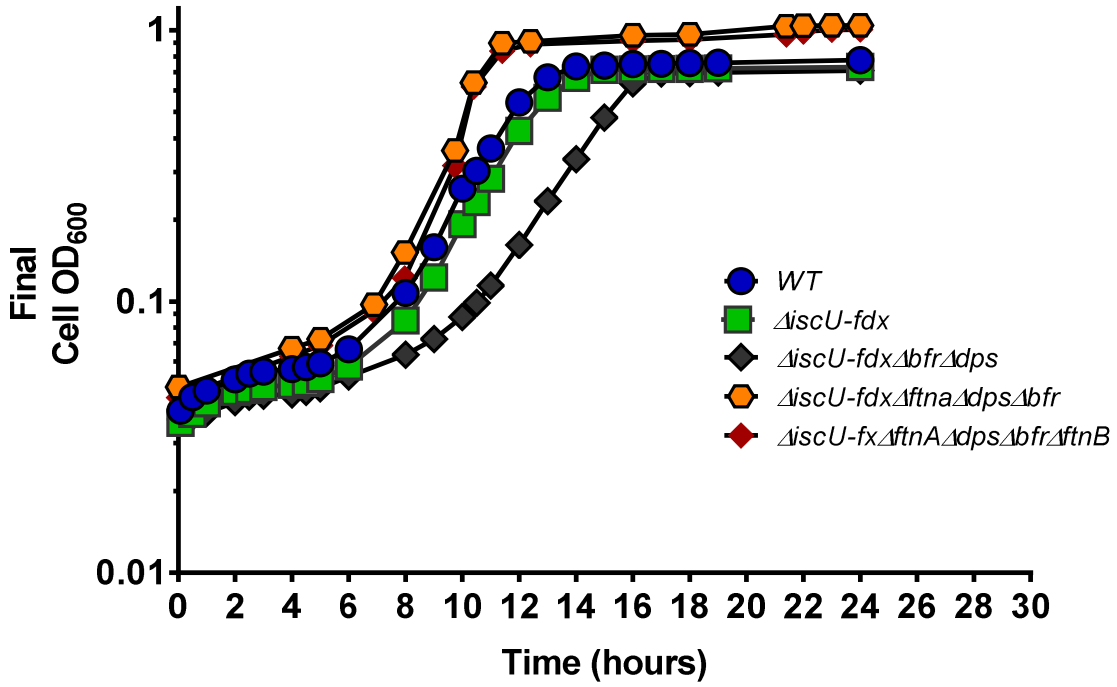

Figure A.4. Additional deletion of *ftnA and ftnB* rescues the mild increase in lag phase duration in LB media with no stress of the Δ*iscU-fdx*Δ*bfr*Δ*dps* strain. All strains were grown in LB media for 18 hours. After this, they were washed and inoculated into fresh 0.2% glucose minimal media and density was measured initially every 30 mins until they exited lag phase, and then hourly. All growths were repeated in triplicate (n=3) and error bars indicate one standard deviation from the mean value.

i

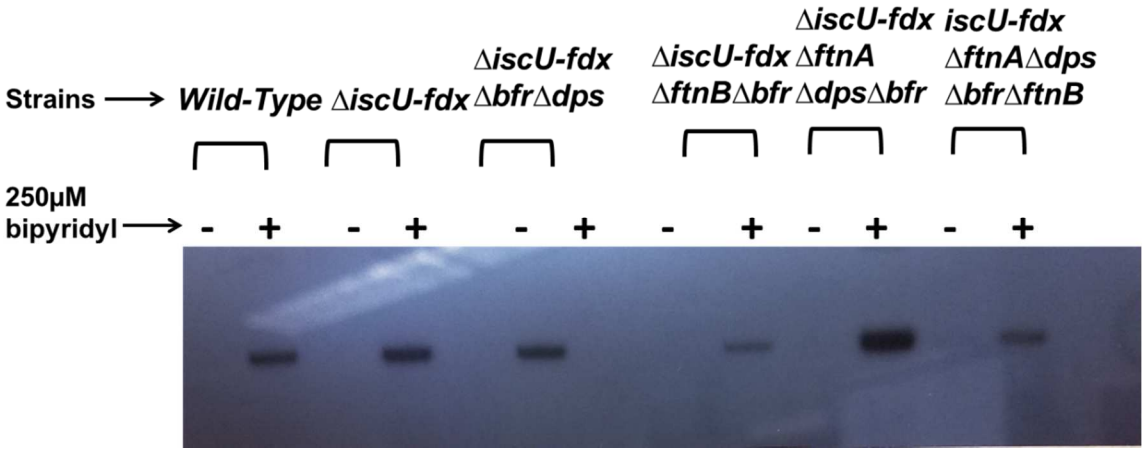

ii

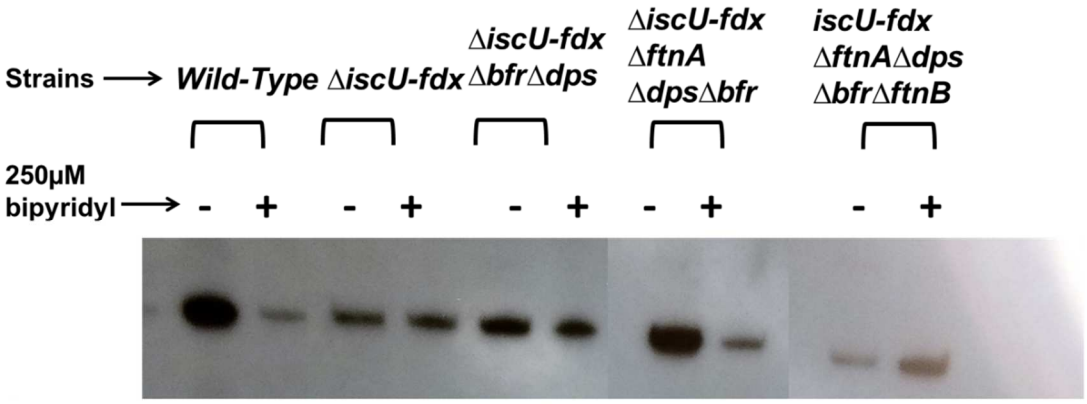

Figure A.5. Transcriptional activity of FepA. Cells were grown in (i) LB or (ii) M9 Glucose minimal media to mid-log phase (0.5), some harvested as the control probe and the remaining induced for 1 hour with 250 μm BIPY for 1 hour.

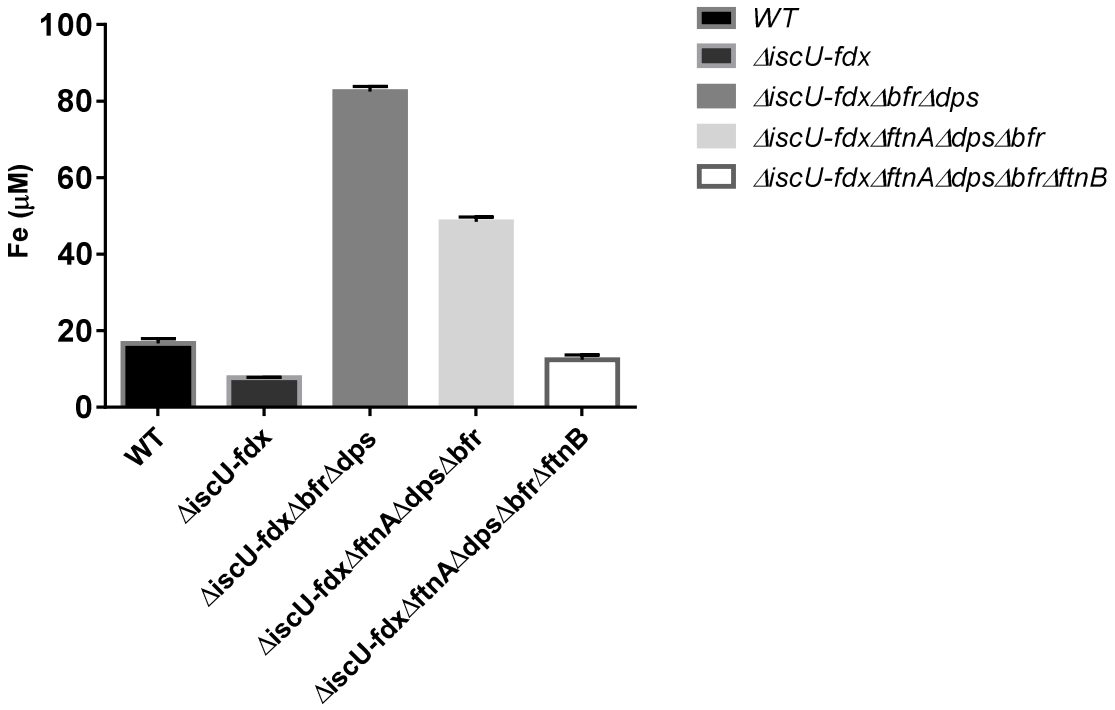

Figure A.6. Labile iron pools are lowest in the Δ*iscU-fdx*Δ*ftnA*Δ*dps*Δ*bfr*Δ*ftnB* strain. Intracellular, DFO-labile iron concentrations are calculated and normalized to cell volume and number.

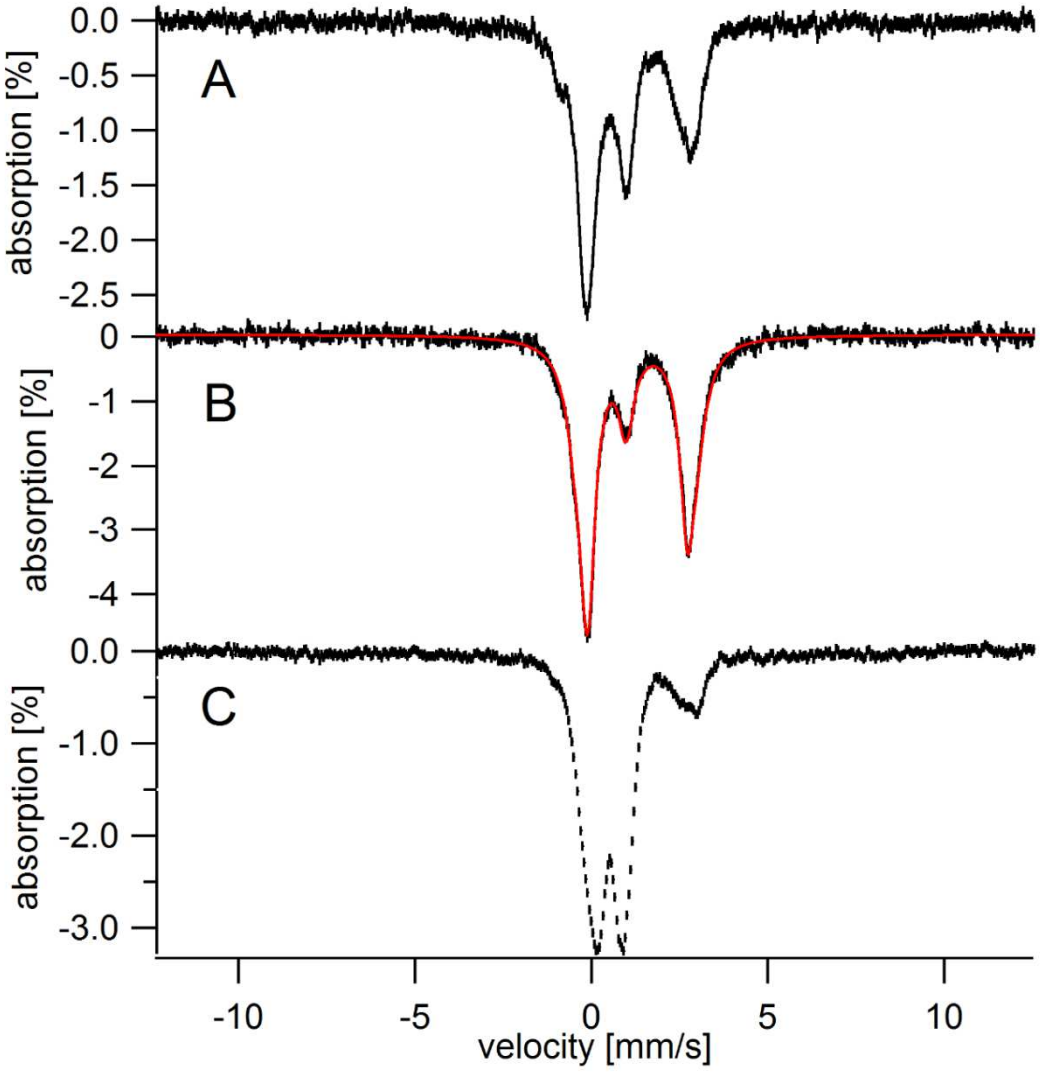

Figure A.7. Mossbauer spectra (5K, 0.05T) of Wild-Type *E.* coli grown in glucose medium. (A) 10 μM Fe in the growth medium and harvested under exponential conditions. (B) 100 μM Fe in the medium and harvested under exponential conditions and (C) 100 μM Fe in the medium and harvested under stationary-state conditions. Spectrum A was simulated using four species including two nonheme high-spin (NHHS) Fe(II) doublets, both reflecting mononuclear Fe(II) complexes with 5-6 O/N donor ligands, a "Central Doublet due to S = 0 $[Fe_4S_4]^{2+}$ clusters and LS Fe(II) hemes combined, and a NHHS Fe(II) site with what appear to be four sulfur donor ligands

Table A.1. Parameters for Wild-type Mossbauer analysis

Spectrum	Site	δ (mm/s)	ΔE_Q (mm/s)	Γ (mm/s)	Area (%)
WT10 μM (A)	#1 $Fe(II)(O/N)_{5-6}$	1.29	2.7	0.62	25
	#2 $Fe(II)(O/N)_{5-6}$	1.30	3.1	0.44	20
	Central Doublet	0.44	1.05	0.55	46
	$Fe(II)(S)_4$	0.70	3.2	0.33	6
WT100 μM (B)	#1 $Fe(II)(O/N)_{5-6}$	1.28	2.7	0.45	42
	#2 $Fe(II)(O/N)_{5-6}$	1.28	3.3	.64	29
	Central Doublet	0.44	1.05	0.54	26
	$Fe(II)(S)_4$	0.71	3.1	0.30	3
WT100 μM (C)	#1 $Fe(II)(O/N)_{5-6}$	1.26	2.7	0.56	10
	#2 $Fe(II)(O/N)_{5-6}$	1.30	3.4	0.43	10
	Central Doublet	0.46	1.2	0.41	18
	$Fe(II)(S)_4$	0.7 (est)	3.2 (est)	0.3 (est)	~ 3 (est)
	$Fe(II)^I$ oxyhydroxide nanoparticles	0.52	0.64	0.54	59

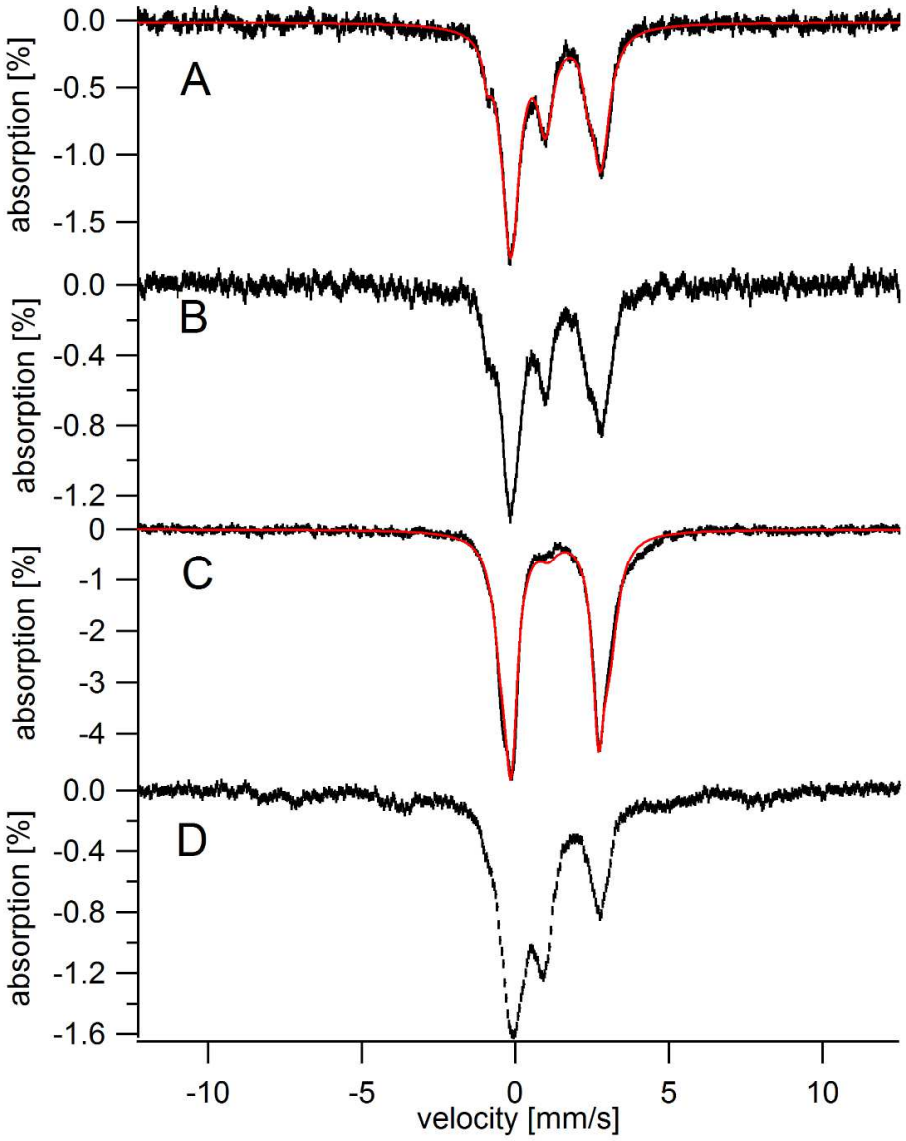

Figure A.8. Mossbauer spectra (5K, 0.05T) of E coli strain Δ*iscU-fdx* grown in glucose medium. (A) and (B) 10 μM Fe in the growth medium and harvested under exponential conditions. (C) 100 μM Fe in the medium and harvested under exponential conditions and (D) 100 μM Fe in the medium and harvested under stationary-state conditions. The 10 μM exponential spectrum (A and B) exhibited three major features, including Sites #1 and #2: NHHS Fe(II) doublets both with parameters typical of 5-6 O/N ligands (called $Fe(II)(O/N)_{5\text{-}6}$) [average: δ = 1.26 mm/s; ΔE_Q = 2.92 mm/s], 54%. Site 3: "Central Doublet" due to S = 0 $[Fe_4S_4]^{2+}$ clusters and LS Fe(II) hemes combined) [δ = 0.45 mm/s; ΔE_Q = 1.15 mm/s], and an $Fe(II)S_4$ species [δ = 0.7 mm/s; ΔE_Q = 3.2 mm/s]. The intensity corresponds to 32%, which is significantly less than we saw in WT spectra. Site 4: 6% was due to $Fe(II)S_4$.

species and also nanoparticles.

In the Δ*iscU-fdx*Δ*bfr*Δ*dps* strain (Figure A.9), Spectra A and B (the 10 μM Fe exponential phase cells) are dominated by a NHHS Fe(II) (O/N)5-6 doublet with parameters [δ = 1.26 mm/s; ΔE_Q = 2.96 mm/s]; this feature represents 58% of spectral intensity. The Central Doublet represented 27% and the Fe(II)S_4 species represented 7%. The spectra look VERY similar to that of Δ*iscU-fdx* grown with 10 μM Fe and harvested at exponential phase. This implies that deleting *bfr and dps* had essentially no effect on the Fe content of the cell. Spectrum C has a 15% effect which is indicates that the concentration of Fe in the sample is very large. Best fits require 2 NHHS Fe(II) (O/N)5-6 doublets, with [δ = 1.21 mm/s; ΔE_Q = 2.8 mm/s and δ = 1.3 mm/s; ΔE_Q = 3.4 mm/s].

The first represents 36% and the second 61%. About 7% of spectral intensity is due to a sextet with parameters [D = 0.25 cm^{-1}; E/D = 0.3; δ = 0.2 mm/s; ΔE_Q = 0.78 mm/s; eta = 2; A = -221 gauss]. There is also a broad shoulder on the right side which was more predominant than on spectra of the previous samples. Cells harvested under stationary state conditions exhibited Mossbauer spectra composed of 3 major species (and perhaps two minor ones). About 60% of spectral intensity was due to a NHHS Fe(II)(O/N)5-6 species with [δ = 1.26 mm/s; ΔE_Q = 3.07 mm/s]. The Central Doublet represented 16% of the spectral intensity. A Non Heme High Spin $Fe(II)^I$ sextet represented 20% of spectral intensity. Simulations of this species required very similar parameters relative to that in the parent Δ*iscU-fdx strain* = 0.25 cm^{-1}; E/D = 0.33; δ = 0.15 mm/s; ΔE_Q = 0.96 mm/s; η = 0.27; A = -197 gauss]. It was also possible to include 2% of the Fe(II)S_4 species and 3% nanoparticles. The strain has more High Spin Fe and less nanoparticles compared to the parent Δ*iscU-fdx* strain.

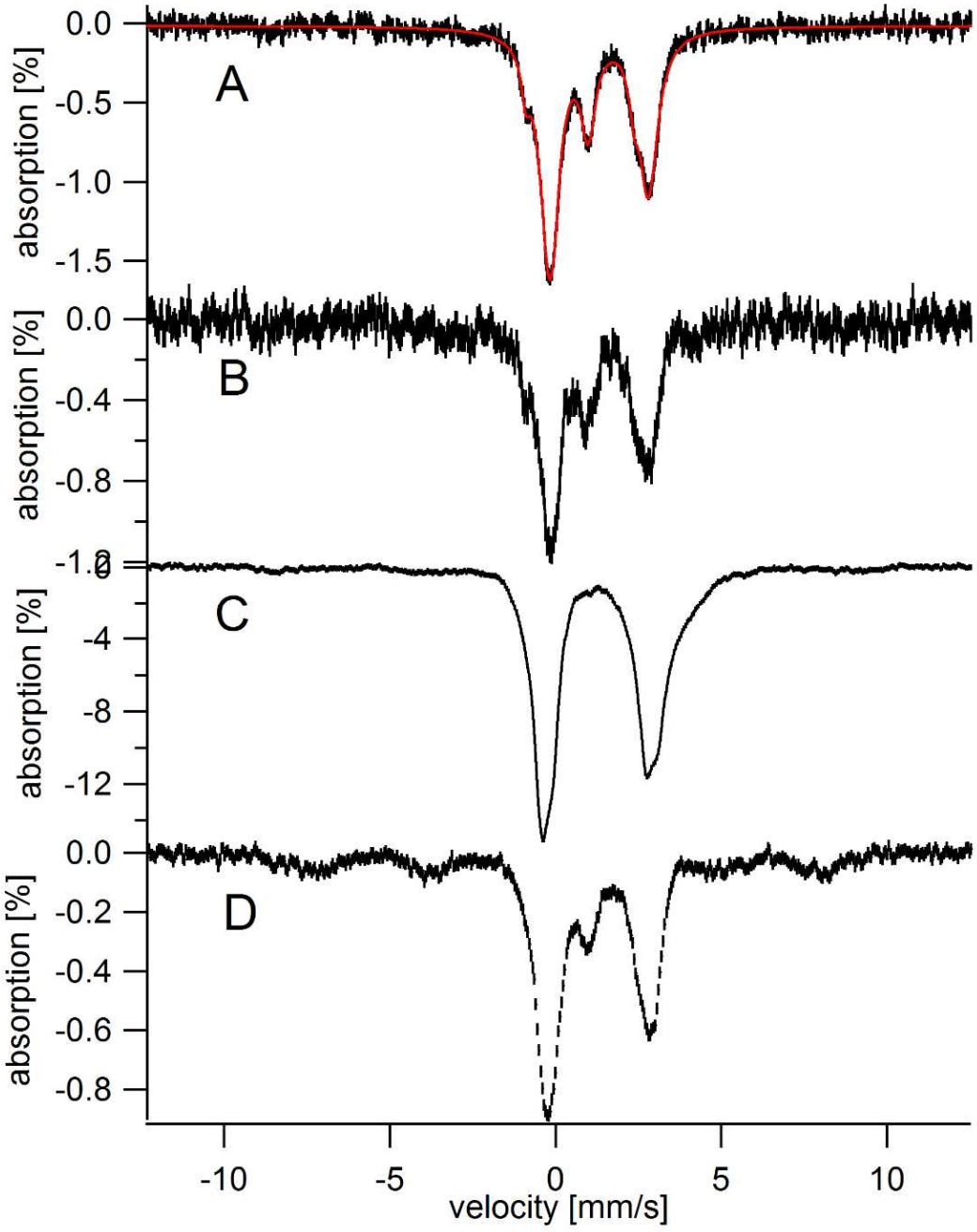

Figure A.9. Mossbauer spectra (5K, 0.05T) of E coli strain Δ*iscU-fdx*Δ*bfr*Δ*dps* grown in glucose medium. (A) and (B) had 10 μM Fe in the growth medium and harvested under exponential conditions (C) had 100 μM Fe in the medium and harvested under exponential conditions and (D) 100 μM Fe in the medium and harvested under stationary-state conditions.

2% of the Fe(II)S_4 species and 3% nanoparticles. The strain has more High Spin Fe and less nanoparticles compared to the parent Δ*iscU-fdx* strain.

The Δ*iscU-fdx*Δ*ftnA*Δ*dps*Δ*bfr* strain (Figure A.10) exponential phase cell strain grown with 10 μM Fe had a lower percent effect than the other samples. This included 31% CD, 57% NHHS Fe(II)(O/N)5-6 [δ = 1.26 mm/s; ΔE_Q = 2.9 mm/s], and 4% Fe(II)S_4. The spectrum with 100 μM Fe had 3.3% effect, with a flat baseline (no sextet) and a hint of the broad shoulder. The NHHS Fe(II)(O/N)5-6 feature was fitted to 2 doublets with [δ = 1.28 mm/s; ΔE_Q = 2.8 mm/s (50%) and [δ = 1.23 mm/s; ΔE_Q = 3.38 mm/s] (28%). The CD represented 22% of the spectral intensity. Spectrum with 100 μM Fe at stationary phase exhibited a broad shoulder and a small Fe(II)I sextet (which represented 14% area). The parameters were [D = 0.25 cm^{-1}; E/D = 0.30; δ = 0.25 mm/s; ΔE_Q = 1.1 mm/s; η = 2; A = -211 gauss]. The CD represented 25% of the spectral intensity. About 64% of spectral intensity was due to NHHS Fe(II) [δ = 1.27 mm/s; ΔE_Q = 3.17 mm/s].

In the Δ*isc* Δ*bfr* Δ*ftnB* strain (Figure A.11), for spectrum the 10 μM Fe spectrum, the NHHS Fe(II) doublet was 46%, the CD was 45%, and the FeS4 was 5%. Two sites were used to fit the NHHS Fe(II) [δ = 1.27 mm/s; ΔE_Q = 2.5 mm/s for site 1 (14%) and δ = 1.31 mm/s; ΔE_Q = 3.07 mm/s for Site 2 (32%). For the 100 μM exponential Fe spectrum, the percent effect was huge (12%), and it was dominated by NHHS Fe(II). There is not much sextet and the unusual shoulder is intense. Two sites were used for the NHHS Fe(II) fit. [δ = 1.24 mm/s; ΔE_Q = 2.83 mm/s for site 1 (55%) and δ = 1.31 mm/s; ΔE_Q = 3.5 mm/s for Site 2 (26%).] The "weird shoulder" fit to [δ = 1.66 mm/s; ΔE_Q = 4.2

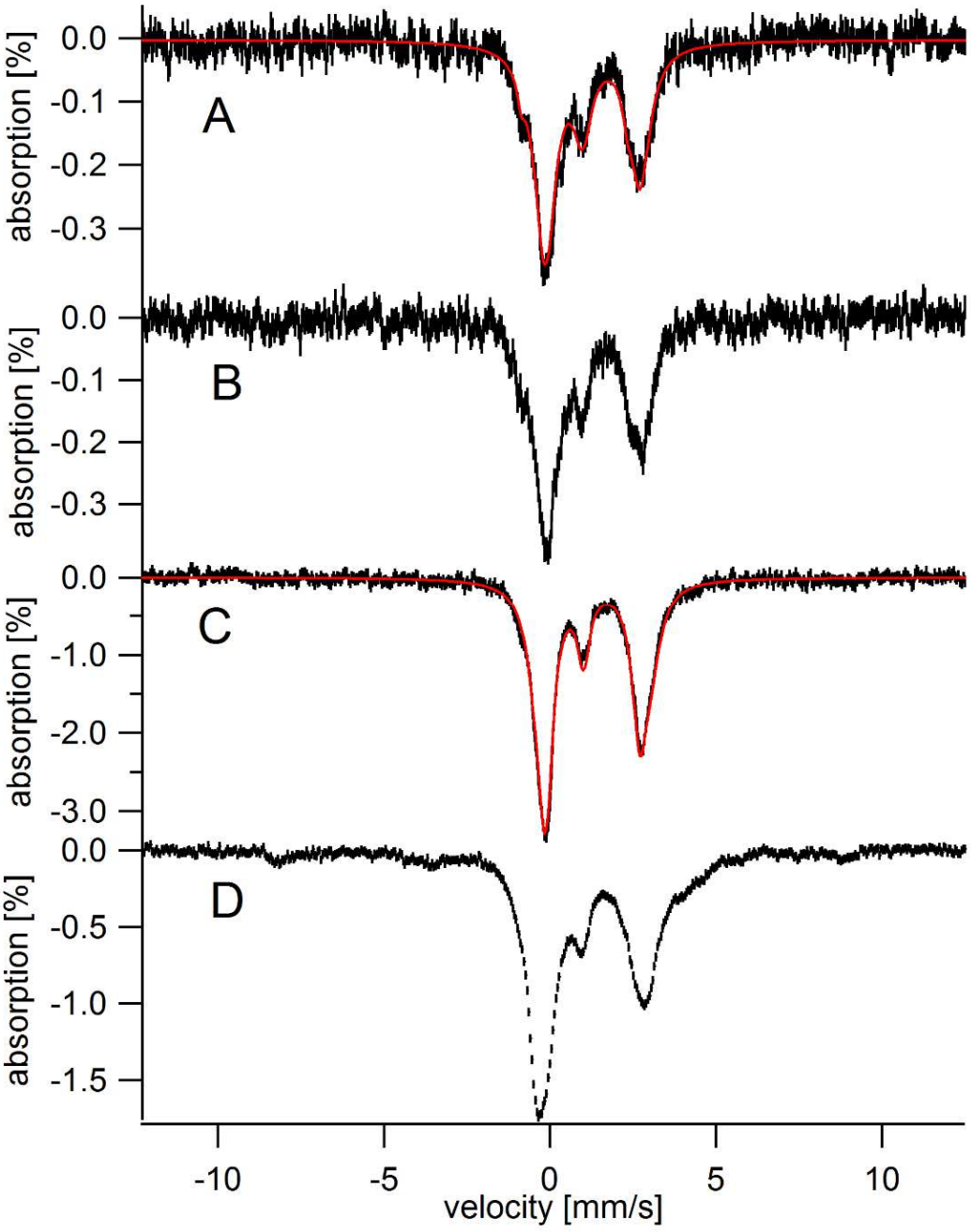

Figure A.10. Mossbauer spectra of *E. coli strain* Δ*iscU-fdx*Δ*bfr*Δ*dps*Δ*ftnA* grown in glucose media. Spectra (A) and B were grown with 10 μM Fe and harvested at exponential phase, (C) grown with 100 μM Fe and harvested at exponential phase and (D) was grown with 100 μM Fe and harvested at stationary phase.

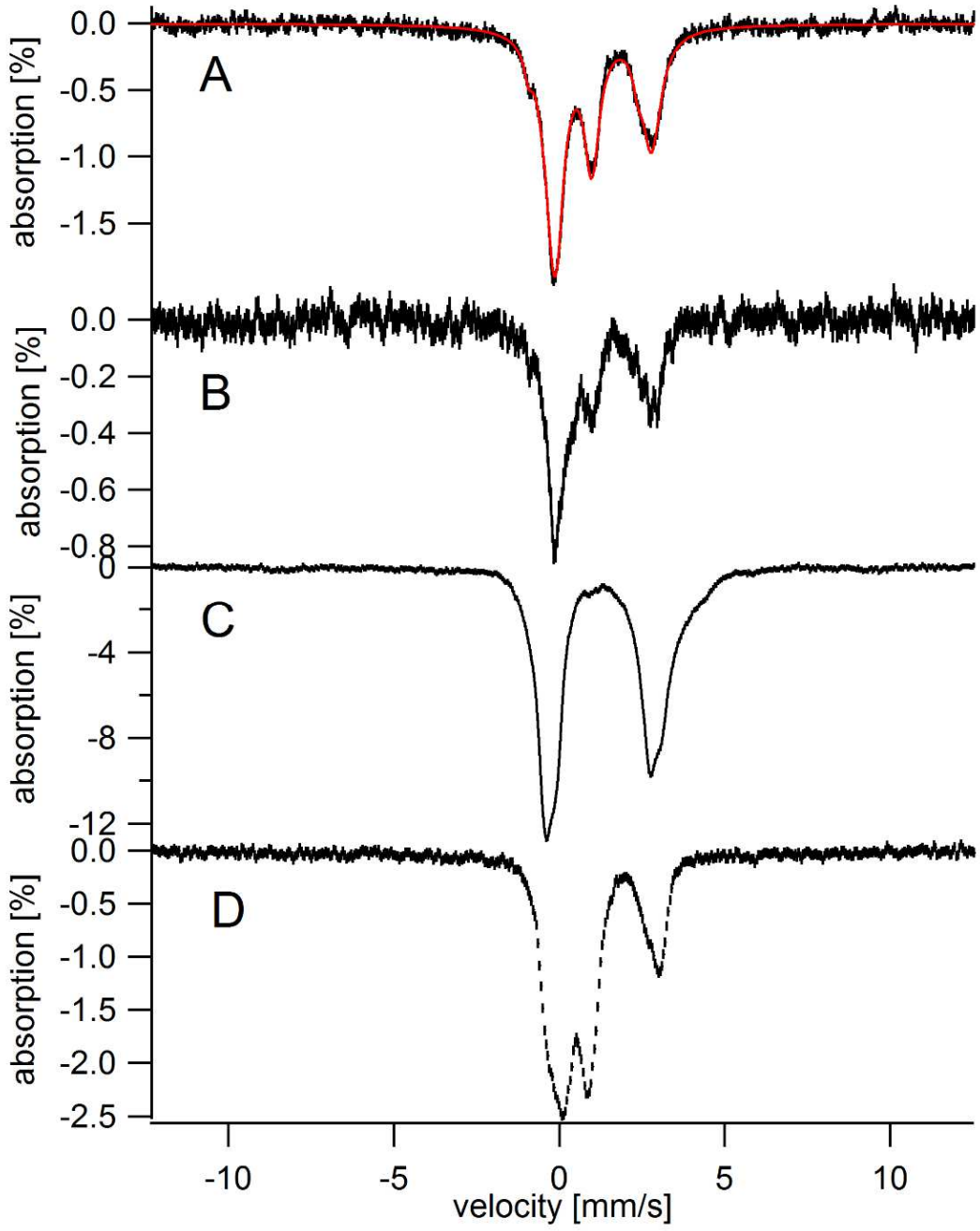

Figure A.11. Mossbauer spectra of *E. coli strain* Δ*iscU-fdx*Δ*ftnB*Δ*bfr* grown in glucose media. Spectra (A) and B were grown with 10 μM Fe and harvested at exponential phase, (C) grown with 100 μM Fe and harvested at exponential phase and (D) was grown with 100 μM Fe and harvested at stationary phase.

mm/s, line width 0.85 mm/s]; it represented 19%. The stationary spectrum had more nanoparticles than the other samples, more similar to WT cells. No sextet was evident. Nanoparticles constituted 48% of the spectral intensity [δ = 0.505 mm/s; ΔE_Q = 0.65 mm/s] whereas the NHHS Fe(II) constituted 35% of spectral intensity. [δ = 1.3 mm/s; ΔE_Q = 3.3 mm/s]. The CD represented 13% of spectral intensity.

APPENDIX B – SUPPLEMENTAL EXPERIMENTS AND RESULTS

Western Blot of FtnA in Wild-type and Δfur cell strains

We directly monitored FtnA protein expression by Western blot in the Wild-type and Δ*fur* cell strains (Figure B1)that we analyzed by Mossbauer. These cells had varying concentrations of ^{57}ferric citrate added to them. They were harvested at mid-log (exponential phase) between an OD_{600} of 0.5-0.6. The gel was run on a 15% SDS-PAGE gel.

Liquid Chromatography-Inductively Coupled Plasma Mass Spectrometry (LC-ICP-MS) of the wild-type and Δfur::kan^R strains show different distinct peaks for their ligands.

After Mössbauer spectroscopy, samples were brought into an anaerobic glove box and thawed for preparation for cell lysis and low molecular weight preparation of that cell lysate. This low molecular weight fraction was passed through a DB peptide column, and the various metal complexes coming off of the column and detected by the ICP-MS. Figures B1-B7 detail the traces of each samples Iron (Fe), Phosphorus (P), Sulfur (S), Copper (Cu), Zinc (Zn), Manganese (Mn), and Cobalt (Co). All analyses were run by Joshua Wofford of Dr Paul Lindahl Lab, Texas A&M.

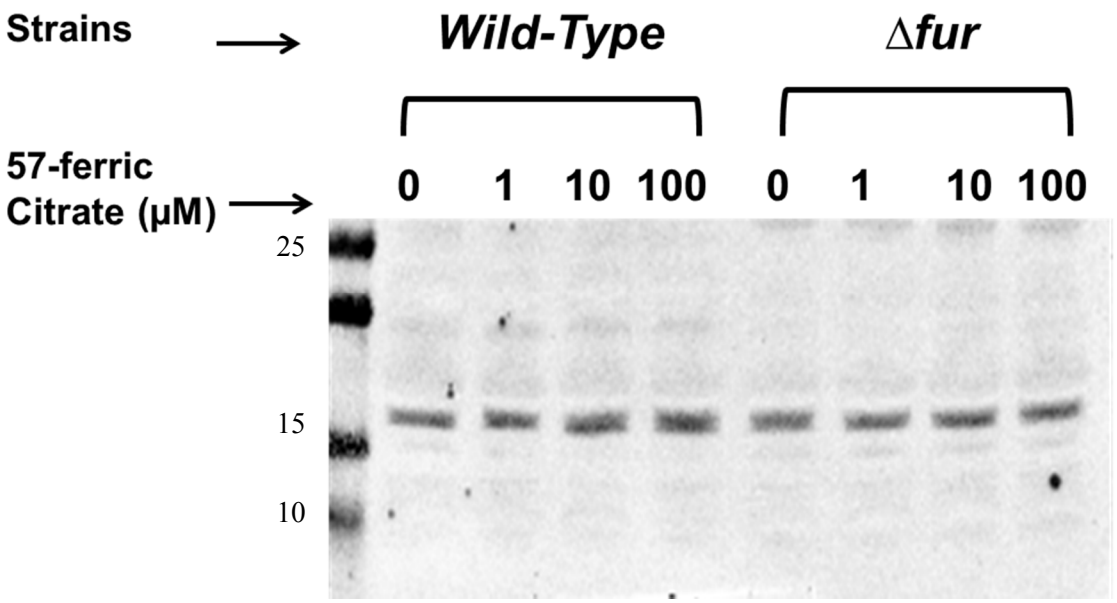

Figure B.1. FtnA expression slightly upregulated in higher iron concentrations in the Wild-type strain. Western blot analysis of equal amounts of total protein from wild-type and Δ*fur* cell strains grown in M9 glucose minimal media with increasing concentrations of ^{57} Fe(III)-citrate addition using α-FtnA antibodies.

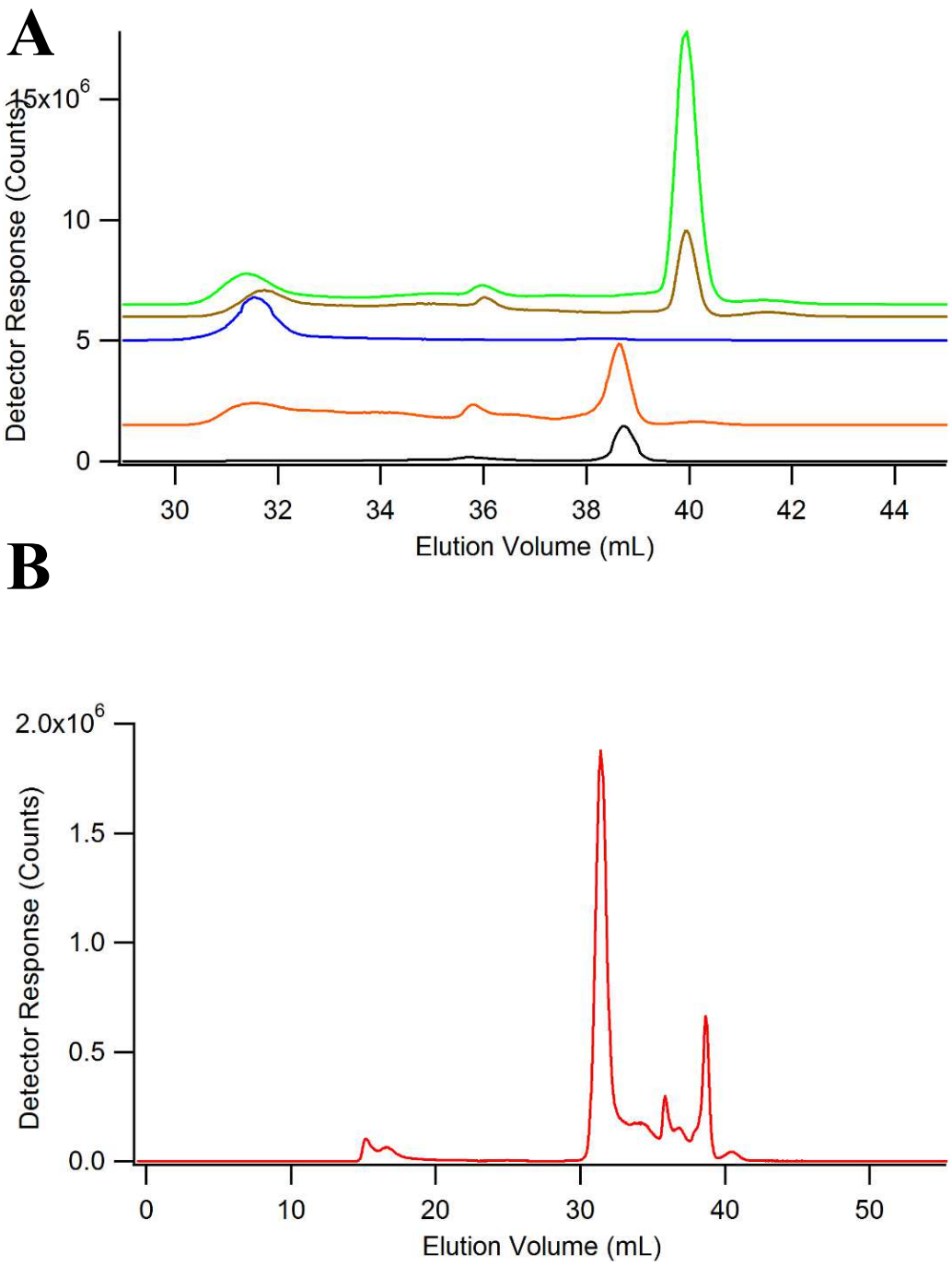

Figure B.2. Iron LC-ICPMS on (A) wild type and (B) 10 µM Δ*fur* samples. Blue Line- 1 µM WT, Gold Line- 10 µM WT, Green Line- 100 µM WT, Red Line 10 µM Δ*fur*, Orange Line- 10 µM WT (odd WT sample), Black line- First 10 µM WT.

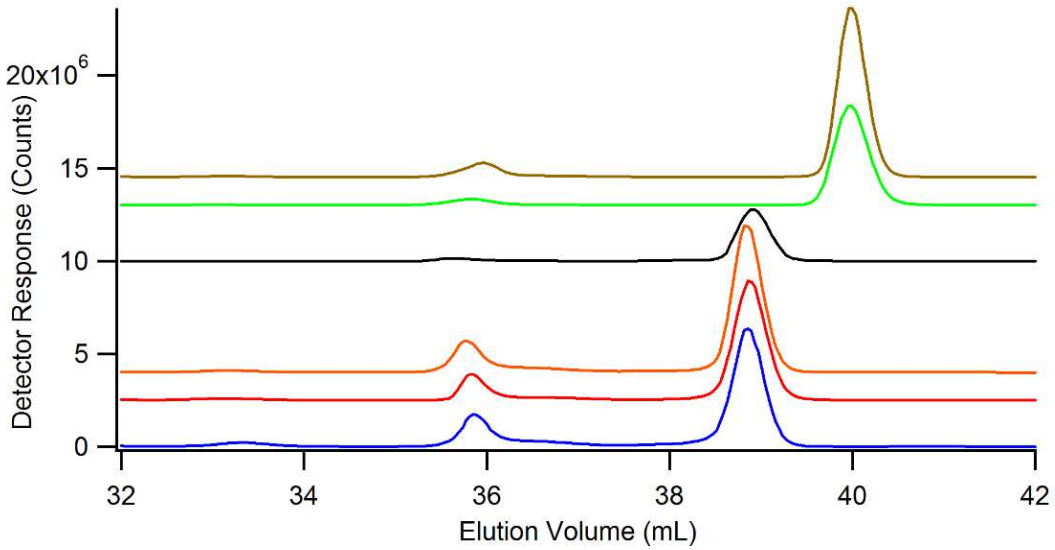

Figure B.3. Phosphorus LC-ICPMS Spectra. Blue Line- 1 µM WT, Gold Line- 10 µM WT, Green Line- 100 µM WT, Red Line 10 µM Δ*fur::kan*^{R}, Orange Line- 10 uM WT (odd 56 Fe), Black line- First 10 µM WT. List of offsets, Blue= -.3 mL, Gold= .5 mL, Red= -.6 mL, Black= -.8 mL, Orange= -.3 mL.

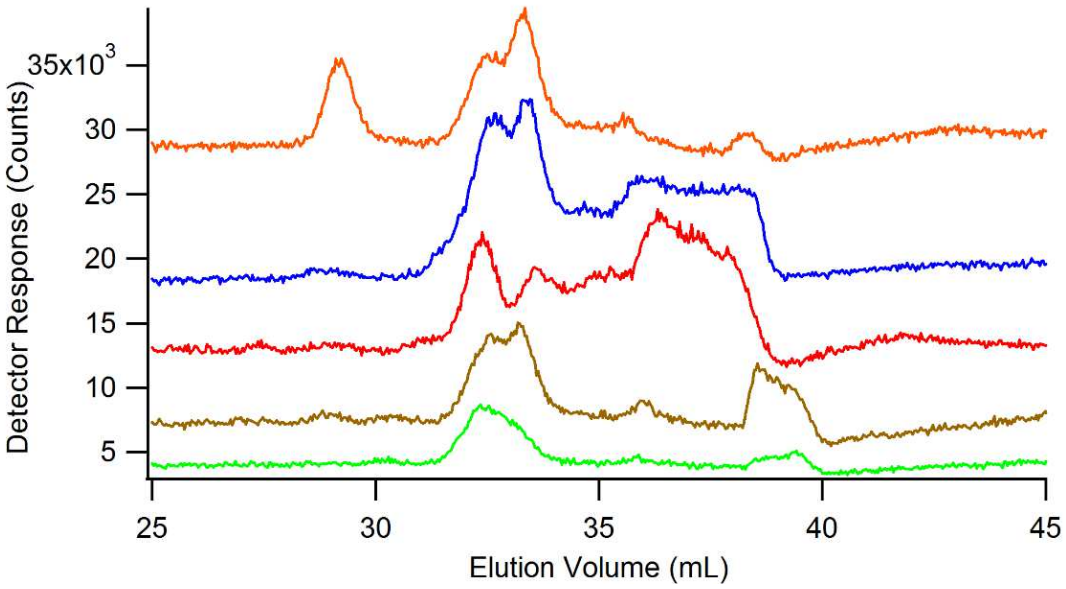

Figure B.4. Sulfur LC-ICPMS on wild type and 10 µM Δ***fur*** **samples**. Blue Line- 1 µM WT, Gold Line- 10 µM WT, Green Line- 100 µM WT, Red Line 10 µM Δ*fur*, Orange Line- 10 µM WT (odd WT sample).

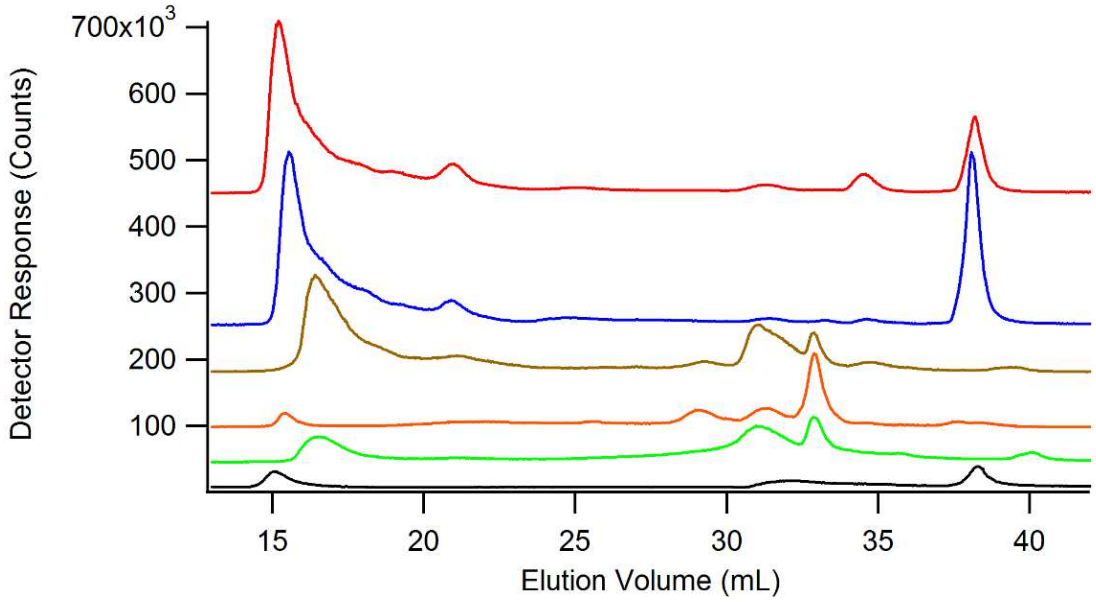

Figure B.5. Copper LC-ICPMS on wild type and10 uM Δ*fur* samples. Blue Line- 1 µM WT, Gold Line- 10 µM WT, Green Line- 100 µM WT, Red Line 10 µM Δ*fur*, Orange Line- 10 µM WT (odd WT sample), Black line- First 10 µM WT.

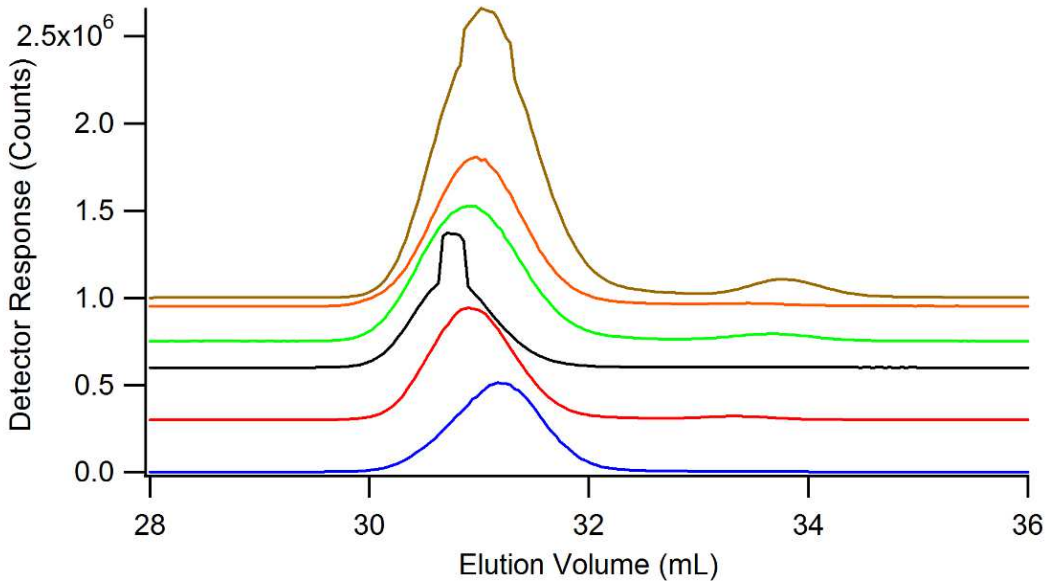

Figure B.6. Zinc LC-ICPMS on (A) wild type and (B) 10 uM Δ*fur* samples. Blue Line- 1 µM WT, Gold Line- 10 µM WT, Green Line- 100 µM WT, Red Line 10 µM Δ*fur*, Orange Line- 10 µM WT (odd WT sample), Black line- First 10 µM WT.

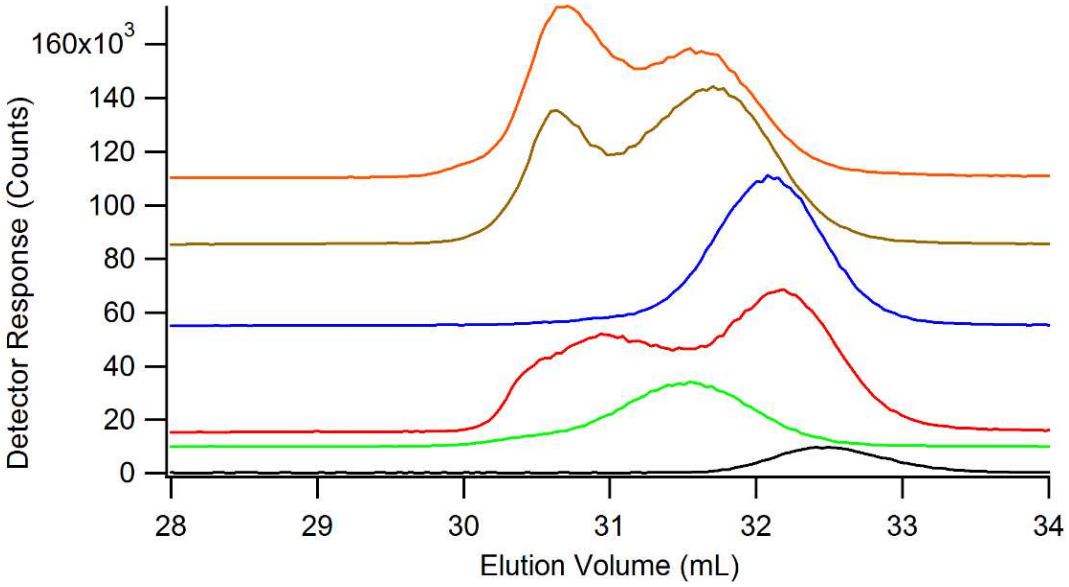

Figure B.7. Manganese LC-ICPMS on wild type and 10 uM Δ*fur* samples. Blue Line- 1 µM WT, Gold Line- 10 µM WT, Green Line- 100 µM WT, Red Line 10 µM Δ*fur*, Orange Line- 10 µM WT (odd WT sample), Black line- First 10 µM WT.

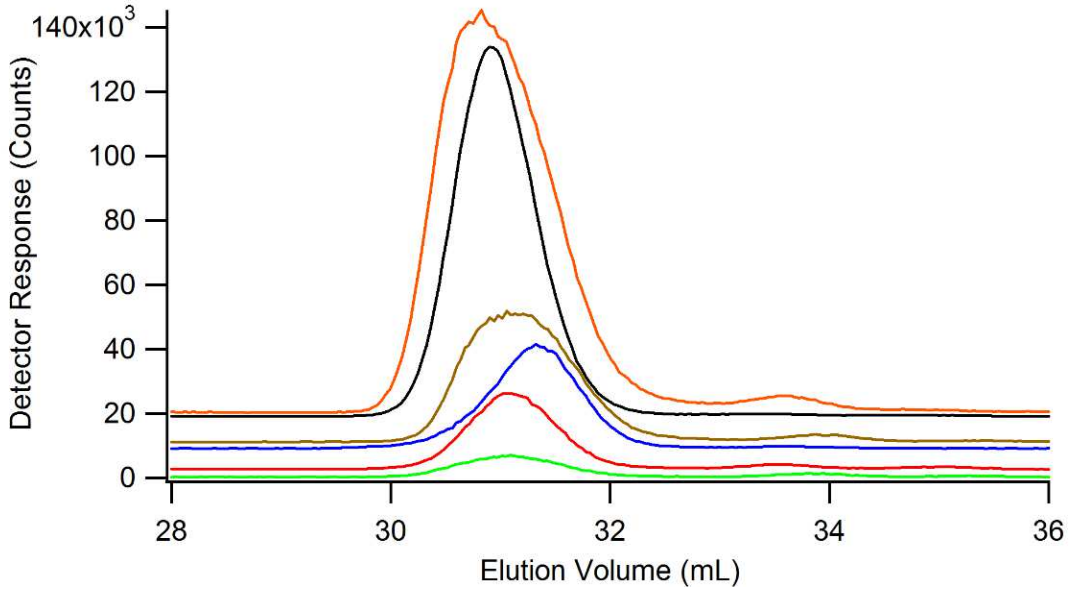

Figure B.8. Cobalt LC-ICPMS on wild type and 10 uM Δ*fur* samples. Blue Line- 1 µM WT, Gold Line- 10 µM WT, Green Line- 100 µM WT, Red Line 10 µM Δ*fur,* Orange Line- 10 µM WT (odd WT sample), Black line- First 10 µM WT.